

**STUDY OF
PHASE SEPARATED
POLYMER DISPERSED LIQUID CRYSTAL
COMPOSITE FILMS**

**A
Thesis
Submitted for the Award of
the Degree of**

DOCTOR OF PHILOSOPHY

By

PRAVEEN MALIK



**School of Physics and Materials Science
Thapar Institute of Engineering and Technology
(Deemed University)
Patiala-147004, India
June - 2005**

A

Thesis

Dedicated

To

My Parents;

For Their Care and Blessings

&

My Sisters;

For Their Love and Support

CERTIFICATE

This is to certify that the thesis entitled “**Study of Phase Separated Polymer Dispersed Liquid Crystal Composite Films**” which is being submitted by Mr. Praveen Malik in fulfillment of the requirement for the award of the degree of Doctor of Philosophy in the School of Physics and Materials Science, Thapar Institute of Engineering and Technology (Deemed University) Patiala, is a record of candidate’s own work carried out by him under my supervision and guidance. The matter presented in this thesis has not been submitted in part or full for the award of any degree in any other University or Institute.



Prof. K. K. Raina

Dean Research and Sponsored Projects

Thapar Institute of Engineering and Technology

(Deemed University)

Patiala-147004, Punjab

Date: 17/6/2005

Place: Patiala

ACKNOWLEDGEMENT

I am extremely thankful to **Prof. S. C. Saxena**, Director, Thapar Institute of Engineering and Technology, Patiala, for providing me all the necessary infrastructure and laboratory facilities to carry out the experimental work in the School of Physics and Materials Science of the Institute.

It is a matter of extreme honour and privilege for me to offer my grateful acknowledgement to my supervisor **Professor K. K. Raina**, Dean Research and Sponsored Projects, Thapar Institute of Engineering and Technology, Patiala for providing me an opportunity to work under his guidance and supervision. He always supported and inspired me with constant encouragement, sincere criticisms and valuable suggestions not only in the experimental and compilation part of the thesis but also in various aspects of my personal life.

He provided an excellent guidance to the present research work and allowed me the necessary freedom to focus on the issues of my interest. I shall always be impressed by his vast and quick intellect, ability to manage several projects at once and his willingness to participate in all aspects of experiments.

I am profoundly obliged to **Prof. N. K. Verma**, Head, School of Physics and Materials Science and Dean of Student Affairs, Thapar Institute of Engineering and Technology, Patiala for his whole-hearted support and needful help during the various stages of my work.

Words are inadequate in expressing my sincere thanks to **Dr. (Mrs) Jasjit Kaur Ahuja**, former Lecturer at the Thapar Institute of Engineering and Technology, Patiala for her support in every moment of difficulty. Her skills, fruitful discussions, constructive suggestions and constant inspiration in this work helped me to fulfil this effort.

The continuous encouragement by **Dr. O. P. Pandey** and **Dr. Kulvir Singh**, Assistant Professor, School of Physics and Materials Science is gratefully acknowledged. Many constructive discussions with Dr. Pandey and Dr. Singh were helpful in planning the experiments and this also improved my understanding of the subject.

I am also thankful to **Dr. S.S. Bawa**, Scientist G, National Physical Laboratory, New Delhi for his incomparable help during the experimentation work by giving me the required training of some new techniques.

I am thankful to **Dr. Satyendra Kumar**, Professor, Liquid Crystal Institute, Kent State University, USA and **Dr. A. M. Bubnov**, Lecturer, Department of Dielectrics, Institute of Physics, Academy of Physics of the Czech Republic, Prague for their invaluable technical suggestions during the experimental work.

I would like to convey my sincere gratitude to my friends and colleagues **Dr. (Mrs) G. Sumana, Dr. Puneet Sharma, Mr. Pankaj Kumar, Mr. Sarabjit Singh, Dr. (Mrs) Samriti Sood, Mrs. Archana Gupta, Mr. Varinder Sapehiya, Mr. Vineet Prakash, Mr. Vivek Srivastava, Ms. Puneet Sharma and Mr. Sanjay Panwar** for their whole-hearted co-operation.

I am grateful to the staff of School of Physics and Materials Science who never turned me down whenever I approached them for any help.

I am greatly indebted to my dearest sisters **Dr. (Mrs) Poonam, Manju, Aruna** and brother-in-law **Dr. Akash** for their patience and constant co-operation whenever I was away from them.

The meaning of my life and work is incomplete without paying regards to the respected parents whose blessings and continuous encouragement have shown me the path to achieve my goals.

I am grateful to DST, DRDO and CSIR, New Delhi for providing the research grant in the form of sponsored projects to carry out this work.

I am also thankful to BDH, UK, E Merck, Darmstadt, Germany and NORLAND Products NJ, for providing the E8, BL036, ZLI-3654 and NOA series polymers used in the present study.

...And above all, I pay my regards to the **Almighty** for his love and blessings.



(Praveen Malik)

CONTENTS

Page No.

Certificate	i
Acknowledgement	ii
List of figures	vii
List of tables	xii
Abbreviations and list of symbols	xiii
List of publications	xv
Chapter 1 Introduction	1-35
Overview	1
1.1 Liquid crystals	2
1.1.1 Types of liquid crystal	2
1.1.2 Order parameter	5
1.1.3 Liquid crystalline phases	6
1.1.3.1 Non tilted phases	6
1.1.3.2 Tilted phases	9
1.1.3.3 Chiral phases	13
1.1.3.4 Other liquid crystalline phases	14
1.1.4 Physical properties of liquid crystal	17
1.1.4.1 Anisotropy	17
1.1.4.2 Liquid crystal alignment	18
1.2 Polymer/liquid crystal dispersed systems	19
1.2.1 Polymer dispersed liquid crystals (PDLCs)	20
1.2.1.1 Preparation methods of PDLC films	22
1.2.1.1 a Encapsulation (NCAP)	23
1.2.1.1 b Phase separation	23
1.2.2 Phase separated composite films (PSCOF)	25
1.2.3 Liquid crystal dispersed polymer (LCDP)	26
1.2.4 Polymer stabilized liquid crystal (PSLC)	26
1.2.5 Polymer/liquid crystal/dyes blends	28
1.3 Droplet configuration in PDLC	28

1.4	Dichroic PDLC	30
1.5	Aim of this research work	32
	References	33-35
Chapter 2	Experimental	36-62
	Overview	36
2.1	Selection of materials	37
2.2	Homogenous alignment and cell construction	39
2.3	Preparation of phase separated polymer dispersed liquid crystals	42
2.3.1	Polymer dispersed nematic liquid crystal samples	42
2.3.2	Guest-host polymer dispersed nematic liquid crystal samples	44
2.3.3	Polymer dispersed ferroelectric liquid crystal samples	46
2.4	Experimental techniques	47
2.4.1	Temperature programmer and hot stage	49
2.4.2	Optical polarizing microscopy	50
2.4.3	UV-VIS spectrophotometer absorbance and transmission studies	50
2.4.4	Droplet size measurements	51
2.5	Optical textures and phase behaviour	52
	References	62
Chapter 3	Polymer dispersed nematic liquid crystal systems	63-87
	Overview	63
3.1	Review of literature	64
3.2	Results and discussion	66
3.2.1	Polymer dispersed nematic liquid crystal	66
3.2.1.1	Droplet morphology	66
3.2.1.2	Electro-optic responses	69
3.2.1.3	Thermo-optic responses	73
3.2.2	Guest-host polymer dispersed nematic liquid crystals	75
3.2.2.1	Droplet morphology	75
3.2.2.2	Electro-optic responses	79

3.2.2.3	Thermo-optic responses	81
3.2.2.4	Electronic- optic responses	83
	References	85-86
Chapter 4	Polymer dispersed ferroelectric liquid crystal systems	87-105
	Overview	87
4.1	Review of literature	88
4.2	Experimental	90
4.2.1	Polarization switching effects	90
4.2.2	Measurement of spontaneous polarization	92
4.3	Results and discussion	93
4.3.1	Droplet morphology	93
4.3.1 (a)	Unaligned polymer dispersed ferroelectric liquid crystal films	93
4.3.1 (b)	Aligned polymer dispersed ferroelectric liquid crystal films	96
4.3.2	Electro-optic and thermo-optic effects in PDFLC films	99
4.3.2 (a)	Temperature dependence on spontaneous polarization	99
4.3.2 (b)	Effect of polymer viscosity on spontaneous polarization	102
4.3.2 (c)	Bias voltage dependence on optical responses	103
	References	105
Chapter 5	Conclusions	106-107

LIST OF FIGURES

Page No.

Chapter 1

1.1	Molecular structure of typical liquid crystal molecule	3
1.2	A general structural template for generating single compound calamitic LCs	3
1.3	A general structural template for discotic liquid crystal	4
1.4	Structural template of (a) main chain polymer liquid crystal (b) side chain polymer liquid crystal	5
1.5	Geometry defining order parameter of a liquid crystal	6
1.6	Order parameter of nematic liquid crystal as a function of temperature	6
1.7	(a) Molecular arrangements of nematic phase (b) The molecules possess a preferred direction of orientation	7
1.8	Molecular arrangement in a SmA phase. The long axes of the molecules in each layer, on an average, are perpendicular to the layer containing the molecules	8
1.9	A view of molecules within a layer of Hexagonal smectic B phase (a) the molecules are perpendicular to the smectic plane as indicated by the circles (b) Local herringbone arrangement of molecules in a layer of the crystal E phase	8
1.10	Molecular arrangement in SmC phase. Molecular tilt at an angle with respect to layer normal is seen	9
1.11	Schematic representation of some tilted phases (a) hexatic smectic F (b) Hexatic Smectic I. Major axis of the ellipse indicates the molecular tilt direction with respect to the hexagon axes	10
1.12	A typical phase sequence of tilted phases	11
1.13	Plan view of different smectic phases	12
1.14	Rotation of director in a helical arrangement about the layer	13

	normal in a cholesteric liquid crystal	
1.15	Helix formation in chiral SmC phase	14
1.16	(a) Platelet texture of blue phase (b) Cubic lattice formed by double twist cylinders as a possible model of a blue phase	15
1.17	A sequence of twisting of smectic blocks in TGBA phase	16
1.18	Planar twist grain boundary TGBA* phase	16
1.19	Micro-texture of banana shaped molecule	17
1.20	Bifurcation of incident light into an ordinary and extra ordinary rays due to the anisotropy in a birefringent liquid crystal	18
1.21	Alignment in liquid crystal: (a) homogenous (b) homeotropic	19
1.22	Dispersed liquid crystal droplets in polymer matrix	20
1.23	Refractive indices of liquid crystal molecule parallel or perpendicular to director, n_e = extra ordinary refractive index and n_o = ordinary refractive index	21
1.24	Operation principle of PDLC film in (a) Opaque state and (b) transparent state	22
1.25	A PDLC film formed by encapsulation method	23
1.26	Evolution of a PDLC material through phase separation	24
1.27	Typical stripe domain pattern of polymer/FLC composite under intermediate pulse field	27
1.28	Liquid crystal droplet configurations dispersed in PDLC systems	30
 Chapter 2		
2.1	Set-up for liquid crystal cell preparation in clean environment	41
2.2	Flow chart showing preparation of phase separated PDLC samples	43
2.3	An assembled (a) empty (b) filled liquid crystal cells	45
2.4	Block diagram of the experimental set-up to study the electro-	48

	optical properties	
2.5	Experimental set-up to study the electro-optical properties of phase separated PDLC films	49
2.6	Measurement of liquid crystal droplet size in PDNLC sample at room temperature	51
2.7	Nematic liquid crystal droplet morphology dispersed in polymer matrix at different temperatures ($^{\circ}\text{C}$) (a) 30 (b) 40 (c) 60 and (d) 68	54
2.8	Dichroic LC droplet morphology in different configurations (a) scattered (b) radial (c) axial and (d) twisted bipolar at room temperature	56
2.9	Droplet morphology in unaligned PDFLC sample at temperatures ($^{\circ}\text{C}$) (a) 30 (b) 60 (c) 73 (d) 78 (e) 82 and (f) 91	60
2.10	Alignment of FLC molecules dispersed in UV curable polymers of viscosities (CPS) (a) 140 (b) 2500 at room temperature	61
 Chapter 3		
3.1	Response of PDNLC sample to an applied voltage (V_{p-p}) (a) 0V (b) 5V (c) 10V and (d) 25V at 55°C	68
3.2	Hypothetical illustration of field induced effects on LC droplets embedded in polymer matrix	72
3.3	Applied voltage dependence of the output transmission at different temperature	73
3.4	Temperature dependence of the applied voltage corresponding to V_{10} , V_{50} and V_{90}	74
3.5	Variation of liquid crystal droplet size as a function of (a) applied voltage at 55°C and (b) temperature at constant applied voltage ($20V_{p-p}$, $f = 1\text{kHz}$)	75
3.6	Schematic representation of LC and dye molecular	76

	arrangement in GHPDNLC sample cell without and with electric field (a) $E = 0$ and (b) $E > 0$	
3.7	Influence of dye concentration (a) 1% (b) 2% and (c) 4% on LC droplet morphology dispersed in polymer matrix	78
3.8	Optical textures of GHPDNLC sample at various applied voltage ($f = 500$ Hz) (a) $0V_{p-p}$ (b) $10V_{p-p}$ (c) $30V_{p-p}$ and (d) $100V_{p-p}$ at room temperature	81
3.9	Variation of optical transmission as a function of applied voltage ($f=500$ Hz) at different dye concentration	82
3.10	Variation of optical transmission as a function of applied voltage ($f=500$ Hz) at different temperatures for 1% dye concentration GHPDNLC sample	83
3.11	Optical transmission as a function of temperature at different applied bias voltage	83
3.12	Bias voltage as a function of temperature at V_{10} , V_{50} and V_{90}	84
3.13	Response time of a GHPDNLC samples as a function bias voltage	85
 Chapter 4		
4.1	Experimental setup to study the polarizing switching responses using reversal field technique	92
4.2	Wave form of the output waveform by the resistor method	92
4.3	Liquid crystal droplet morphology of unaligned PDFLC sample at polymer viscosities (CPS) (a) 140 (b) 1000 (c) 2500 and (d) 5000	96
4.4	Variation of liquid crystal droplet size as a function of polymer viscosity in unaligned PDFLC at 30°C	97
4.5	Polymer viscosity dependence on the alignment of liquid crystal droplets in aligned PDFLC samples at polymer viscosities (CPS) (a) 140 (b) 1000 (c) 2500 and (d) 5000	99

	viscosities (CPS) (a) 140 (b) 1000 (c) 2500 and (d) 5000	
4.6	Temperature dependence on spontaneous polarization in aligned PDFL C sample	100
4.7	Wave form of polarization hump at different temperatures (°C) (a) 30 (b) 40 (c) 50 (d) 65 and (e) 70	101
4.8	Temperature dependence on spontaneous polarization in unaligned PDFLC sample	102
4.9	Effect of polymer viscosity on spontaneous polarization at different temperatures in (a) aligned PDFLC sample (b) unaligned PDFLC sample	104
4.10	Optical transmission as a function of applied voltage in polymers of different viscosities	105
4.11	Response time as a function of applied voltage dependence in different polymer viscosities for unaligned PDFLC samples at room temperature	105

LIST OF TABLES

Page No.

2.1	Physical properties of liquid crystal materials used	37
2.2	Physical properties of liquid crystal materials used	38
2.3	Physical properties of UV curable polymers	38
2.4	Molecular structure and physical properties of anthraquinone dichroic dye	39

ABBREVIATIONS AND LIST OF SYMBOLS

LC	Liquid crystal
NLC	Nematic liquid crystal
FLC	Ferroelectric liquid crystal
PDLC	Polymer dispersed liquid crystal
PIPS	Polymerisation induced phase separation
TIPS	Temperature induced phase separation
SIPS	Solvent induced phase separation
ITO	Indium tin oxide
PDFLC	Polymer dispersed ferroelectric liquid crystal
PDNLC	Polymer dispersed nematic liquid crystal
GHPDNLC	Guest-host polymer dispersed nematic liquid crystal
NOA	Norland optical adhesive
CPS	Centi poise
n_o	Ordinary refractive index
n_e	Extra ordinary refractive index
n_p	Polymer refractive index
V_{th}	Threshold voltage
τ	Rise time
P_s	Spontaneous polarization
μ	Polymer viscosity
T_c	Critical temperature
β	Critical exponent
ρ_p	Polymer resistivity
ρ_{LC}	Liquid crystal resistivity
V_t	Terminal velocity
R	Droplet radius
Cr	Crystalline
Iso	Isotropic

N	Nematic
N*	Cholesteric
SmA	Smectic A
SmC	Smectic C
SmC*	Smectic C*
K	Twist elastic constant
l	Liquid crystal droplet anisotropy
d	Film thickness
c	Constant
E_{eff}	Effective electric field
E'_{eff}	Threshold field
E_a	Applied electric field
σ_{Pol}	Polymer conductivity
σ_{LC}	Liquid crystal conductivity

LIST OF PUBLICATIONS

Referred Journals

- [1] Effect of polymer viscosity on morphological and electro-optic properties of aligned polymer dispersed ferroelectric liquid crystal composite films, **Praveen Malik**, Jasjit K. Ahuja and K. K. Raina, *Current Applied Physics*, **3** (2003) 325-329
- [2] Droplet orientation and optical properties of polymer dispersed liquid crystal composite films, **Praveen Malik** and K.K. Raina, *Optical Materials*, **27** (2004) 613-617.
- [3] Electro-optic properties of UV curable polymer dispersed ferroelectric liquid crystal thin films, **Praveen Malik**, G. Sumana and K.K. Raina, *Integrated Ferroelectrics*, (In press) 2005
- [4] Domain switching and dielectric spectroscopy investigations in ferroelectric liquid crystals, K. K. Raina, **Praveen Malik**, Rajbir Singh, V. K. Aggrawal and Chandra Prakash, *Integrated Ferroelectrics* (In Press) 2005

Communicated Papers

- [5] Opto-electronic responses of a guest host polymer dispersed liquid crystal device, **Praveen Malik**, P. Kumar and K. K. Raina, *Japn. J. Appl. Phys.*, (2005)
- [6] Dielectric spectroscopy of new ferroelectric liquid crystalline material laterally substituted by methyl Group, **Praveen Malik**, K.K. Raina, Jasjit K Ahuja, Alexej Bubnov, Vera Hamplová, and Miroslav Kašpar, *Journal of Physics and Chemistry of Solids*, (2005)

Referred Conference Proceedings (International/National)

- [7] Effect of polymer viscosity on morphological and electro optic properties of unaligned polymer dispersed ferroelectric liquid crystal composites films,

- Praveen Malik** and K. K. Raina, *Proc. of National Conference on Materials and Related Technologies*, Ed. K. K. Raina, September 19-20 (2003) 174-182
- [8] Electro-optic responses of ferroelectrics liquid crystalline materials with large spontaneous polarization, K. K. Raina, **Praveen Malik**, Pankaj Kumar and Alexij Bubnov, *Proc. of National Seminar on Ferroelectrics and Dielectrics XIII*, Ed. R. P. Tandon, Allied Publisher, Nov 23-25 (2004), New Delhi
- [9] Effect of polymer viscosity on morphological, polarizing switching and optical properties of polymer dispersed ferroelectric liquid crystal thin films, **Praveen Malik**, Pankaj Kumar, K. K. Raina and Chandra Prakash, *Proc. of National seminar on Ferroelectrics and Dielectrics XIII*, Ed. R. P. Tandon, Allied Publisher, Nov 23-25 (2004), New Delhi
- [10] Synthesis and characterization of novel acrylate based side chain ferroelectric liquid crystal polymers, G. Sumana, K. K. Raina, **Praveen Malik**, Pankaj Kumar, Puneet Sharma, Shikha Kapila, Alexij Bubnov and Chandra Prakash, *Proc. of National seminar on Ferroelectrics and Dielectrics XIII*, Ed. R. P. Tandon, Allied Publisher, Nov 23-25 (2004), New Delhi
- [11] Influence of dichroic dye on morphological and electro-optical properties of polymer dispersed liquid crystal composite thin film, **Praveen Malik**, P. Kumar and K. K. Raina, *Proc. on Advanced Condensed Matter Physics*, Ed. K. K. Raina, Feb. 11-12 (2005) 174-182
- [12] Charge induced droplet orientation and optical properties of polymer dispersed liquid crystal thin films, **Praveen Malik**, Pankaj Kumar and K. K. Raina, 7th *International conference on Optoelectronics, Fibre optics, and Photonics*, CUST, Kochi, 9-11 December 2004, (To appear in proceeding of SPIE).

Conference/Symposium/Seminar Attended

- [13] Attended National Conference on Mathematical and Statistical Techniques, SBAS, T.I.E.T, Patiala, Dec 6-8, (2001)

- [14] Effect of temperature on the electro-optic properties of polymer dispersed ferroelectric liquid crystal thin films. **Praveen Malik**, Jasjit K. Ahuja and K. K. Raina, Presented at *5th Punjab Science Congress*, Patiala, Feb 7-9, (2002)
- [15] Storage effect and electro-optic properties in UV cured High Polarization polymer dispersed ferroelectric liquid crystals, **Praveen Malik**, Jasjit K. Ahuja and K. K. Raina, *Twelfth National Seminar on Ferroelectric and Dielectrics (NSFD-XII)*, MRC, IISC, Bangalore, Dec. 16-18, (2002)
- [16] *International Conference on Liquid Crystal and Other Soft Materials*, **Praveen Malik**, RRI, Bangalore, Dec. 18-20, (2002)
- [17] *4- Asian Meeting on Ferroelectrics*, **Praveen Malik**, IISC Bangalore, Dec 12-15 (2003)
- [18] Opto-electronic properties of polymer-liquid crystal dispersed composite films, **K. K. Raina**, **Praveen Malik**, **G. Sumana** and **S. Khosla**, *ICMAT Singapore*, Dec. 7-12, (2003)

Best presentation award

- [19] Effect of polymer viscosity on morphological, polarizing switching and optical properties of polymer dispersed ferroelectric liquid crystal thin films, **Praveen Malik**, Pankaj Kumar, K. K. Raina and Chandra Prakash, *Proc. of national seminar on ferroelectric and dielectric XIII*, Ed. R. P. Tandon, Allied Publisher, Nov. 23-25 (2004)

Chapter -1

Introduction

Overview

This chapter reviews the properties of liquid crystal systems in general and polymer dispersed liquid crystal in particular. We have tried to review the recent development in behavior of tilted, non-tilted and chiral liquid crystalline phases with emphasis on their structural considerations. The preparation methods of polymer dispersed liquid crystal composite films and others liquid crystal dispersed polymer systems are discussed in detail. The operation principle of these composite films, liquid crystal droplet configuration dispersed in polymer matrix is given. The guest-host polymer dispersed liquid crystal systems also discussed in this chapter.

1.1 Liquid crystals

In 1888, Reintzer and Lehmann discovered that some organic substances exhibit one or more intermediate phase(s) between crystalline solid and isotropic liquid phases [1-4]. These types of phases are termed as the liquid crystalline phase; mesophase or mesomorphic phase and the materials are called "liquid crystal". In these phases they retain the ability to flow like ordinary liquid, but also possess long-range orientation order. Some liquid crystals may have positional order as well.

1.1.1 Types of liquid crystal

A number of different types of molecules form liquid crystal (LC) phases when heated above their melting point. However, they are all anisotropic, they differ either in their shape or different solubility properties [2]. The three major classification of LCs are:

- Lyotropic liquid crystals
- Thermotropic liquid crystals
- Polymer liquid crystals

Lyotropic liquid crystals are formed by the change in concentration of solvent or solute. e.g. amphiphilic molecules in water.

Substances that exhibit liquid crystalline properties at certain temperature range are called thermotropic liquid crystals. The phase of a thermotropic liquid crystal changes from crystalline solid to liquid crystal when the temperature is raised above its melting point (T_M). When the temperature is further increased, the phases of the substance change from liquid crystalline phase to isotropic liquid phase. This final temperature is called the clearing point. (T_c) (Fig. 1.1). Thermotropic liquid crystal which are stable at temperature above the melting point of the compound are called enantiotropic. In certain cases the liquid crystalline state is only stable at temperature below the melting point and can be obtained only with decreasing the temperature, phases of this kind are called monotropic.

Discotic liquid crystals are formed by disc shaped molecules, in which one molecular axis is shorter than other two. In 1977, S. Chandrasekhar et al. reported the mesomorphism in disc shaped molecules (hexa-alkanoylbenzene). Such compounds known as discotic LCs and again rigidity in the central part of the molecule is essential. The core of a typical discotic LC molecule is usually based on benzene, triphenylene or truxene with 6 or 8 chains, each resembling a typical calamitic LC molecule. Fig. 1.3 shows a general structural template for discotic LCs.

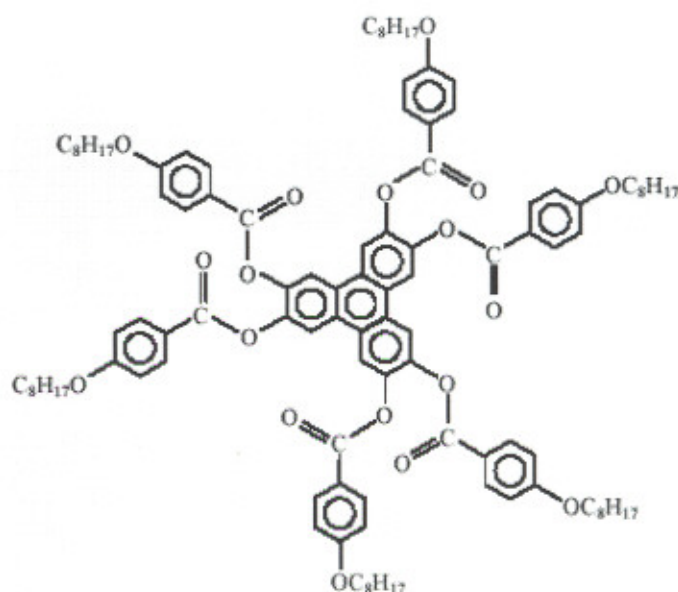


Fig. 1.3 A general structural template for discotic liquid

The disc shaped central core unit is usually benzene or a polyaromatic such as triphenylene or phthalocyanine, but columnar phases have been generated with alicyclic cores such as cyclohexane and carbohydrate. In order to maintain the disc-like structure, the central core is usually symmetrical and the peripheral dendritic units are present in number that are appropriate for the central core [2]

Another class of materials that combine the properties of liquid crystal and polymer are called polymer liquid crystals (PLCs) [5-6]. These hybrids show the same mesophases characteristic of ordinary liquid crystals, yet retain many of the useful and versatile properties of polymers. For normally flexible polymers to display liquid crystal characteristics, rod-like or disk-like elements called mesogens must be incorporated into their chains. The placement of the mesogens plays a significant role in determining the

type of PLC that is formed. Main chain polymer liquid crystal (or MCPLC) are formed when rigid elements are incorporated into the backbone of normally flexible polymers Fig. 1.4(a). These stiff regions along the chain allow the polymer to orient in a manner similar to ordinary liquid crystals, and thus display liquid crystal characteristics.

Conversely, side chain polymer liquid crystals (or SC-PLC) are formed when the mesogens are connected as side chains to the polymer by a flexible "bridge" (called the spacer.) as shown in Fig. 1.4(b)

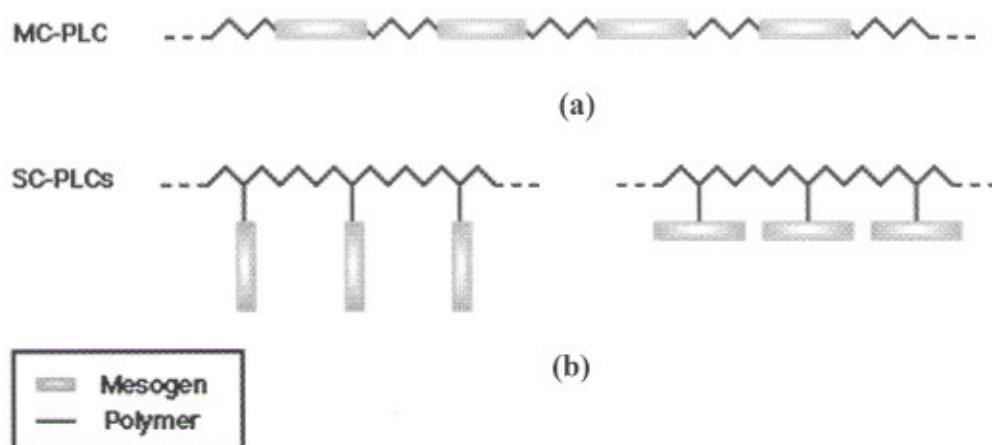


Fig. 1.4 The structural template of (a) main chain polymer liquid crystal (b) side chain polymer liquid crystal

1.1.2 Order parameter

The amount of orientation order in liquid crystals can be obtained by averaging macroscopic molecule orientation with respect to director. This can be achieved in a number of ways.

The order parameter (S) can be defined as the average of the second Legendre

$$S = \langle P_2(\cos \theta) \rangle = \left\langle \frac{3}{2} \cos^2 \theta - \frac{1}{2} \right\rangle \quad (1.1)$$

Where θ is the angle between the rod axis of a molecule and the director n as shown in Fig. 1.5. If all liquid crystal molecules align perfectly parallel to the director then $S = 1$.

If all the molecules orient completely at random directions, directions with equal probability $S = 0$. Typically, the order parameter in liquid crystal phases ranges from 0.3 to 0.9 (Fig. 1.6).

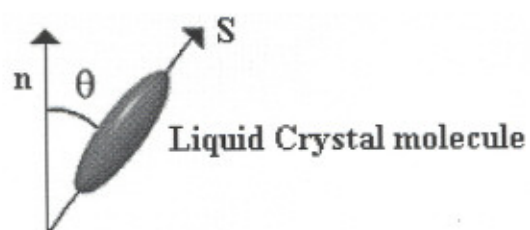


Fig. 1.5 Geometry defining order parameter of a liquid crystal

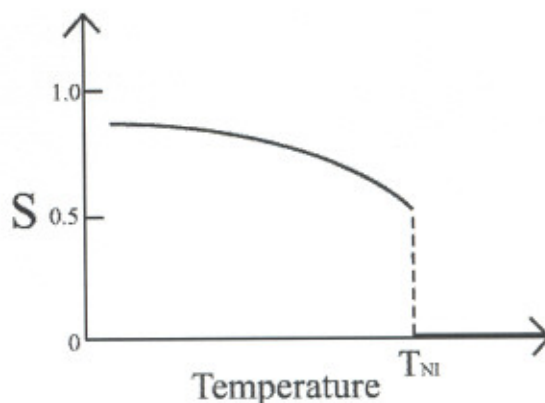


Fig. 1.6 Order parameter of nematic liquid crystal as a function of temperature

1.1.3 Liquid crystalline phases

In 1922, G. Friedel [5] classified the liquid crystalline phases into three major groups viz: Nematics, Cholesterics and Smectics based upon the orientation and positional order of the molecules.

1.1.3.1 Non-tilted phases

This is a subclass of liquid crystalline phases, which are free from chirality and molecular tilt. However these phases differ from each other in the type and extent of order and symmetry they possess.

Nematic phase

In these systems, the molecules possess only long range orientation but no positional order [Fig. 1.7(a, b)]. Depending on the molecular structure, nematics possess slightly different properties based upon their molecular structure and chemical behaviour like uniaxial and biaxial liquid crystals.

Uniaxial nematic liquid crystals have long axes of the molecules tending to align along the director (\hat{n}) as shown in Fig. 1.7 (a). Biaxial nematic liquid crystal usually consists of molecules that are elongated in one direction and flatter in the perpendicular direction [7-8]. The LC molecules are ordered in two directions: the long axes are oriented around one director and the broadsides are oriented around another director perpendicular to the first one.

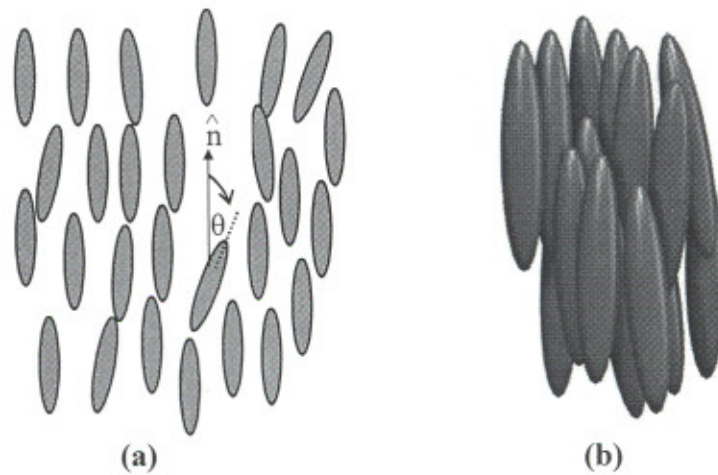


Fig. 1.7 (a) Molecular arrangements of nematic phase (b) the molecules possess a preferred direction of orientation

Smectic A phase

These phases are more ordered than nematics and possess positional and orientation order. These phases usually occur at temperatures below the nematic domain. From the structural point of view, all the smectics have layered structures and are perpendicular to the layer plane with a well-defined interlayer spacing that can be measured by x-ray diffraction. In this system the molecules can move freely around the long axes within the layer. Optically smectic A is uniaxial with the optical axis direction coinciding with the director [Fig. 1.8].



Fig. 1.8 Molecular arrangement in a SmA phase. The long axes of the molecules in each layer, on an average, are perpendicular to the layer plane containing the molecules

Smectic B or Hexatic B phase

These two names of same phase, abbreviated as HexB describe a phase, which is characterized by a layered structure, just like the SmA phase. In this phase the LC molecules are locally hexagonally packed and are perpendicular to the plane as shown in Fig. 1.9.

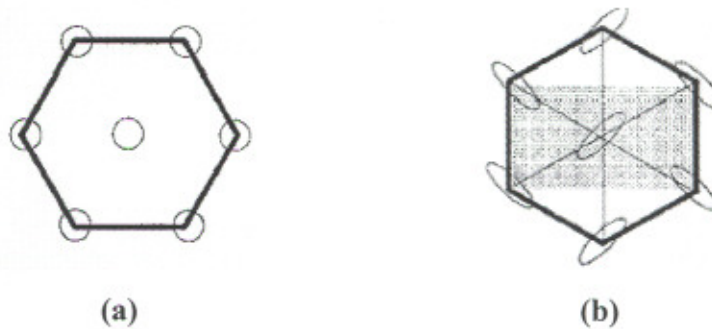


Fig. 1.9 (a) A planar view of molecules within a layer of a hexagonal smectic B phase (a) the molecules are perpendicular to the smectic plane as indicated by the circles (b) Local herringbone arrangement of molecules in a layer of the crystal E phase

Crystal B

These phases are different from true crystal in one important aspect. The phase in which the position of LC molecules is fixed have freely rotation about their long axis. The average molecular orientation is perpendicular to smectic layers and within each layer molecules are ordered in a triangular lattice.

Crystal E

As in the crystal B phase, the molecules within this phase are arranged on a triangular or hexagonal lattice and are perpendicular to smectic layers. This phase is different from the crystal B phase in the rotational motion of molecules. In the crystal E phase, the thermal motion of molecules is reduced to the extent that they are arranged themselves in a herringbone pattern within a smectic layer.

1.1.3.2 Tilted phases

There is a complete set of smectic phases in which the long axis of molecules is not perpendicular to the layer normal, but makes a relatively large angle. Just like the non-titled phases these phase possess different structure and order. This section includes smectic C, smectic F, smectic I, crystal G, crystal J, Crystal H and Crystal K phases.

Smectic phase

In this phase molecules are arranged like the SmA phase, but the only difference is the long axes of the molecules are arranged at an angle θ to the layer normal as illustrated in Fig. 1.10. Optically, SmC is biaxial with one of the axes coinciding with the director, and one along the surface normal. On the temperature scale, SmC is usually located lower than SmA.



Fig. 1.10 Molecular arrangement in SmC phase. Molecular tilt at an angle with respect to layer normal is seen

Smectic F and Smectic I phase

These phase may be thought of as tilted analogues of the HexB phase. However, with a hexagonal arrangement within smectic planes, the molecules can tilt along two distinct

directions with respect to the hexagonal lattice. In the HexF phase, the tilt is in a direction perpendicular to the slides of the hexagon. If molecules tilt towards the corner, it is known as HexI phase. HexI phase is always the higher temperature phase. The molecular arrangement in these phase are shown in Fig. 1.11.

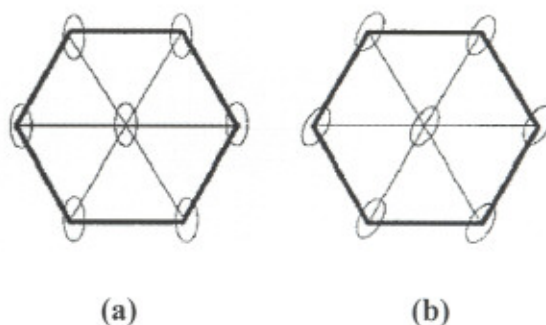


Fig. 1.11 Schematic representation of tilted phases (a) hexatic smectic F (b) hexatic smectic I. Major axis of the ellipse indicates the molecular tilt direction with respect to the hexagon axes.

Crystal G and crystal J phases

The crystal G and crystal J phases are the phases normally obtained at temperatures lower than the HexF and HexI phases. In these phases the molecules are tilted with respect to the layer normal by approximately 25 to 30°. The local order is hexagonal which is distorted due to molecular tilt, with molecules having rotational freedom comparable to the untilted crystal B phase.

Crystal H and crystal K phase

The crystalline H and K phases are tilted versions of the crystal E phase. The molecules in the crystalline H and K phase are tilted in a manner similar to the crystal G and J and (HexI) phases, i.e. along the direction perpendicular to a side (towards a corner) of the underlying hexagonal structure. The general sequence of tilted phases with decreasing temperature is shown in Fig. 1.12. Fig. 1.13 shows the view of smectic phases.

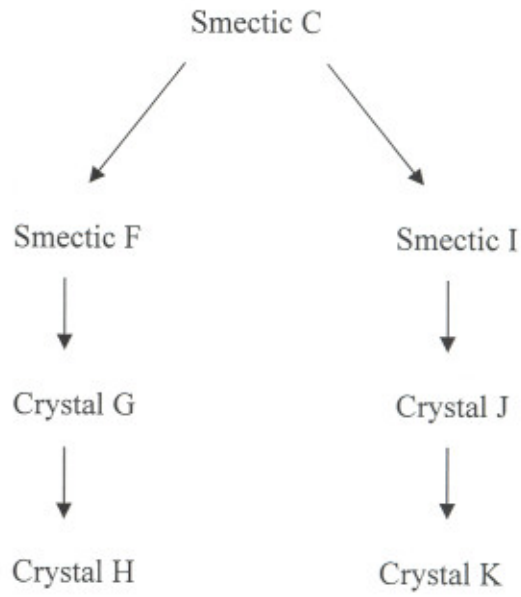
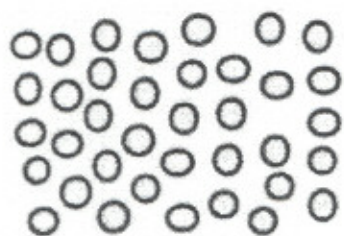


Fig. 1.12 A typical phase sequence of tilted phases

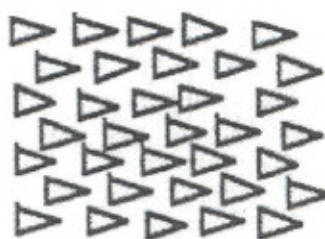
25-12-05

Non tilted phases

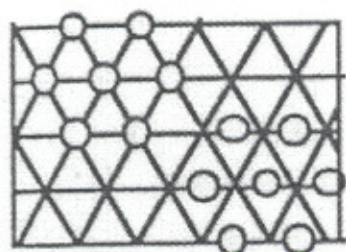
Tilted phases



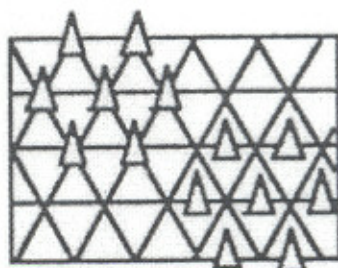
Smectic A



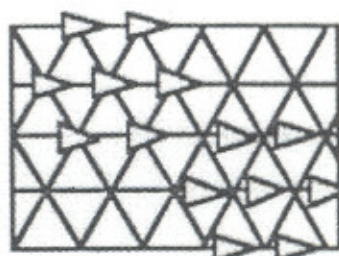
Smectic C



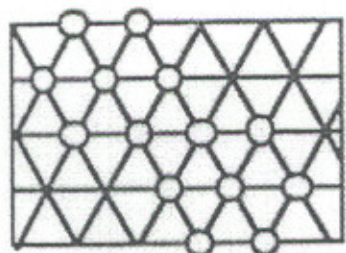
Smectic B



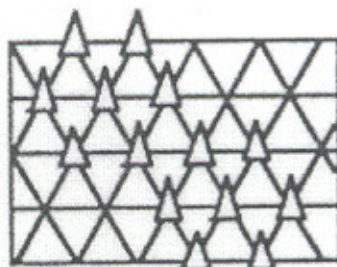
Smectic F



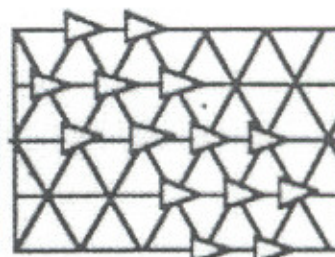
Smectic I



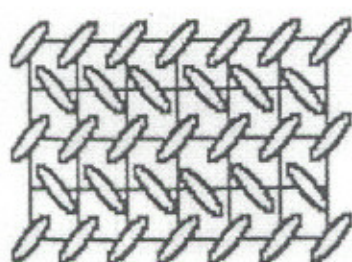
Crystal B



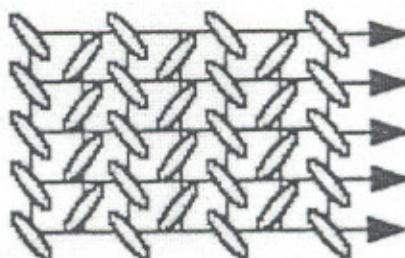
Crystal G



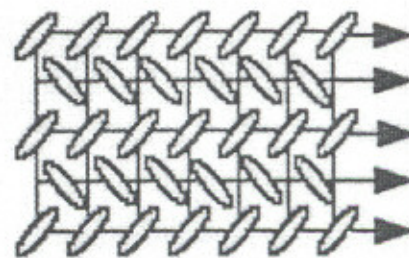
Crystal J



Crystal E



Crystal H



Crystal K

Fig. 1.13 Plan view of different smectic phases

1.1.3.3 Chiral phases

Chiral based liquid crystalline phases show lower symmetry and are thus not identical to their mirror image. Such materials exhibit unusual properties and wide range of applications [3-4].

Cholesteric or chiral nematic phase

This phase can be generated by adding a small amount of chiral molecules to nematic materials. These chiral molecules produce intermolecular forces that favour alignment between molecules at a slight angle with respect to one another. This leads to the formation of a structure similar to thin 2-D nematic like layers with the director in each layer twisted with respect to those above and below. Helix pitch is an important characteristic of this phase. The helical pitch controls the selective reflections of the cholesteric phase and makes them suitable for electro-optic display devices. It is represented by N^* and the arrangement of molecules is shown in Fig. 1.14.

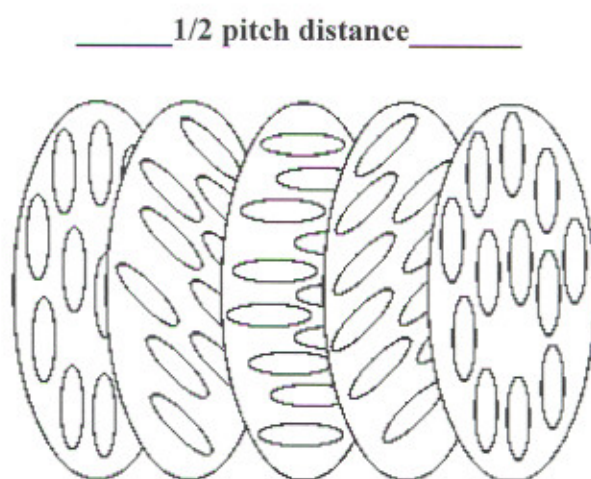


Fig. 1.14 Rotation of director in a helical arrangement about the layer normal in a cholesteric liquid crystal

Chiral smectic phases (SmC*)

Smectic phases where long axis of molecule is tilted at an angle with respect to the layer normal, as in SmC phase, can form different helical structures. In these phases the director rotates from layer to layer through a change in tilt direction and describes a helix [Fig. 1.15]. These phases are denoted by SmC*.



Fig. 1.15 Helix formation in chiral smectic C phase

1.1.3.4 Other liquid crystalline phases

(i) Blue phase

Blue phases (BP) are exhibited by the liquid crystal materials usually of short pitch ($< 700\text{nm}$) and highly chiral character observed in narrow temperature range between chiral nematic and isotropic liquid phase [9,10]. Blue phases are isotropic in nature and have three-dimensional distribution of helical director axes leading to frustrated with cubic symmetry and lattice constant of the wavelength of visible light. The three stable blue phases are referred as blue phase I (BPI), blue phase II (BP II) and blue phase III (BP III) respectively in that order with increasing temperature. BPI and BP II exhibits three-dimensional periodic structure, however highest temperature phase BP III appears to be amorphous. Several other BPs phases of different cubic symmetry exist but only in the presence of external electric field. Fig. 1.16(a, b) shows platelet texture and typical cubic lattice formed by double twist cylinders as possible model of blue phase respectively.

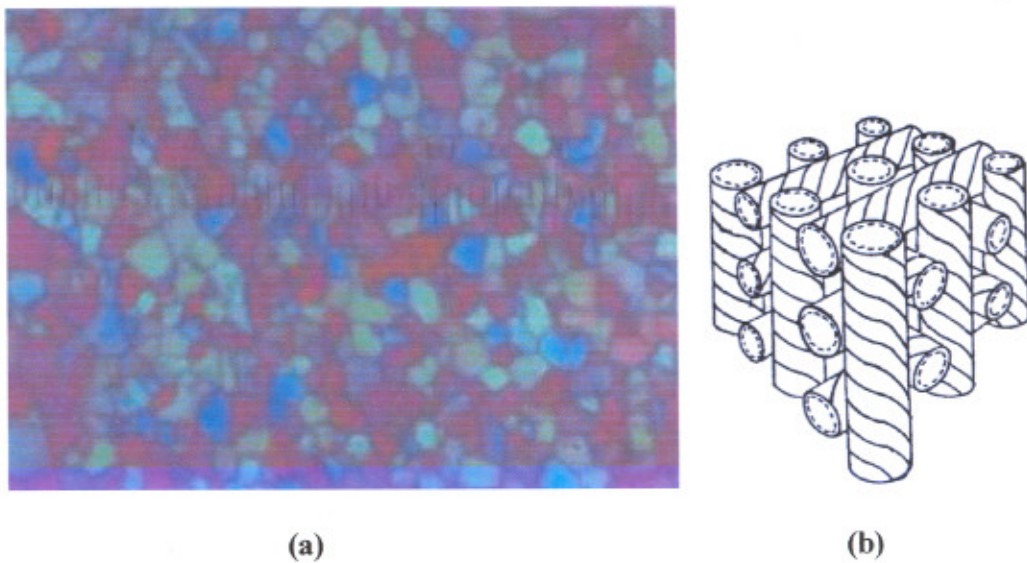


Fig. 1.16 (a) Platelet texture of blue phase (b) cubic lattice formed by double twist cylinders as a possible model of a BP

(ii) Twist grain boundary mesophase

Twist grain boundary (TGB) phases are frustrated defect phases, which can be observed in often only at narrow temperature intervals between the cholesteric and the SmA^* phase or between SmA and isotropic phase of highly chiral liquid crystals. TGBA phase are first predicted theoretically by Renn and Lubensky [11,12] and experimentally by Goodby et al. [13-15]. These phases exhibit simultaneously a helical twist and block of smectic layering. The twist grain boundary phase is formed when the layers of a smectic A phase are forced to twist by the presence of chiral molecules. The system accommodates the conflicting demands of constant layer spacing and a net twist by breaking up (Fig. 1.17) into a sequence of blocks, each with intact layers and no twist, but each rotated by a fixed angle relative to its neighbouring blocks. The interface between adjacent blocks is a twist grain boundary. Depending on the character of the smectic blocks (SmA^* , SmC , SmC^*), TGBA*, TGBC and TGBC* phases are predicted. For the existence of these phases molecule should have strong molecular chirality (i.e. a very tight pitch and a high enantiomeric excess). Planar twist grain boundary TGBA* phase is shown in Fig. 1.18 in which TGBA* helix axis is perpendicular to the substrate plane, i.e. out of the plane of the image.

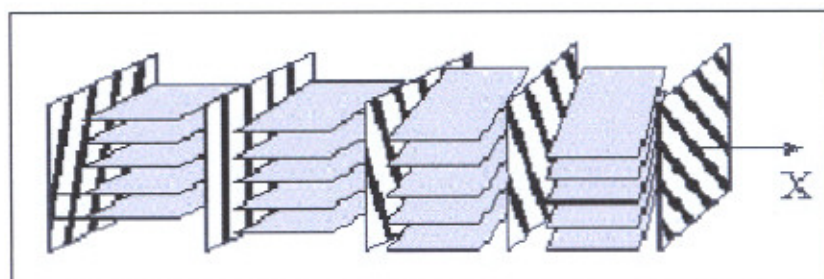


Fig. 1.17 A sequence of twisting of smectic blocks in TGBA phase

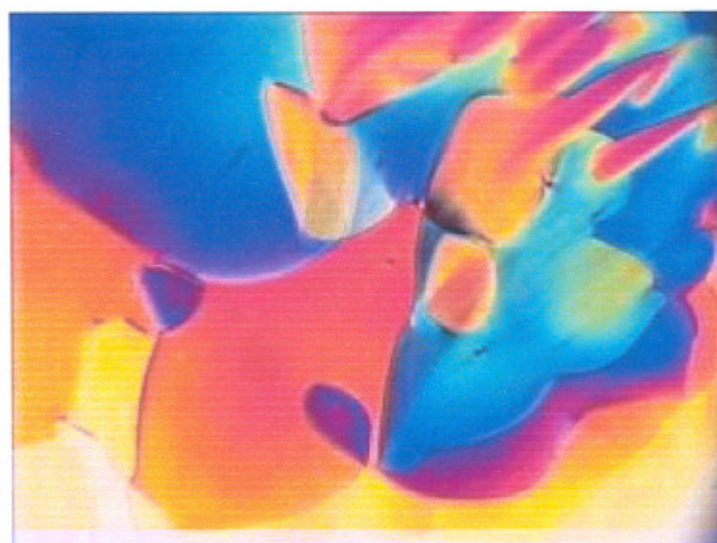


Fig. 1.18 Planar twist grain boundary TGBA* phase

(iii) Banana-shaped or bent-core liquid crystals

In recent years lot of emphasis has been given to understanding the structure and properties of banana shaped liquid crystal compounds. These are achiral, but the special molecular packing induces chirality into the smectic layers [16]. These organic molecules due to their bent core or V shape are called ‘bananas’. Bend core molecules basically consists of a V-shaped core and alkyl tags at the two ends of the V-bend.

Different phases were observed for this new form of mesophase, and referred as B1, B2, B3, B4, B5, B6 and B7. (B3 and B4 are known to be crystalline phases) [17,18]. Recently it has been reported that the smectic phase of achiral banana –shaped molecular systems could form helical superstructures [19]. Matsunaga and co-workers synthesized some banana materials and found that they can form smectic LCs but they did not pay any

attention to the electrical properties [20,21]. Watanabe et al. reported that a ferroelectric smectic phase with C_{2v} symmetry might be formed for some chain types of LC polymers, if two different aliphatic spacers with odd numbers of carbons are incorporated into the backbone in regularly alternating fashion and they segregate into different monodomains. They prepared homologous series of banana shaped molecules, which form the SmA_b , $HexB_b$ and smectic blue phase in order of decreasing temperature, and then discovered the ferroelectricity in the SmA_b and $HexB_b$ phases. They reported spontaneous polarization more than 150 nC/cm^2 even in the higher order smectic phase below the SmA_b phase, and concluded that this phase is also ferroelectric. A typical micro texture of banana shaped molecule is shown in Fig. 1.19.

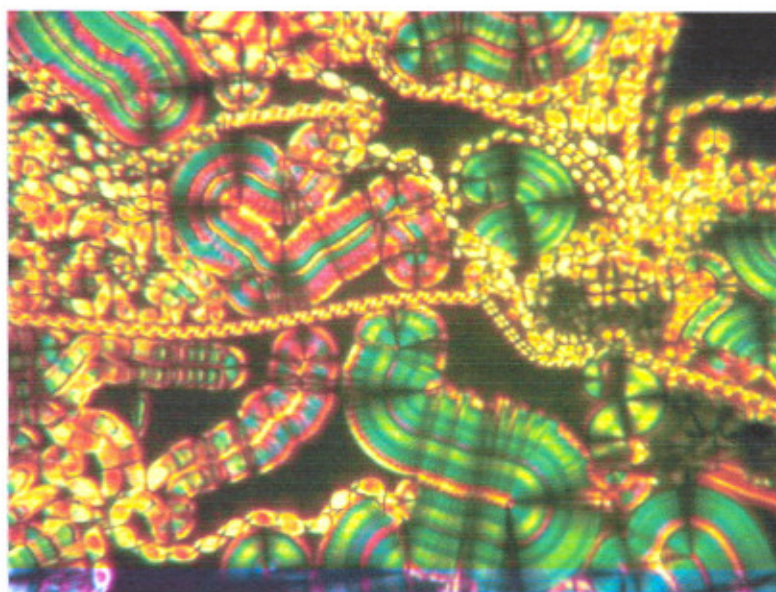


Fig. 1.19 Micro-texture of banana shaped molecule

1.1.4 Physical properties of liquid crystal

1.1.4.1 Anisotropy

Liquid crystals are anisotropic in nature due to the presence of small degree of order among their molecules. This property distinguishes them from ordinary liquids (which are isotropic in nature).

The optical anisotropy can be explained by a typical example of birefringence as illustrated in Fig. 1.20 where an electromagnetic wave pass through the nematic LC sample and the outgoing light gets bifurcate into two rays of different path and wavelength called ordinary (O-ray) and extraordinary ray (e-ray).

The optical anisotropy is determined by $\Delta n = n_{\parallel} - n_{\perp}$.

Where n_{\parallel} and n_{\perp} gives the indices of refraction in the direction parallel and perpendicular to the nematic axis respectively. If Δn is positive then material is said to be positive uniaxial LC and if negative then materials is said to be negative uniaxial.

The effect of electric field gives rise to dielectric anisotropy in these systems. It is given by

$$\Delta \epsilon = \epsilon_{\parallel} - \epsilon_{\perp}$$

where ϵ_{\parallel} and ϵ_{\perp} refer to the dielectric constant parallel and perpendicular to the nematic axis respectively. The response of nematics to an electric field depends upon both the sign and magnitude of $\Delta \epsilon$. If $\Delta \epsilon$ is positive, lowest energy state in the presence of field will be that in which the nematic axis is parallel to field and for negative value of $\Delta \epsilon$ the lowest energy state will be the one in which the nematic axis is perpendicular to the field [2].

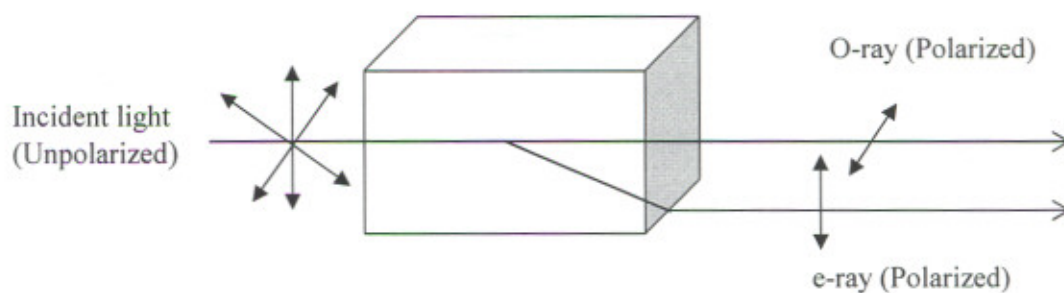


Fig. 1.20 Bifurcation of incident light into an ordinary and extraordinary rays due to the anisotropy in a birefringent liquid crystal

1.1.4.2 Liquid crystal alignment

Surface alignment is necessary for maximizing the contrast of the display so that the orientation of the molecules is same throughout the liquid crystal sample whether the field is off or on. In the liquid crystal sample, various kinds of molecular alignment can

be induced by treating the supporting substrate differently. Depending on the pre-treatment of the substrate, the optic axis of the LC molecules may be oriented either parallel (homogenous) or perpendicular (homeotropic) to the surface of the substrate. If the substrate is covered with a thin film of amphiphilic molecules, which deposit their polar end to the substrate, liquid crystal molecules will be aligned such that the director is perpendicular to the supporting substrates. This configuration is called homeotropic alignment. If the supporting substrate is applied with a thin layer of polymer stretched in one direction by rubbing with a nylon cloth, the liquid crystal molecules will be aligned such that the director is parallel to the supporting substrates in the direction of the rubbing. This configuration is named as homogenous or planar alignment. These two configurations are illustrated in Fig. 1.21. Other sample geometries such as twisted and super twisted alignments are often employed in display applications.

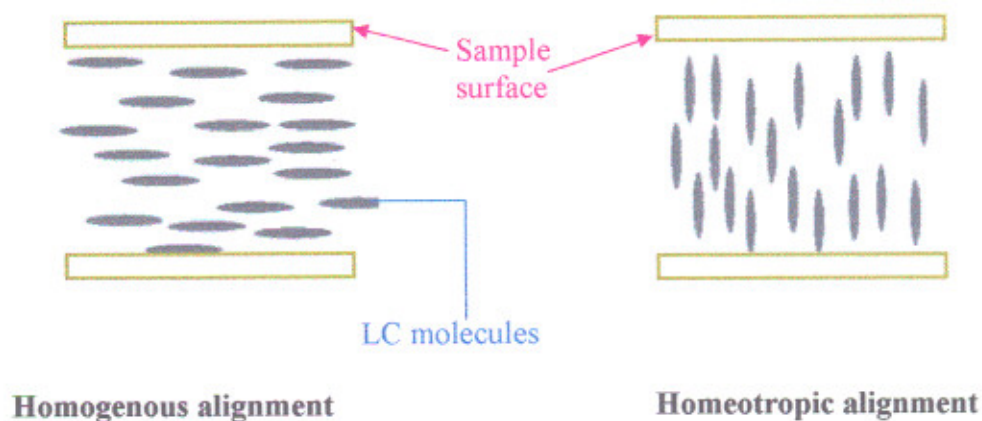


Fig. 1.21 Alignment in liquid crystal: (a) homogenous (b) homeotropic

1.2 Polymer/liquid crystal dispersed systems

Polymer/liquid crystal composites have been studied intensively because of their fundamental importance and applications. They can be fabricated into different categories of systems depending on the preparation conditions, concentration of polymer which can be as large as 70% or as small as 2%. These are characterized as:

1.2.1 Polymer dispersed liquid crystals (PDLCs)

In the recent years a great scientific interest has grown in polymer dispersed liquid Crystals (PDLCs), a new class of composite materials both from a basic and as well as application point of view [22-25]. In their most common form they essentially consist of micron or sub-micron size droplets of low molecular weight liquid crystal randomly dispersed in transparent polymer matrix [25]. A typical dispersion for nematic liquid crystal in polymer matrix is shown in Fig. 1.22.

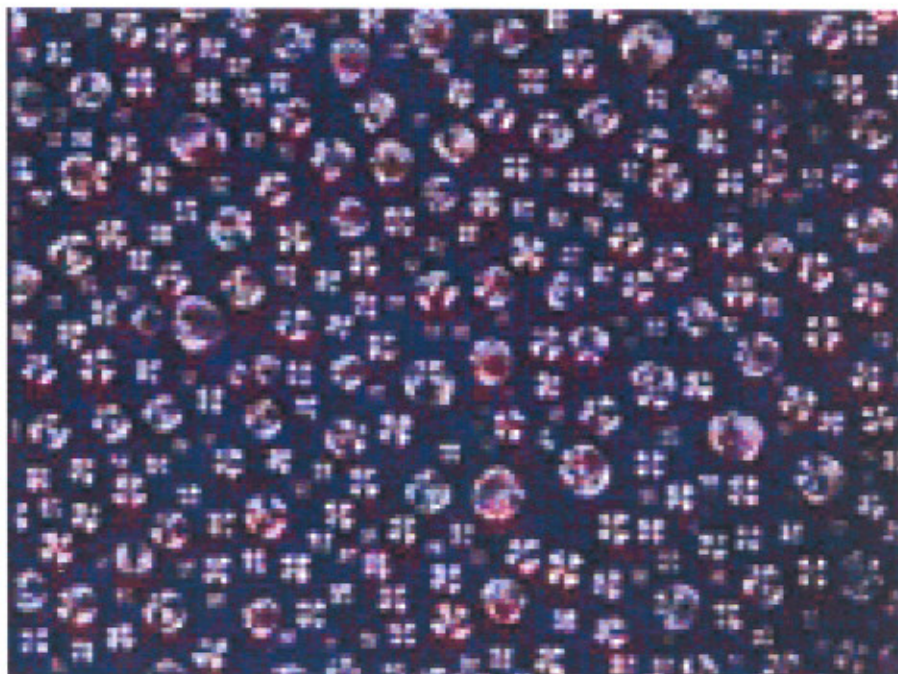


Fig. 1.22 Dispersed liquid crystal droplets in polymer matrix

They are likely to be one of the most potential candidates for the fabrications of flexible, large-scale displays, for outdoor applications area, switchable windows, holographic grating and other light shutter devices [23-26]. They have some advantage over conventional twisted nematic (TN) liquid crystal displays and super twisted nematic (STN) liquid crystal displays in that we can make large area flexible, high contrast ratio displays devices without using the polarizers. These PDLCs films can be switched from

optical response is based on the electrically controlled light scattering properties of the droplets [25-27].

In the absence of an external electric field, the director orientation of liquid crystal droplets varies randomly from droplet to droplet. In this case LC refractive indices $n_{||}$ and n_{\perp} i.e. extra ordinary (n_e) and ordinary (n_o) refractive indices are different from polymer refractive index (n_p) and produce a strong light scattering that makes the sample translucent white appearance (opaque state). While in the presence of sufficient amount of external electric field the molecules of LC droplet collectively reorients with their direction parallel to applied electric field and sample appears transparent. The transparency in the film appears due to the matching of the refractive indices of liquid crystal (n_o) to polymer (n_p) i.e. $n_o \sim n_p$. Refractive indices of liquid crystal in parallel or perpendicular to the director is shown in Fig. 1.23.

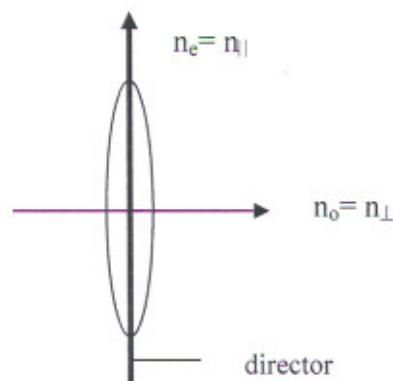


Fig. 1.23 Refractive indices of liquid crystal molecule parallel or perpendicular to director, n_e = extra ordinary refractive index and n_o = ordinary refractive index

Fig.1. 24 shows the LC droplet orientation dispersed in polymer matrix in opaque and transparent state. The applied electric field aligns the nematic liquid crystal droplets to non-scattering state or transparent state. The competition between the applied field and the elastic and viscous torque of the liquid crystal governs the response and switching times of such films.

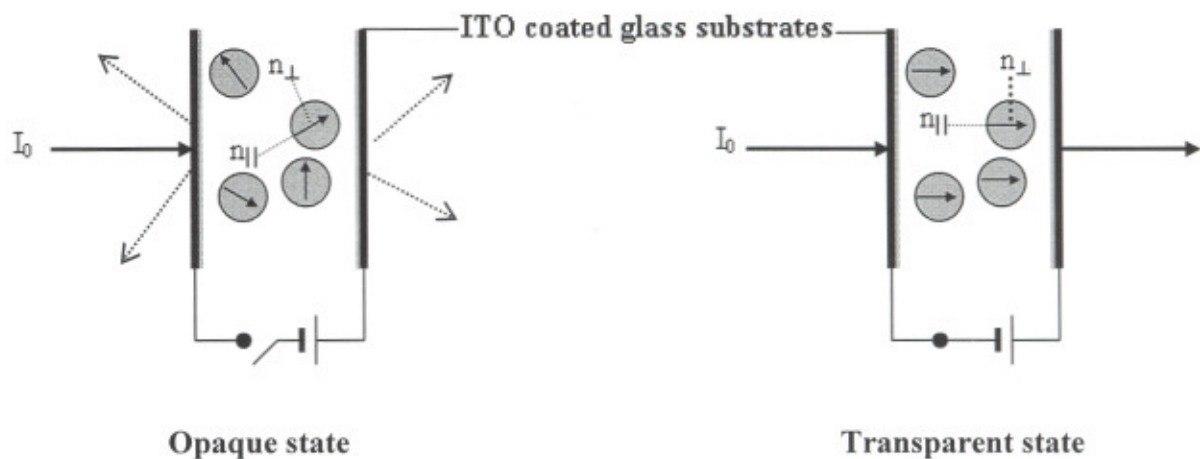


Fig. 1.24 Operation principle of PDLC film in (a) opaque state (b) transparent state

The transparent condition in the film arises when the applied voltage creates an electric field, which aligns the LC droplets such that their refractive index (nearly matches to that of the polymer), substantially reducing the scattering power of the droplets. Upon removal of the voltage, the droplets return to their original scattering orientation. The light scattering properties state is dependent on the optical heterogeneities in the composite film, such as spatial distortion of the nematic director and mismatching in refractive indices of the components. The electro-optical properties of PDLC displays depend on LC concentration, film thickness, size and shape of liquid crystal droplets, anchoring energy on the boundary surface, and physical properties of both components, e.g. elasticity and viscosity parameters, dielectric anisotropy of liquid crystal, and resistivities and refractive index ratios of the liquid crystal and polymer.

1.2.1.1 Preparation methods of PDLC films

Polymer dispersed liquid crystals are usually produced in two distinct ways: encapsulation and phase separation, each method produces PDLCs with different properties and characteristics.

(a) Encapsulation (NCAP)

Early attempts to produce PDLCs were made with a technique known as micro encapsulation. Micro encapsulation is a technique that has been applied to obtain small capsules of drug release, of food products and even of cholesteric liquid crystals in temperature indicating devices. In this method, a liquid crystal is mixed with a polymer dissolved in water. When the water is evaporated, the liquid crystal is surrounded by a layer of polymers. A cross section of PDLC film formed by this method is shown in Fig. 1.25. Thousands of these tiny capsules are produced and distributed through the bulk polymer. Droplets with this method tend to be non-uniform in size and can even be interconnected with each other. Materials manufactured by encapsulation are referred to as 'nematic curvilinear aligned phase' (NCAP) [28-29].

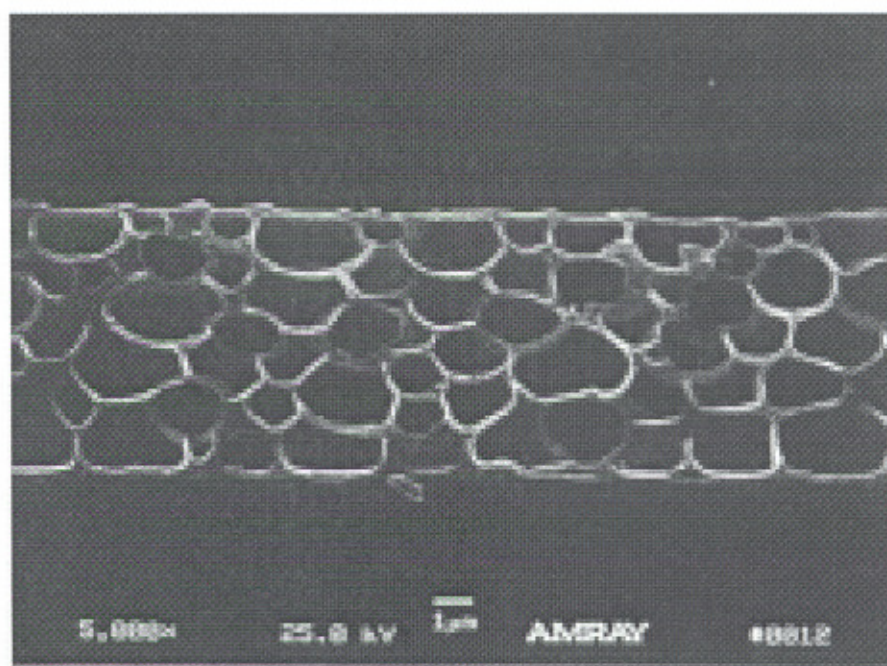


Fig. 1.25 A PDLC film formed by encapsulation method

(b) Phase separation

In order to obtain PDLC by phase separation, a homogenous mixture of polymer (prepolymer) and liquid crystal is first produced. The liquid crystal droplets are then formed by the separation of the two phases. The phase separation can take place in one of the following three ways.

(i) **Polymerization induced phase separation (PIPS)**

Polymerization induced phase separation (PIPS) occur when a liquid crystal is mixed with a solution that has not undergone polymerization (a pre-polymer). This technique is useful when, pre-polymer materials are miscible with the low molecular weight liquid crystal compounds [24,25,30,31]. Once a homogenous solution is formed, the polymerization reaction is initiated either thermally (thermoset polymer) or optically (photo-curable polymer). As the reaction progresses, the liquid crystal molecules come out of solution and begin to form micro droplets. The droplets grow until the polymer binder becomes solid enough that the molecules are trapped and can no longer move easily. The complete PIPS process is illustrated by line diagram in Fig. 1.26. The two main factors that influence the size of liquid crystal droplets in PIPS method are the cure temperature and the type and proportions of materials used. The cure rate affects the speed of polymerization as well as the diffusion rate and solubility of the liquid crystal in the polymer. These factors can greatly influence the size of the liquid crystal droplets, which translates into different macroscopic optical properties.

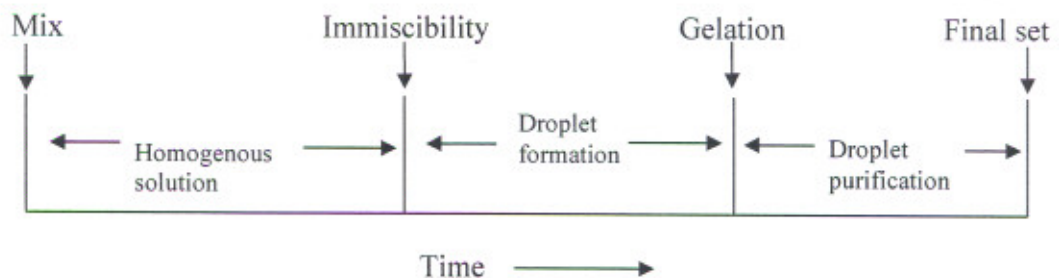


Fig. 1.26 Evolution of a PDLC material through phase separation

(ii) **Thermally induced phase separation (TIPS)**

Thermally induced phase separation (TIPS) can be used when the polymer binder has a melting temperature below its decomposition temperature. In this method, a homogenous mixture of liquid crystal and a melted polymer is formed. The solution is cooled at a specific rate to induce the phase separation. Liquid crystal droplets begin to form as the polymer hardens. The droplet continues to grow until the glass transition temperature of the polymer is crossed.

In this method, droplet morphology and droplet size is affected the most by the cooling rate of polymer melt/liquid crystal solution. Fast cooling rates tend to produce small droplets because there is not sufficient time for large particles to form. Therefore, droplet size and cooling rate are relatively inverse to each other.

(iii) Solvent induced phase separation (SIPS)

Solvent induced phase separation (SIPS) is useful with thermoplastics, which melt above the decomposition temperature of the thermoplastic or the liquid crystal, or where solvent coating techniques are used. The liquid crystal and polymer are dissolved in a common solvent, forming a homogenous solution. The solvent is then removed by evaporation, resulting in phase separation and polymer solidification. The LC droplets come out of solution and start growing until all the solvent removed from the solution. In this case droplet size is dependent on the rate of solvent removal.

Apart from these two methods PDLC film can also be prepared by imbibing porous structures with liquid crystal, glass-dispersed systems and dispersed silica systems. To date these alternative schemes have not been seen in widespread application.

1.2.2 Phase separated composite films (PSCOF)

Recently it has been seen that cells can be prepared by containing a very thin layers of liquid crystal in contact with a thin layer of polymer. This system is referred as phase separated composite films. The technique used to construct the PSCOF structure is essentially same as that used for making PDLC samples [32-33]. It is a joint effect of strong light absorption, slow polymerisation, phase separation, and fast diffusion of small molecules. In this method one of the plastic substrates or glass substrates is spin coated with a thin layer of polymer (such as polyvinyl alcohol) and then rubbed to force LC alignment. The plates are separated by a spacer layer (commonly glass beads). The prepolymer and liquid crystal are mixed at same ratio and phase separation is initiated by exposure to UV light. The mechanism responsible for the formation of PSCOF is non-uniform polymerisation. The LC molecules absorb UV light more strongly in the mixture. As a result, an intensity gradient is produced in the sample. Thus, prepolymer molecules first undergo polymerization near irradiated surface and then the LC molecules expelled out from the polymerised volume. The phase separation results in a solidified film of

polymer on the substrate close to the UV source and the liquid crystal between the polymer film and the second substrate. The LC acquires a homogenous alignment on the rubbed polymer layer. PSCOF method has a number of advantages as:

Simple fabrication process and unique structure, easy control of LC cell thickness, mechanical, ruggedness and flexibility and deal method for active matrix LC devices etc.

1.2.3 Liquid crystal dispersed polymer (LCDP)

Liquid crystal dispersed polymer (LCDP) or some times called liquid crystal/gel dispersions systems are those, in which a small amount of polymer is dispersed in a continuous liquid crystal matrix [34-37]. In these composites polymer makes some kind of network structure, which aligns the liquid crystal molecules. In these systems no LC droplets are formed. Here the matching of refractive indexes is not important as in the case of PDLC due to small polymer concentration.

The alignment can be altered by external fields, so these systems can also be used for light shutters.

1.2.4 Polymer stabilized liquid crystal (PSLC)

Polymer stabilized liquid crystal (PSLC) consists a small amount of polymer (typically less than 5 wt%) in a liquid crystal matrix to form a polymer network [38]. Most PSLC and PDLC systems studied to date involve nematic or cholesteric liquid crystals and despite their versatility and potential applications, their usefulness is limited by the relatively slow response time of these liquid crystals. Due to short time of switching ferroelectric liquid crystals are likely candidates to improve upon existing technology, as they may exhibit response times up to 500,000 times faster than nematic based systems.

These composite can be divided into three groups as:

(i) Surface stabilized ferroelectric liquid crystal (SSFLC)

Surface stabilized ferroelectric liquid crystal (SSFLC) composite device is prepared by mixing a small amount of polymer (< 3 wt%) with the ferroelectric liquid crystal (FLC) materials between ITO coated rubbed glass substrates. Sakaigawa et al. [39] have investigated the combination of the FLC material and the polymer which provides the stripe domain distribution as shown in Fig. 1.27. The most important feature is the phase

separation of dispersed polymer from FLC mixture in the nematic phase and the following realignment process at the smectic phase. Thus the micro-scale phase separated polymer aligns along the smectic layer. When the polymer is separated randomly from the nematic phase, it will be aligned along the smectic layer in the smectic phase, by cooling from the nematic phase.

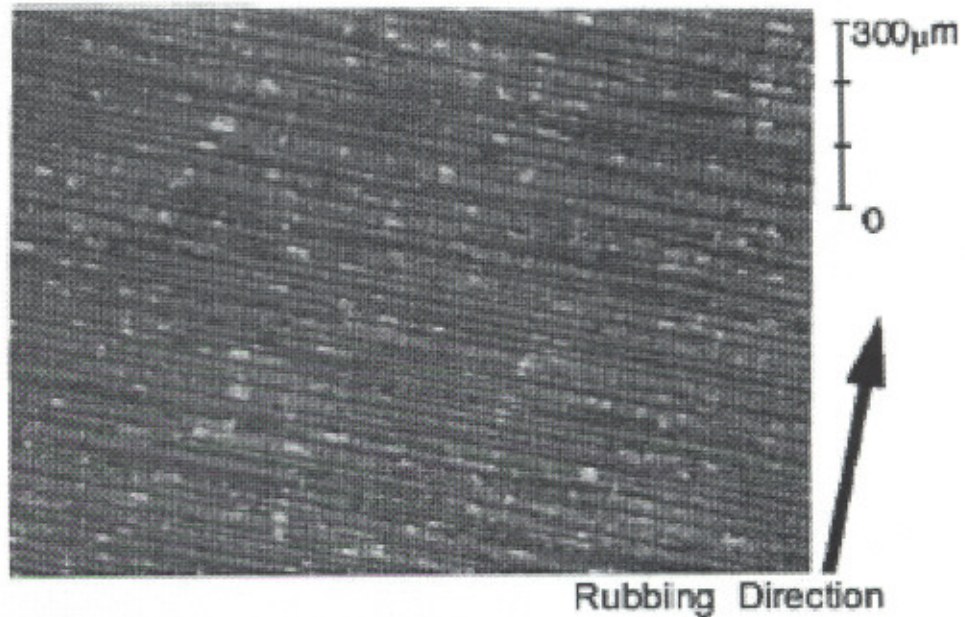


Fig. 1.27 Typical stripe domain pattern of polymer/FLC composite under intermediate pulse field

(ii) Polymer network stabilized ferroelectric liquid crystal (PNSFLC)

Polymer network stabilized ferroelectric liquid crystals with homogenous alignment have been produced in cells without a surface alignment layer [39-40]. In this technique a crosslinkable monomer was mixed into a FLC and polymerised in a magnetic field to form a polymer network that will stabilize the alignment of the FLC. The final morphology of composite and alignment of FLC are affected by the curing temperature at which the UV curing of the sample started.

(iii) *Shear aligned polymer dispersed ferroelectric liquid crystal (SAPDFLC)*

Molsen et al. [41] have shown that thicker than in case of SSFLC devices can be fabricated using PDFLCs. The essential uniform alignment of the liquid crystal molecules is achieved by shearing the material during the phase separation that occurs between the liquid crystal and polymer during photoinduced crosslinking. The size of droplets and the quality of the alignment of the smectic layers are determined by rate of shearing, phase separation and polymerisation of the matrix.

1.2.5 Polymer/liquid crystal/dyes blends

Liquid crystals/polymer/dyes blends-color PDLC films are made by incorporation of dyes (isotropic or dichroic) in the PDLC films [42-46]. The colour contrast of PDLC film incorporating an isotropic dye is the result of the change in the path length of light passing through the film in the scattering and transparent state. The rate of absorbance of an isotropic dye in the ON and OFF states is a direct measure of the scattering efficiency of the PDLC film.

The dichroic dyes dissolved in the liquid crystal droplets produce higher color contrast than the isotropic dyes. The dichroic dye is aligned by the liquid crystal in the droplets and therefore its absorption is modulated by alignment of LC with an electric field. In the OFF state the alignment of dichroic dye varies randomly from droplet to droplet. In the ON state the droplet directors and the dichroic dye are aligned normal to the film surface. Some amount of dichroic dye dissolved in the polymer binder will be randomly aligned and unaffected by the applied electric field. Only the dye dissolved in the droplet will exhibit dichroic properties and improve the contrast of the PDLC display compared to the use of isotropic dyes.

1.3 Droplet configuration in PDLC

The configuration of the liquid crystal droplets in a polymer matrix is the focus of much current research. Many different configurations have been observed and they depend on factors such as droplet size, shape, surface anchoring and applied fields. This section will describe some of the most common configurations exists in PDLC systems.

The radial configuration occurs when the liquid crystal molecules are anchored with their long axes perpendicular to the droplet walls. If the anchoring strength is strong or droplet is larger enough, then radial structure is stable. The radial structure possesses a splay-type deformation with a point volume defect at the center topologically classified as 'hedgehog' [46]. This arrangement is shown in the Fig. 1.28(a).

The axial configuration of the liquid crystal droplets also occurs when the molecules are oriented perpendicular to the droplet wall [47]. Axial configuration is most stable when surface anchoring is weak and droplet size is sufficiently small or if there is an applied electric field E of suitable strength. This configuration creates a line defect that runs around the equator of the spherical droplet, as seen in Fig. 1.28(c). When an electric field is applied to a radial droplet, the molecules adopt the axial configuration. The radial configuration is returned when the field is removed.

The bipolar configuration is obtained when the elongated molecules of the nematic liquid crystal are anchored tangentially to the droplet wall. This structure is characterized by the presence of two point defects at the poles of the droplet and is shown in the Fig. 1.28(b). These point defects in bipolar configuration are classified as 'boojums' [48]. Boojums can exist only at the surface and cannot move into the volume of the droplet. However hedgehog can exist, either on the surface of the droplet or in its interior.

In a typical PDLC sample, there are many droplets with different configurations and orientations. When an electric field is applied, however, the molecules within the droplets align along the field and have corresponding optical properties. In the following diagram, the director orientation is represented by the black lines on the droplet. There are numerous other possible director configuration which can arise in PDLC systems depending on anchoring condition e.g. ellipsoidal, twisted bipolar droplet, escaped radial, toroidal [49,50] and axial droplet structures.

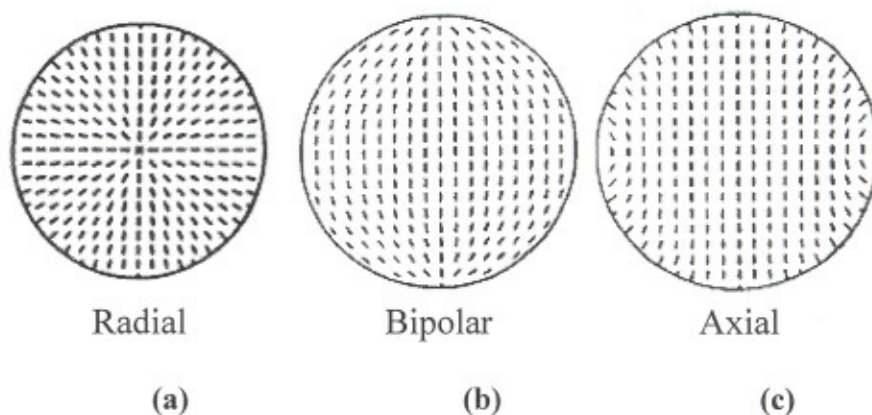


Fig. 1.28 Liquid crystal droplet configurations in PDLC systems

1.4 Dichroic PDLC

Dichroic dyes can be used in PDLC films to produce devices, which show large absorbance changes, and therefore are useful for the construction of displays. A major electro-optical effect in PDLC films is found when the films contain dichroic dyes. In dichroic dye designed for use in LCs, the dye molecule are typically long, rigid entities, and will tend to align with the director field when dissolved into a liquid crystal solvent. Dichroic dye absorbs light more along one axis than the others. Usually, the major component of the transition moment of dyes is along the long molecular axis (Plechoric) or short molecular axis (Negative dichroic or N-type). Plechoric dye (Positives dichroic or P-type) dyes [51-54] absorb the E vector of light which is directed along the long molecular axis of dye, while 'Negative dichroic' absorb the E vector of light which is directed perpendicular to the long molecular axis [52-55]. Normally, these dyes have a narrow absorption spectrum, the wavelength of maximum absorption being designed as λ_{\max} . The colour seen is basically the light, which is not absorbed by the dye. In most cases the zero field state is highly absorbing, and the application of an electric field produces a weakly-absorbing film. The presence of a dichroic dye does not seem to affect the scattering properties of PDLC films substantially. The zero field state of typical films are translucent as well as absorbing, while the high field state is transparent as well as weakly absorbing. Dichroic PDLC can be prepared by two methods:

(i) Emulsion type dichroic PDLC films

The optimal configuration for dichroic effects for PDLC films is a system where dye has low solubility in polymer matrix, is oriented randomly within the film plane in the high absorbance state, and is oriented perpendicular to the film plane in the low absorbance state [38]. These conditions can be readily achieved for films constructed using this method.

(ii) Phase separated type dichroic PDLC films

The dichroic PDLC film formed by phase separation methods is not as advantageous as it for emulsion based film. First, the dye and polymer begin as a single homogenous phase [38]. When the system phase separates into droplets and a polymer matrix, substantial amounts of dye and liquid crystal can be left behind into the polymer. Dye dissolved in polymer matrix is no longer able to change its orientation in response to an electric field. A second difference between emulsion-based and phase separation based films are the average orientation of the nematic droplets. Even if both types of films form bipolar droplets, phase separated films tend to form droplets with a random 3 dimensional distribution of symmetry axes, compared to a random two dimensional distribution of symmetry axes, in the emulsion case.

The usefulness of the dichroic dyes in displays devices is determined by the following properties [51-53,56].

- The chemical and photochemical stability of the dye
- The color or hue (λ_{\max} , wavelength of maximum absorption or emission)
- Extinction coefficients
- Dichroic ratio [56]
- Order parameter of dye [56]
- Non-ionic nature
- The solubility of dye in host
- Influence of dye on the viscosity of the host [52-53]
- The purity and high resistivities

- The compatibility of dye with the host, which is usually determined by its order parameter, solubility, viscosity, and the absence of chemical reaction with the host.

1.5 Aim of this research work

Several researchers and technologists did quite significant research work to understand the material properties of liquid crystal dispersion in polymer matrix. We noticed that there were still some unanswered questions and few gaps in understanding the nature of droplet morphology and process of phase separation in these systems under the influence of electric field. Thus an attempt was made to consider the appropriate combination of liquid crystal and polymer material which would enhance the optical transmission considering the proper droplet morphology, their electrical and electro-optic characteristics. For this purpose, low molar mass nematic and ferroelectric liquid crystal mixtures were dispersed in the polymer matrix (optical adhesive) to study their behaviour in detail. Understanding the influence of anthraquinone dye on the optical characteristics of polymer dispersed nematic liquid crystal films was also one of the objectives of this work.

The clear understanding and scientific curiosity to investigate the properties of this soft condensed matter was the main motivation to carry out this experimental work.

REFERENCES

- [1] P. J. Colling, *Liquid Crystal: Nature's Delicate Phase of Matter*, Princeton: University Press (1990)
- [2] P. J. Colling and M. Hird, *Introduction to Liquid Crystal: Chemistry and Physics*, Taylor and Francis Ltd (1997)
- [3] P. G. De Gennes, *The Physics of Liquid Crystal*: Oxford University Press (1975)
- [4] S. Chandrasekhar, *Liquid Crystal 2nd Edn.* Cambridge: Cambridge University Press (1992)
- [5] A. Cifferi, W. R. Krigbaum, R. B. Meyer, *Polymer Liquid Crystals*, Academic Press: Network (1982)
- [6] C. B. Mcardle, *Side Chain Liquid Crystal Polymer*, Champan and Hall: Newyork (1989)
- [7] B. M. Mulder, *Liq. Cryst.*, **1** (1986) 539
- [8] B. R. Acharya, A. Primak and S. Kumar, *Phys. Rev. Lett.*, **92** (2004) 145506
- [9] D. C. Wright and N. D. Mermin, *Rev. Mod. Phys.*, **61** (1989) 385
- [10] Basic term relating to low –molar mass and polymer liquid crystals, IUPAC, *Pure and Appl. Chem.*, **73** (2001) 845
- [11] S. R. Renn and T.C. Lubensky, *Phys. Rev. A.*, **38** (1988) 2132
- [12] T. C. Lubensky and S. R. Renn, *Phys. Rev. A.*, **41** (1990) 4392
- [13] J. W. Goodby, M. A. Waugh, S. M. Stein, E. Chin, R. Pindak and J. Patel, *Nature*, **337** (1989) 449
- [14] K. J. Ihn, J. A. N. Zasadzinski, R. Pindak, A. J. Slaney, and J. Goodby, *Science*, **258** (1992) 275
- [15] J. W. Goodby, I. Nishiyama, A. J. Slaney, C. J. Booth, and K. J. Toyne, *Liq. Cryst.*, **14** (1993) 37
- [16] A. Jakli, M. Muller, D. Kruerke and G. Heppke, *Liq. Cryst.*, **24** (1998) 467
- [17] G. Pelzl, S. Diele, and W. Weissflog, *Advanced Materials*, **11** (1999) 707
- [18] W. Weissflog, H. Nadasi, U. Dunemann, G. Pelzl, S. Diele, A. Eremin, and H. Kresse, *J. Mater. Chem.*, **11** (2001) 2748

- [19] C. K. Lee, A. Primak, A. Jakli, E. J. Choi, W. C. Zin, and L. C. Chien, *Liq. Cryst.*, **28** (2001) 1293
- [20] H. R. Brand, P. E. Cladis and H. Pleiner, *Eur. Phys. J. B*, **6** (1998) 347
- [21] W. Helfrich, *Phys. Rev. Lett.*, **24** (1970) 201
- [22] B. G. Wu, J. L. West and J. W. Doane, *J. Appl. Phys.*, **62** (1987) 3925
- [23] J. W. Doane, A. Golemme, J. L. West, J. B. Whitehead and B. G. Wu., *Mol. Cryst. Liq. Cryst.*, **165** (1988) 511
- [24] P. S. Drazic, *Liquid Crystal Dispersion*, World Scientific, Singapore (1995)
- [25] P. S. Drazic, N. A. Vaz, B. G. Wu and S. Zumer, *Appl. Phys. Lett.*, **48** (1986) 269
- [26] P. S. Drazic, *J. Appl. Phys.*, **60** (1986) 2142
- [27] F. Simoni, *Non linear Optical Properties of LC & PDLC*, World Scientific, Singapore (1997)
- [28] J. L. Ferguson, *SID Digest*, (1985) 68
- [29] J. L. Ferguson, US Patent 4, **435** (1984) 047
- [30] J. L. West, *Mol. Cryst. Liq. Cryst.*, **157** (1998) 427
- [31] N. A. Vaz, G. W. Smith and G. P. Montgomery, Jr., *Mol. Cryst. Liq. Cryst.*, **146** (1987) 17
- [32] V. Vorflusev and S. Kumar, *Science*, **283** (1999) 1903
- [33] T. Qian, J. H. Kim, S. Kumar and P. Taylor, *Phys. Rev. E.*, **61** (2000) 4
- [34] A. Jakli, *Mol. Cryst. Liq. Cryst.*, **251** (1994) 289
- [35] R. A. M. Hikmet, *Liq. Cryst.*, **9** (1991) 3
- [36] R. Stannarius, G. P. Crawford, L. C. Chien and J. W. Doane, *J. Appl. Phys.*, **70** (1991) 135
- [37] R. A. M. Hikmet and J. A. Higgins, *Liq. Cryst.*, **12** (1992) 831
- [38] P. S. Drazic, *Liquid Crystal Dispersion*, World Scientific, Singapore (1995)
- [39] A. Sakaigawa, T. Sako and M. Kodan, *Mol. Cryst. Liq. Cryst.*, **328** (1999) 201
- [40] W. Zheng and G. H. Milburn, *Liq. Cryst.*, **27** (2000) 1423
- [41] H. Molsen and H. S. Kitzerow, *J. Appl. Phys.*, **75** (1994) 710
- [42] G. Cipparrone, A. Mazzulla, P. Pagliusi, A. V. Sukhov and R. F. Ushakov, *J. Opt. Am*, **18** (2001) 182

- [43] J. Wu, C. M. Wang, W. Y. Li and S. H. Chen, *Jpn. J. Appl. Phys.*, Part 1, **37** (1998) 6434
- [44] P. S. Drzaic, R. Wiley and J. McCoy, *Proc SPIE – Int. Soc. Opt. Engg.*, **1080** (1989) 41
- [45] D. Higgins, X. Liao, J. Hall and E. Mei, *J. Phys. Chem B.*, **105** (2001) 5874
- [46] G. E. Volovik and O. D. Laurentovich, *Zh. Eksp. Teor. Fiz.*, **85** (1983) 1997 [*Sov. Phys. JETP*, **58** (1983) 1159]
- [47] J. H. Erdmann, S. Zumer, and J. W. Doane, *Phys. Rev. Lett.*, **64** (1990) 1907
- [48] J. W. Doane, *MRS Bulletin*, **16** (1991) 22
- [49] G. H. Springer and D. A. Higgins, *J. Acc. Chem. Soc.*, **122** (2000) 6801
- [50] D. A. Higgins, J. E. Hali and A. Xie, *J. Acc. Chem. Soc.*, **38** (2005) 137
- [51] B. Bahadur, *Mol. Cryst. Liq. Cryst.*, **209** (1991) 39
- [52] B. Bahadur, *Liquid Crystal -Applications and Uses*, Vol.3 (Ed.: B. Bahadur), World Scientific, Singapore, (1992)
- [53] H. V. Ivashchenko and V. G. Romyantsev, *Mol. Cryst. Liq. Cryst.*, **150A**, **1** (1987)
- [54] Literature on Dichroic dyes, mixtures and hosts from BDH (England), E. Merck (Germany), Hoffman La Roche (Switzerland) Mitsui (Japan)
- [55] G. Pelzl, H. Zschke and D. Demus, *Displays*, **141** (1985)
- [56] B. Bahadur R. K. Sarna and V. G. Bhide, *Mol. Cryst. Liq. Cryst.*, **75** (1981) 121

Chapter -2

Experimental

Overview

This chapter describes the experimental design and characterization techniques to study the various polymer dispersed liquid crystal sample cells and their physical parameters. Thermal polarizing microscopy has been used to investigate the optical textures under different condition of sample preparation and temperatures.

We also describe criteria for selection of materials, description of instruments and their characterization of physical properties of materials.

2.1 Selection of materials

A variety of materials have been investigated to study the optical and electro-optical properties of liquid crystal systems. The selection of materials plays an important role on the performance of PDLC devices. The selections of materials in the present study has been carried out on the basis of their physical properties individually e.g. refractive index matching/mismatching of LC and polymers, their purity, resistivity, chemical and photo stability, mutual miscibility, non-ionic nature of dye in case of guest host materials etc.

In this work, we used commercially available nematic liquid crystals namely E8, BL036 and ferroelectric liquid crystal ZLI-3654 (BDH UK) [1]. A series of UV curable polymers like (NOA-73, NOA-65, NOA-63, NOA-68) (Norland, NJ) [2] were used as matrix elements. NOA-65 was used as matrix material in nematic whereas NOA-65, NOA-73, NOA-63 and NOA-68 were used in ferroelectric dispersed systems. These polymers are clear, colourless, liquid photopolymers that cure under UV light of maximum absorption within the range of 350-380 nanometers. We also investigated the effect of small amount of dichroic dye (e.g. anthraquinone) [3] on liquid crystal droplet morphology and other associated properties. The physical properties of the above materials are given in Table 2.1- 2.4.

Table 2.1 Physical properties of liquid crystal materials used [1]

Ferroelectric liquid crystal mixture ZLI-3654

<i>Properties</i>	<i>Values</i>
<i>Phase sequence</i>	<i>K-30⁰C SmC*-62⁰C SmA76⁰C Ch 86⁰C I</i>
<i>Tilt angle at 20⁰C</i>	<i>25⁰</i>
<i>Spontaneous Polarization (nC/cm²)</i>	<i>-29</i>
<i>Switching Time (μsec)</i>	<i>44</i>
<i>Pitch (μm)</i>	<i>3</i>

Table 2.2 Physical properties of liquid crystal materials used [1]

Nematic liquid crystals E8, BL036

<i>Materials</i>	<i>Phase sequence</i>	<i>Refractive index</i>
E8	Crystal $\xrightarrow{-12^{\circ}\text{C}}$ Nematic $\xrightarrow{72^{\circ}\text{C}}$ Isotropic	$n_e = 1.77$ $n_o = 1.52$
BL036	Nematic $\xrightarrow{95^{\circ}\text{C}}$ Isotropic	$n_e = 1.79$ $n_o = 1.52$

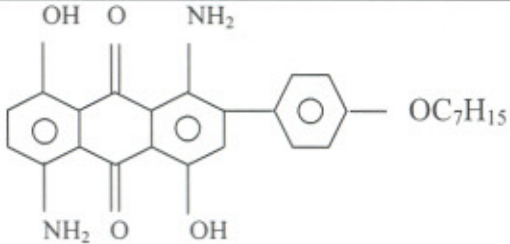
Table 2.3 Physical properties of UV polymers used [2]

UV curable polymers

<i>Physical Properties</i>	<i>Polymers</i>			
	NOA- 73	NOA- 65	NOA- 63	NOA- 68
<i>Polymer Viscosity at 25° C (CPS)</i>	140	1000	2500	5000
<i>Refractive index at cured polymer</i>	1.56	1.52	1.56	1.54
<i>Tensile (Psi)</i>	200	1500	5000	2500
<i>Modulus (Psi)</i>	160	2000	240,000	20,000

Table 2.4 Molecular structure and physical properties of anthraquinone dichroic dye [3]

Anthraquinone dye

<i>Properties</i>	<i>Value</i>
<i>Structure</i>	
<i>Solubility</i>	<i>100%</i>
<i>Colour</i>	<i>Blue</i>
λ_{max}	<i>630 nm</i>

2.2 Homogenous alignment and cell construction

Polymer dispersed liquid crystal (PDLC) samples were prepared using conducting indium tin oxide (ITO) coated glass substrates. These substrates were procured from Bharat Electronics Limited (BEL), Bangalore. We also used some commercial cells obtained from M/S Linkam Instruments, UK. These substrates were highly transparent with resistivity of the order of few 140-180 ohm-m.

The substrates were initially washed with soap solution, rinsed with acetone (purity 99.9%), distilled water and then dried in a vacuum chamber. These substrates were then put in dust free (laminar flow) chamber to ensure proper cleaning conditions. For PDLC devices there is no need of any surface treatment and polarizers to get the higher contrast and better optical properties [4-6].

The characterization with respect to switching responses etc was carried out in homogenous (planar) cells. Out of the two basic forms of alignment for liquid crystalline compounds or mixtures i.e. the homeotropic and homogenous [7-11], we used

homogenous alignment method. In this method constituents molecules of LC phase are oriented parallel to the supporting substrates.

In order to obtain planar alignment, these substrates were initially treated with polyamide (nylon) solution. This procedure was immediately followed by deposition of a coating of a nylon (6/6) polymer. The 0.5% (wt. to vol.) solution of nylon prepared in 60% m-cresol and 40% methanol (vol. to vol.) was used [12-13]. A drop of this solution was spin coated on ITO coated substrate at a varying rotation speed (4000 rpm) for about a minute in a spin coating unit as shown in Fig. 2.1. The excess solvent if any, on the glass substrates was evaporated by keeping the coated glass plates at about or 130°C in an oven for about an hour. Both the glass plates were rubbed uni-directionally with a velvet cloth. The conducting sides of these rubbed ITO coated glass substrates were joined together and separation between the substrates was maintained with the help of mylar spacer of thickness 10 μm . These two glass plates were sealed with optical adhesive (UV curable polymer), and then cured the cell in presence of UV light.

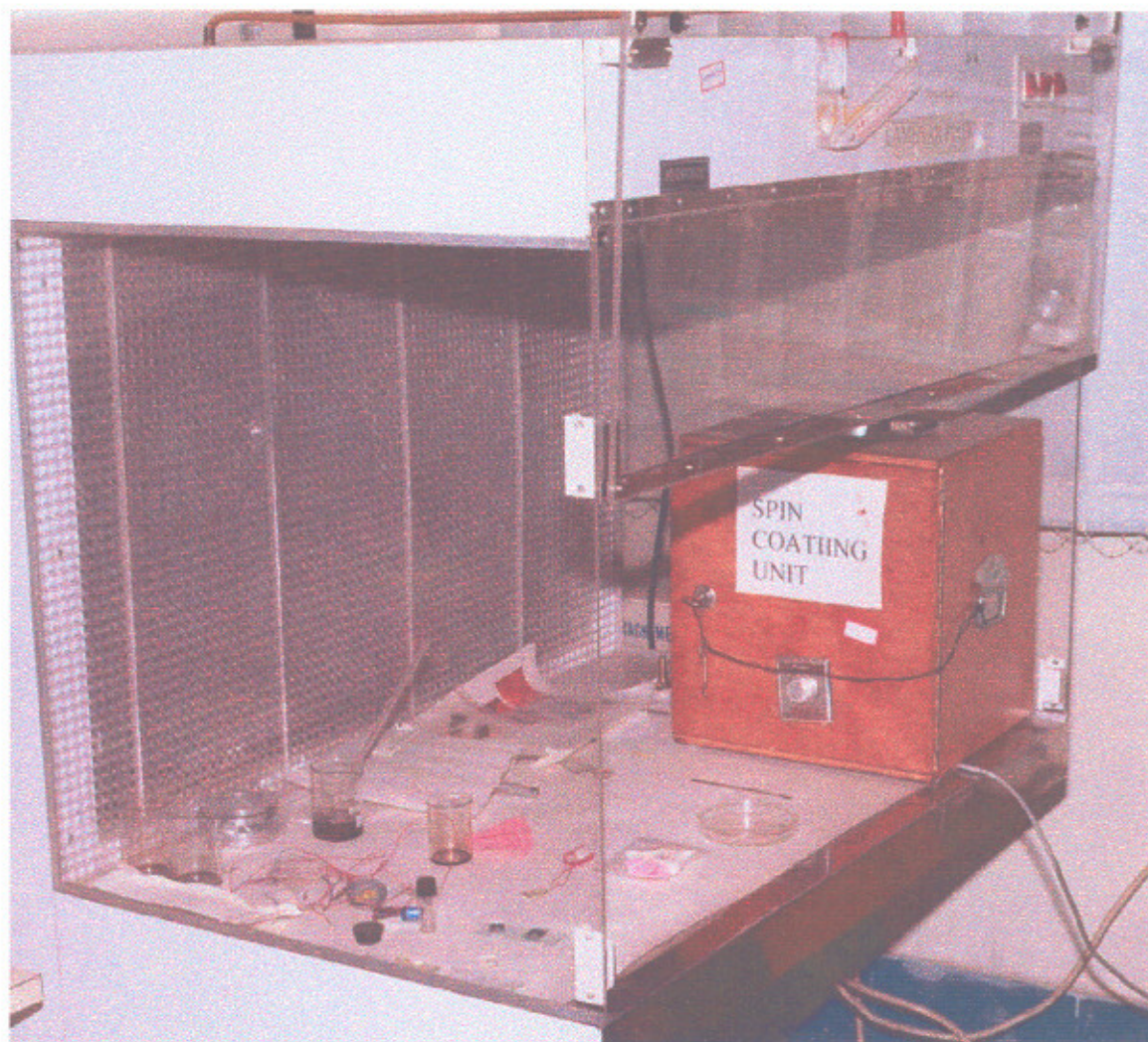


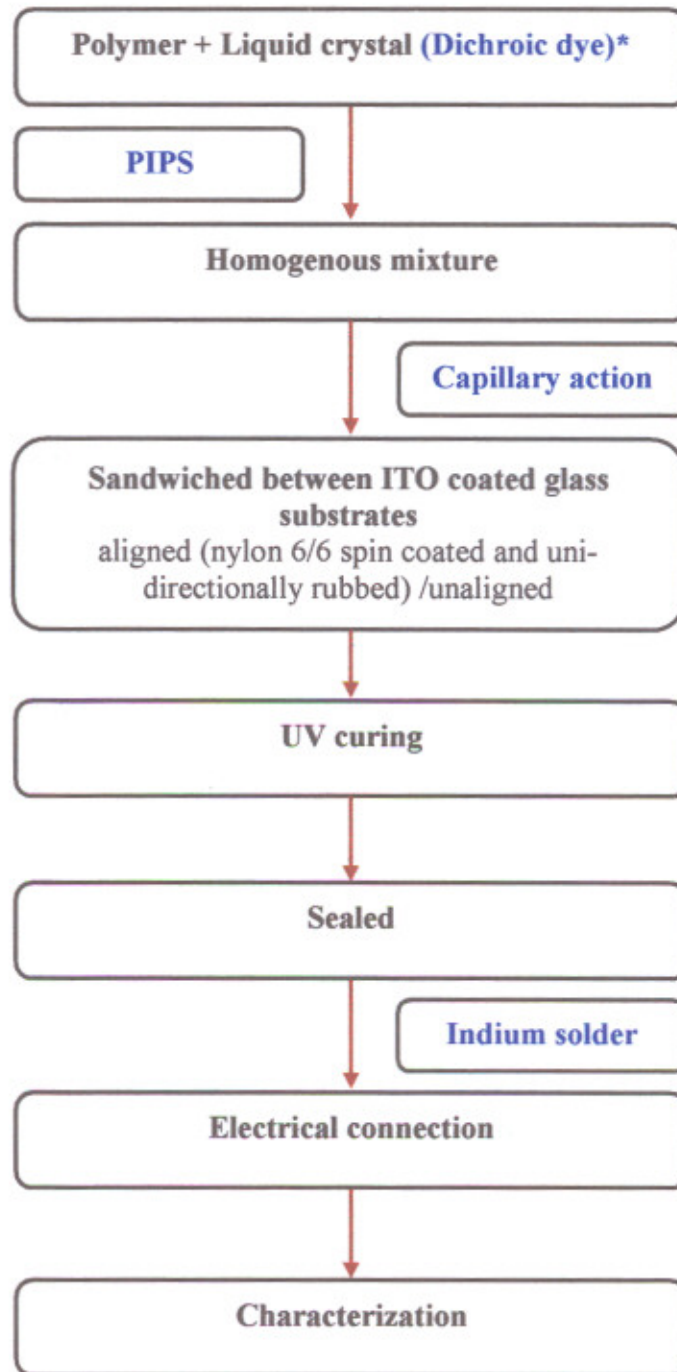
Fig. 2.1 Setup for liquid crystal cell preparation in clean environment

2.3 Preparation of phase separated polymer dispersed liquid crystal samples

Polymer dispersed liquid crystal samples were prepared with standard polymerisation induced phase separation (PIPS) method. In this technique, polymer and liquid crystal were mixed in equal or in different wt./wt. ratio in a vial. To homogenise the mixture, both the polymer and LC mixture were heated in an oven up to the isotropic temperature of LC for about an hour and vial was then shaken rigorously. This mixture was then filled between conducting ITO coated glass substrates by capillary action. The sample was first heated to isotropic temperature of liquid crystal and then cooled down to room temperature. After cell filling, the other edges of glass plates were also sealed. The cells were then exposed to UV light of intensity about 2mW/cm^2 (power 125W) for about an hour at room temperature. The UV light creates the phase separation between liquid crystal and polymer. Liquid crystal droplets were dispersed in polymer matrix and gives rise to different orientation and properties depending on LC droplet morphology. However these liquid crystal droplets align inside the polymer matrix in the direction of rubbing done on the glass substrates. The electrodes were connected at the ITO coated substrate surface using indium solder for a better contact. The complete process of PDLC sample preparation is shown in Fig. 2.2 in the form of flow chart.

2.3.1 Polymer dispersed nematic liquid crystal samples

Phase separated polymer dispersed nematic liquid crystal (PDNLC) samples were prepared using UV polymer (NOA-65) and nematic liquid crystals (E8, BL036) as base materials. Both LCs (E8, BL036) and polymer (NOA-65) have the same refractive index 1.52. We expected a better phase separated and scattered PDLC sample. We selected 70:30 wt./wt. ratio [liquid crystal (E8) /polymer by weight] in a vial. This homogenous mixture was heated to isotropic temperature in an oven and then properly dispersed after shaking to ensure proper mixing. A thin sample cell consisting of two ITO coated glass substrates of thickness $10\ \mu\text{m}$ was used. The homogenous mixture was then introduced between two conducting ITO coated glass substrates by capillary action after heating the mixture to its isotropic phase. The sample cell was sealed and exposed to UV light (intensity $\sim 2\ \text{mW/cm}^2$) for about an hour. During UV exposure, the sample cell was kept at a temperature of $\sim 20^\circ\text{C}$.

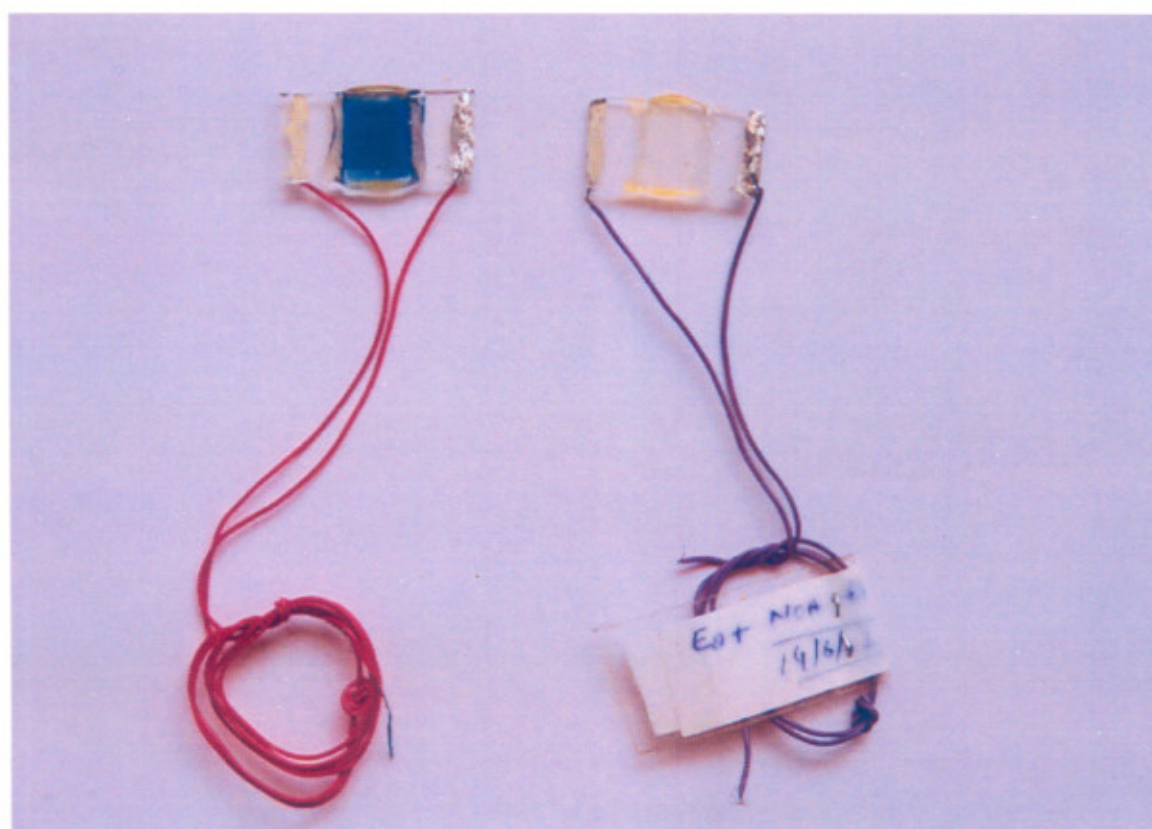
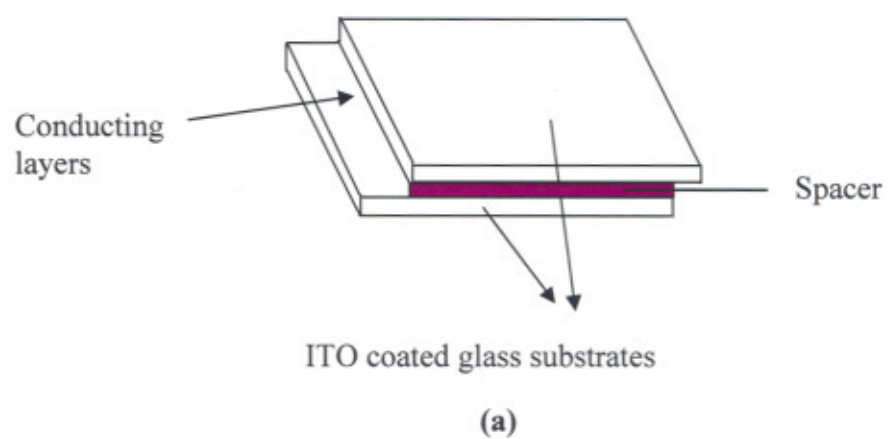


(* if guest-host polymer dispersed liquid crystal samples were prepared)

Fig. 2.2 Flow chart showing preparation of phase separated PDLC samples

2.3.2 Guest-host polymer dispersed nematic liquid crystal samples

It has been felt by researchers and technologists that dispersion of dichroic dyes would enhance the optical properties of LC systems in a guest-host polymer dispersed nematic liquid crystal (GHPDNLC) and PDNLC in particular. As a curiosity to access the change in properties, we prepared GHPDNLC samples by first dissolving the dye (1%, 2% and 4% wt./wt.) in liquid crystal, and then dispersed into the polymer material. The NLC (BL036) and polymer were taken in equal 50:50 wt./wt. ratio. Although the method of preparation of PDNLC and GHPDNLC is similar but care is taken in GHPDNLC samples that dye does not accumulate at one place and should be uniformly dispersed. These GHPDNLC mixtures were also filled between ITO coated glass substrates of thickness 10 μm and cured as discussed earlier in section 2.3.1. The preparation method of GHPDNLC sample is same as shown in flow chart in Fig. 2.2. An assembly of liquid crystal cell in empty and filled state is shown in Fig. 2.3.



(b)

Fig. 2.3 An assembled (a) empty (b) filled liquid crystal cells

2.3.3 Polymer dispersed ferroelectric liquid crystal (PDFLC) samples

A series of four UV curable polymers of different viscosity in the range of 140 CPS to 5000 CPS namely (NOA-73, NOA-65, NOA-63, NOA-68) were used as matrix for dispersion of multi-component ferroelectric liquid crystal mixture ZLI-3654.

Four PDFLC samples of different polymer viscosities were prepared in a fixed ratio of liquid crystal and polymer to 30:70 wt./wt. The cells gap between the substrates was fixed 10 μm in all the samples. We mentioned these cells as unaligned PDFLC samples.

In order to study the effect of surface treatment on the ITO coated glass substrates and hence on the droplet morphology, droplet size, switching properties, optical properties and other physical properties, a set of another four PDFLC samples of thickness 10 μm in the same ratio of LC and polymer to 30:70 wt./wt. were also prepared and studied thoroughly. We called these cells as aligned PDFLCs samples. The alignment procedure was adopted using Nylon 6/6 as discussed earlier in section 2.2.

Unaligned and aligned PDFLCs samples were sealed and exposed to UV light at the same intensity $2\text{mW}/\text{cm}^2$ for an hour at room temperature. Electric connections with ITO coated glass substrates were made in all the samples using an indium solder. After sealing and curing, all the samples (PDNLC, GHPDNLC, unaligned PDFLC, aligned PDFLC) were placed in a LINKAM temperature programmer cum hot-stage.

The optical micro-texture and LC droplet morphology were viewed at a magnification of 10X through Olympus polarizing microscope fitted with charge coupling device (CCD) camera. The LC droplet morphology, its size and alignment was detected and acquired on a P IV computer using Linksys and RTVMS software. The electric field was applied using a function generator and the output responses were detected on a digital storage oscilloscope using wavestar software.

The detailed investigation on LC droplet morphology, behaviour of droplet in the polymer matrix and other parameters in each systems as a function of temperature, electric field, surface treatment, polymer viscosity etc are discussed and are given in the chapter 3 and 4.

2.4 Experimental techniques

In order to study the liquid crystal droplet morphology and phase transition temperatures, Olympus polarizing microscope (Model- BX51P) and Linkam temperature programmer cum hot stage (Model TP94 and THMS 600) were used as major instruments. The electric field was applied to the sample through Scientech function generator (Model ST 4060), Philips function generator (Model FG8002). The optical textures were captured through the CCD camera (Model- Mintron OS-35111) fitted on polarizing microscope and interfaced with P IV computer. A block diagram of our experimental set up for the investigation of optical textures, electro-optic properties and other parameters of liquid crystal is shown in Fig. 2.4. The temperature of the PDLC sample cell was controlled using temperature controller interfaced with computer through RS232 port and the output response as a function of field was recorded on Tektronix Oscilloscope (Model TDS2024).

All the optical textures have been investigated with electric field and temperature under crossed polarizers at a magnification of 10X. The complete experimental set-up to study electro-optical properties is also shown in Fig. 2.5.

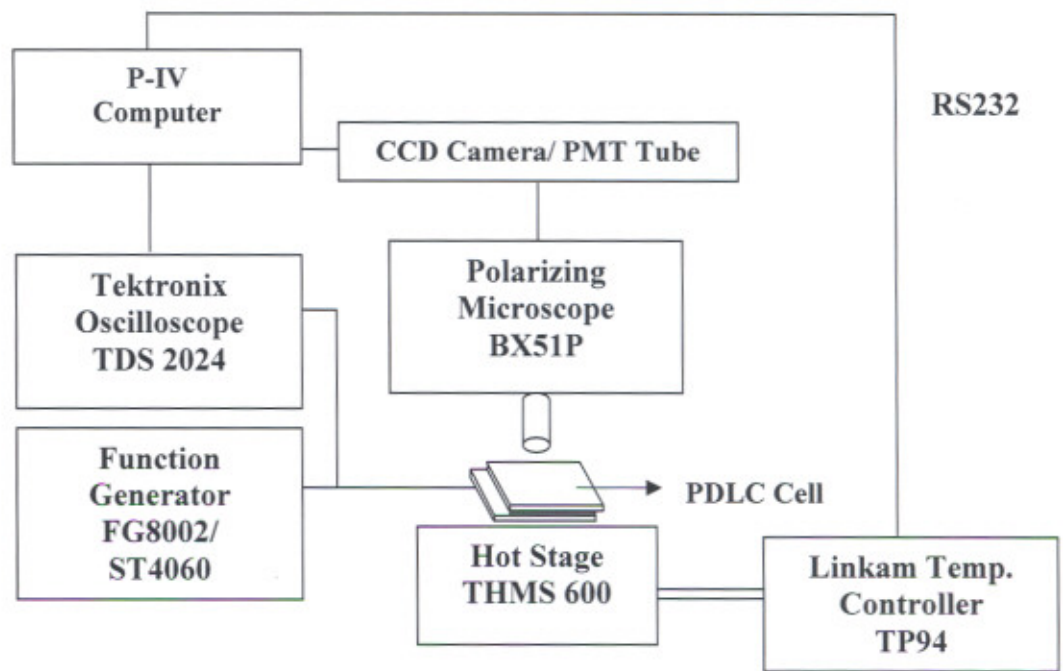


Fig. 2.4 Block diagram of the experimental set-up to study electro-optical properties

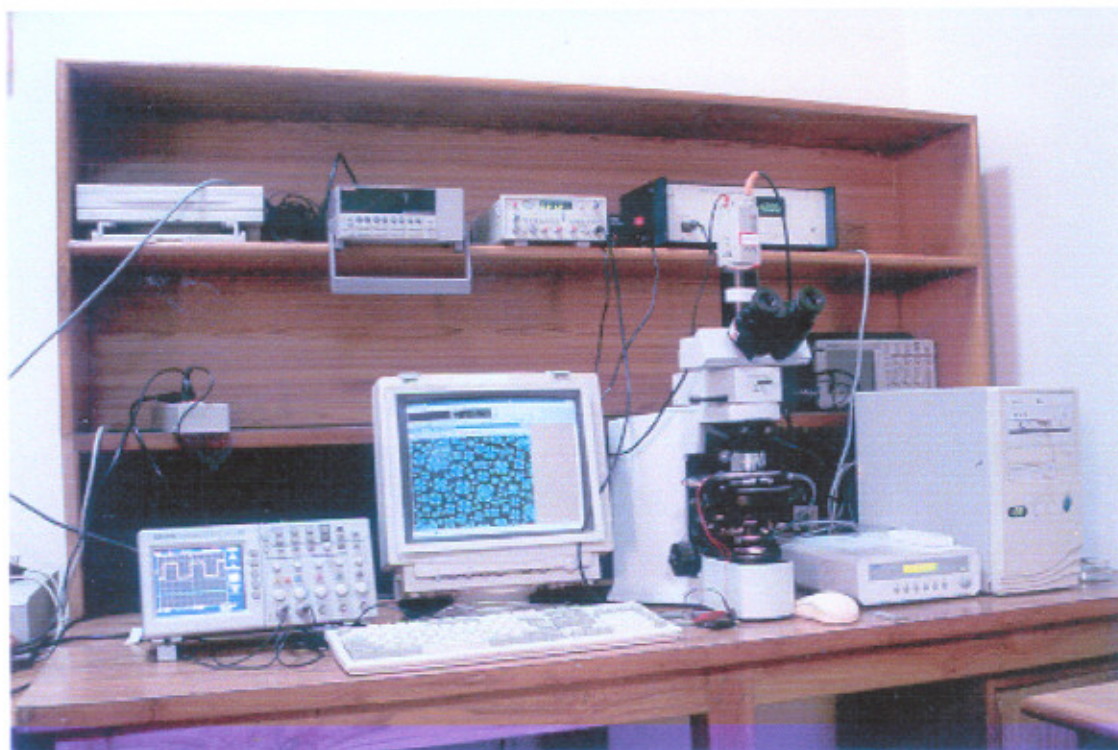


Fig. 2.5 Experimental set-up to study the electro-optical properties of phase separated PDLC films

2.4.1 Temperature programmer and hot stage

In thermal microscopy studies, we used Linkam temperature programmer TP94 and hot stage THMS 600. The TP94 is specifically designed for precise temperature control of the Linkam heating/freezing stages. The stage sensor is digitally linearized to give accurate temperature readout, the controls and their functions have been carefully chosen for simple and easy operation. The temperature range is -196°C to 600°C . Heating or cooling rates can be changed almost instantly using the three rate keys. The heat ranges

are from 0.1 to 0.9°C/min at 0.1 degree intervals from 1.0 to 9.0°C/min at 1.0 degree intervals and from 10 to 90°C degree intervals.

A varying dc signal is used to control the stage and results in an even application of power, which avoids the bursts seen with conventional burst fire ac techniques. An optional remote control gives single key control of three programmable heating/cooling rates and the HEAT, COOL and HOLD functions. The three programmable heating/cooling rates are held in memory when power is switched off. The temperature and limit values can also be stored and recalled using the remote control facility.

2.4.2 Optical polarizing microscopy

The optical studies observed in nematic liquid crystals, ferroelectric liquid crystal and guest host systems were investigated using an Olympus optical polarizing microscope (Model BX51P) at 10X magnification under crossed polarizers using long working distance objective lens at 10X. The optical micro-textures of LC materials were also investigated as a function of temperature, voltage and other physical parameters.

2.4.3 UV-VIS Spectrophotometer for absorbance and transmission studies

The absorbance of incident light by dye molecule in dye doped polymer dispersed liquid crystal sample cells were investigated by using ultra violet visible (UV-VIS) Spectrophotometer (Model- SPECORD 200PC) in the wave length range of 190 –1100 nm with an accuracy of ± 0.5 nm interfaced with PIV computer.

The out put responses of the PDLC sample cells were measured with the help of photo multiplier tube (PMT) (Model RCA931-A) fitted on the polarizing microscope and interfaced with computer as shown in Fig. 2.4. PMT covert the output intensity in the form of current and it was measured with the help of electrometer (Keithley Model – 6514) of three and half to six and half digits. The range of current measurement was 20PA to 20mA with $\pm 5\%$ error.

2.4.4 Droplet size measurements

The LC droplet sizes were measured using the Linksys software by taking the mean of two major axes and minor axis diameter of droplet. To measure the precise droplet size measurement, different droplet were chosen and the mean of randomly existing about 80 droplets were taken. The droplet size of small droplets exhibiting between the two major droplets was also taken. Fig. 2.6 depicts the measurement of LC droplet size by drawing the horizontal and vertical scale bar on the major and minor axes of the droplet.

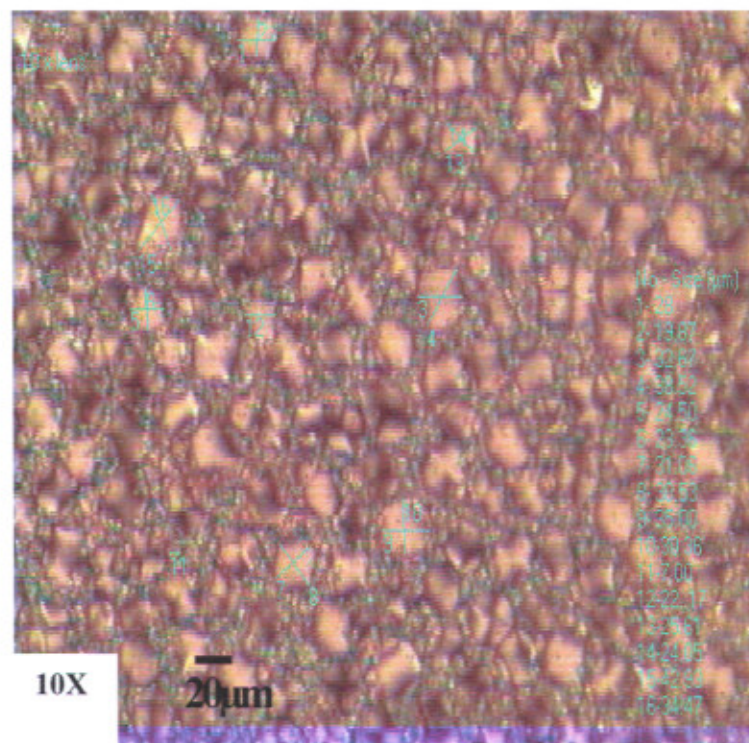
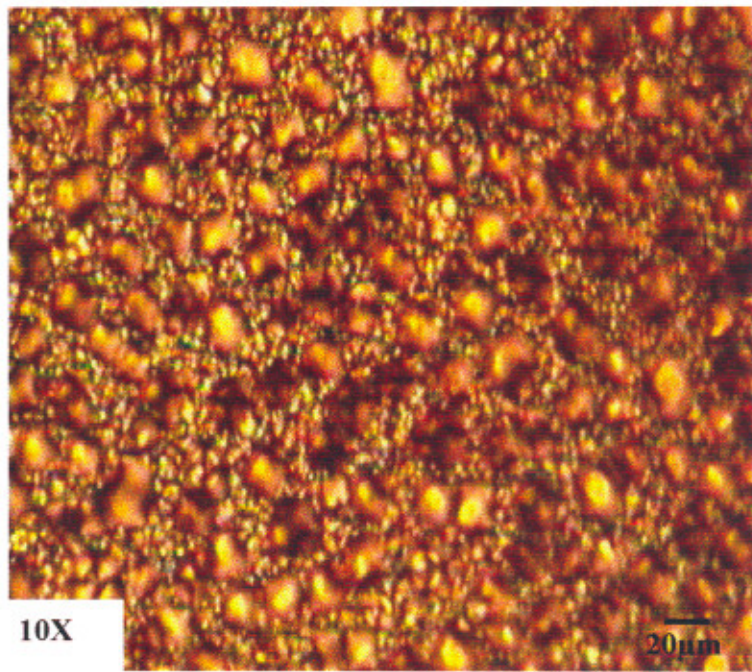


Fig 2.6 Measurement of LC droplet size in a PDNLC sample at room temperature

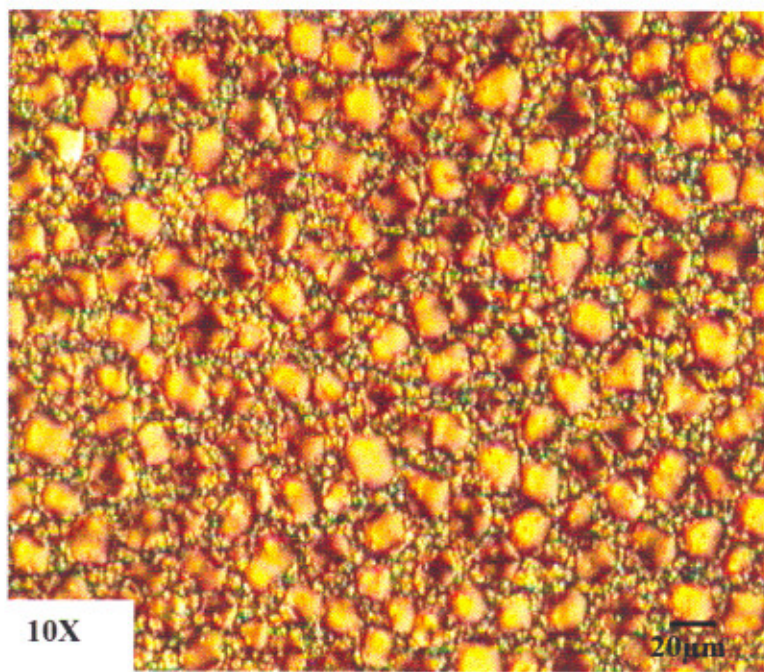
2.5 Optical textures and phase behaviour

(a) Textures in polymer dispersed nematic liquid crystal and guest-host polymer dispersed nematic liquid crystal samples

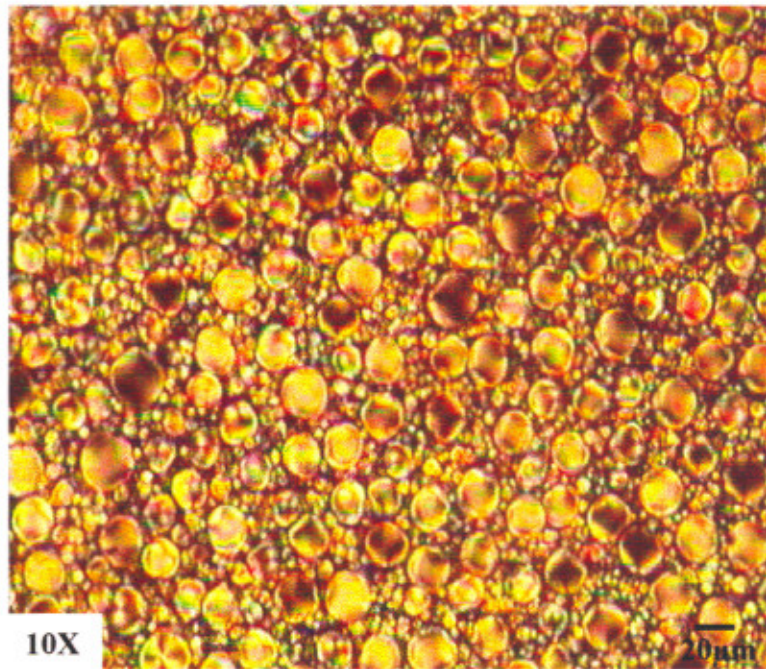
The micro-textures of nematic liquid crystal droplets in PDNLC samples at different temperature under zero bias are shown in Fig. 2.7. It depicts the change in phase sequence from nematic to biphasic region at isotropic temperature [Fig. 2.7(d)]. Fig. 2.8 shows the micro-textures of 1% dichroic dye doped GHPDNLC systems at room temperature under zero voltage in bipolar, radial and axial configurations. However the major contribution in the sample was due to bipolar liquid crystal droplets. These texture morphologies showed that LC droplets exhibit various configurations like bipolar, radial, axial and twisted bipolar etc. Some other micro-droplets were also observed. The electro-optical and thermo-optical responses of these systems (PDNLC and GHPDNLC) are strongly dependent on LC droplet morphology, size and their orientation phenomena surrounded by the polymer network. In early studies, UV-VIS absorption and light scattering methods were used to monitor the LC dynamics. Recently, nuclear magnetic resonance, Fourier transform, infrared spectroscopy and several time resolved microscopies and spectroscopies have been employed. All such method yields valuable information on the LC dynamics but do not provide sufficient spatial resolution to resolve the reorientation dynamics within individual LC droplets. More recently Higgins et al. studied the droplet orientation dynamics and optical properties in PDNLC and guest-host PDNLC sample using Near- Field Scanning Optical Microscopy (NSOM) [14,15]. This method provides high-resolution optical images of the droplets and their dynamics, as well as topographic information, allowing for development of detailed co-relation between droplet size/shape attributes and the dynamics. Higgins et al. observed the well known radial and axial bipolar droplet. However a new type of droplet called "toroidal" was also discovered. The details of the electric field effects on PDNLC and GHPDNLC samples are given in chapter 3.



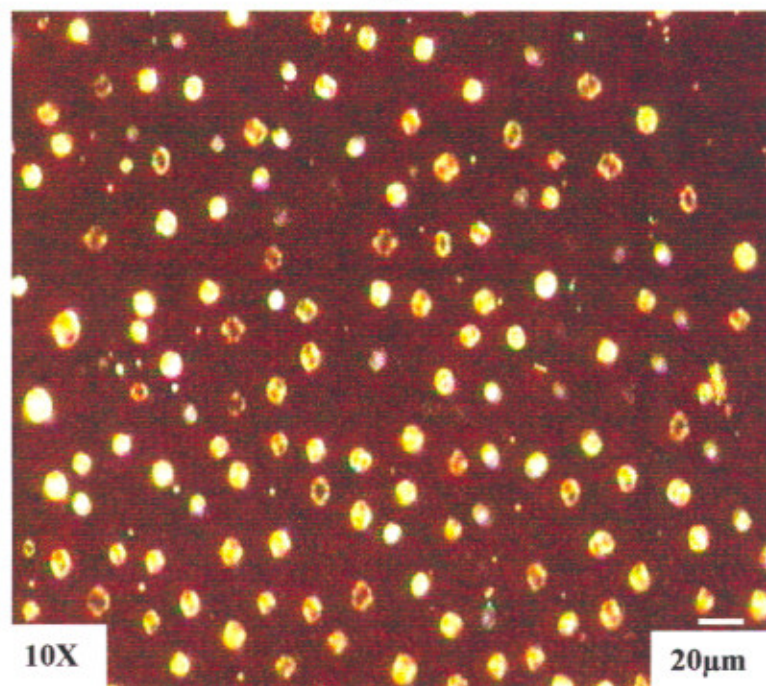
(a)



(b)

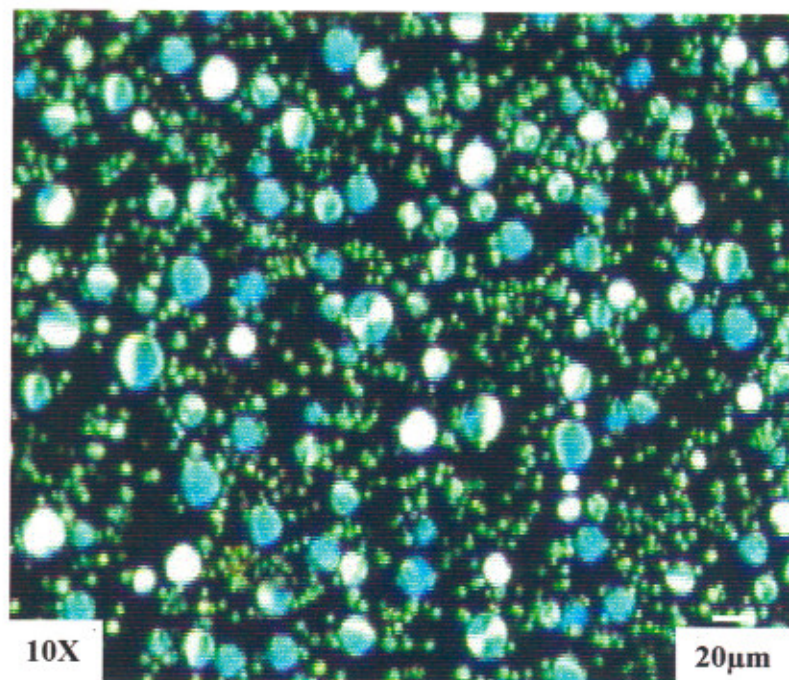


(c)

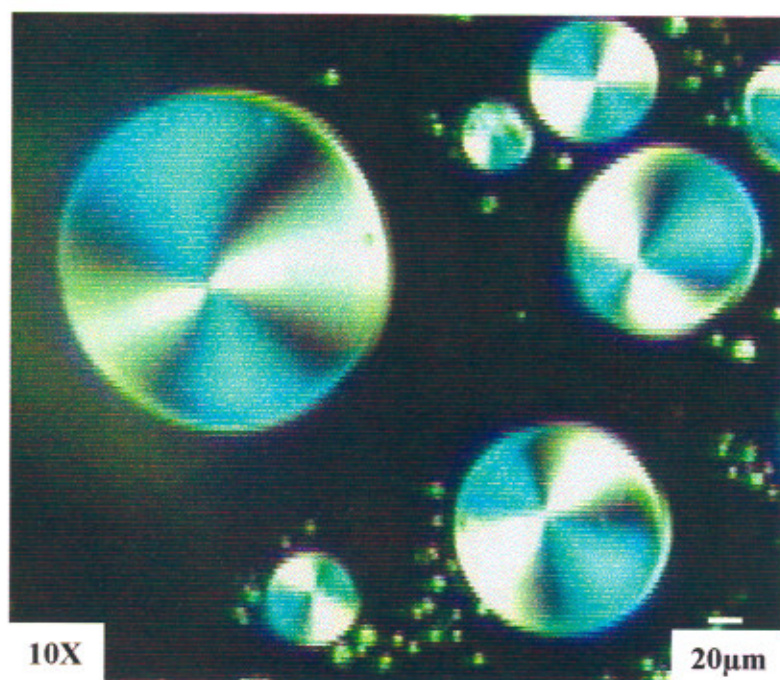


(d)

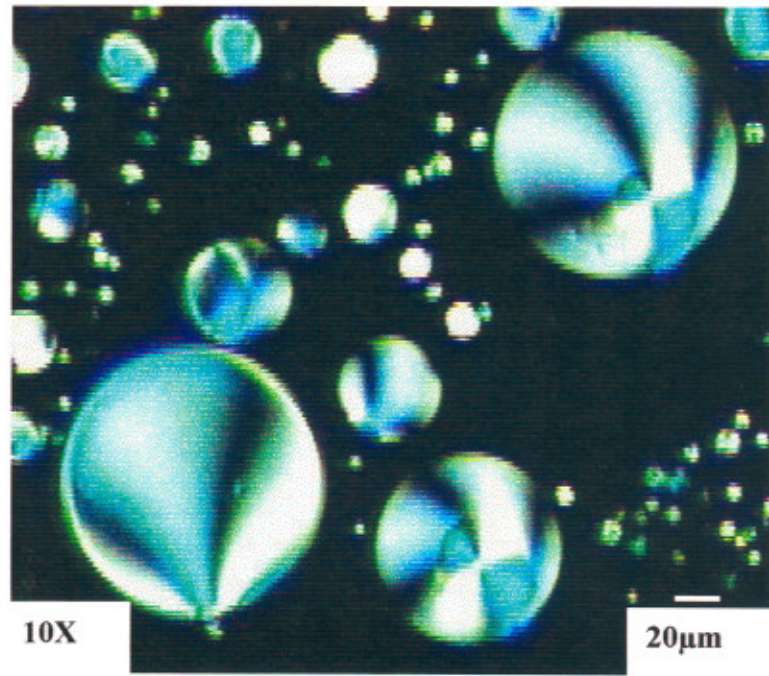
Fig. 2.7 Nematic liquid crystal droplet morphology dispersed in polymer matrix at different temperature ($^{\circ}\text{C}$) (a) 30 (b) 40 (c) 60 and (d) 68



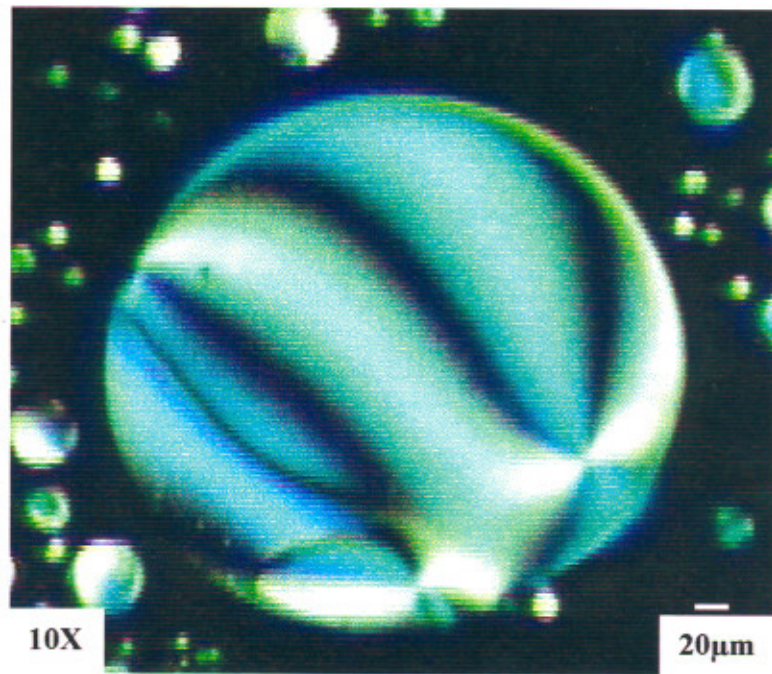
(a)



(b)



(c)



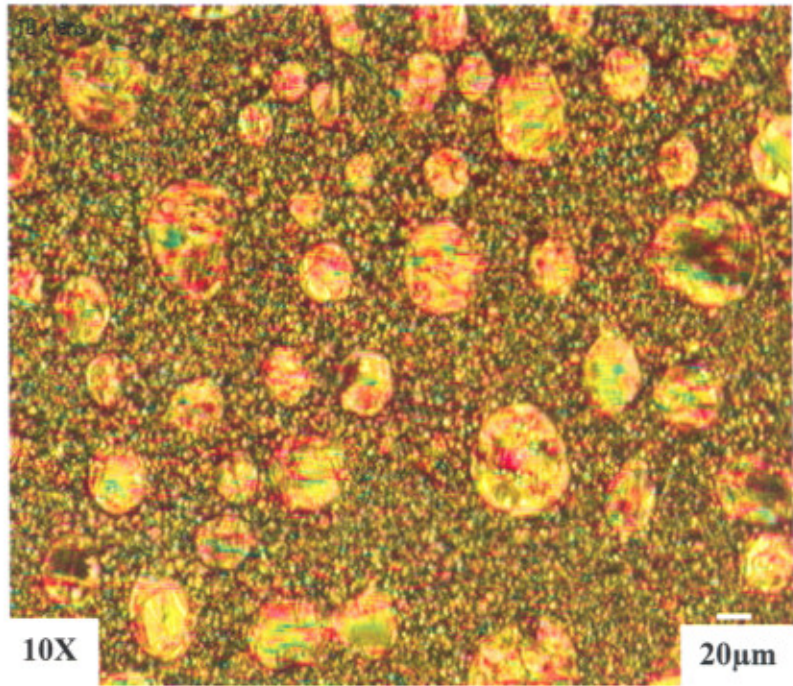
(d)

Fig. 2.8 Dichroic LC droplet morphology in different configuration (a) scattered (b) radial (c) axial and (d) twisted bipolar at room temperature

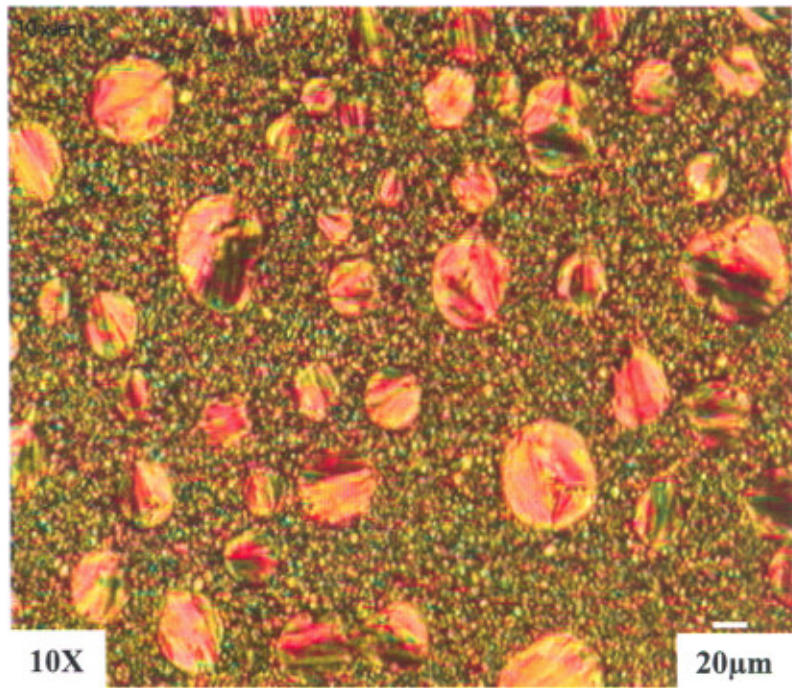
(b) Textures in unaligned and aligned PDFLC samples

The dispersion of FLC material in NOA-65 polymer in unaligned samples at different temperature is shown in Fig. 2.9. It depicts that FLC droplets are not uniform as in the case of nematic LC dispersion. The non-uniformity of FLC droplets may be due to the inherent property of FLC materials. The phase changes of FLC material inside the droplet can be seen from Fig. 2.9(a) to Fig. 2.9(e) with an increase in isotropic temperature about 5-6°C. The increase in isotropic temperature may be due to the fact that, in these PDLC systems some amount of LC materials always mixed with polymer.

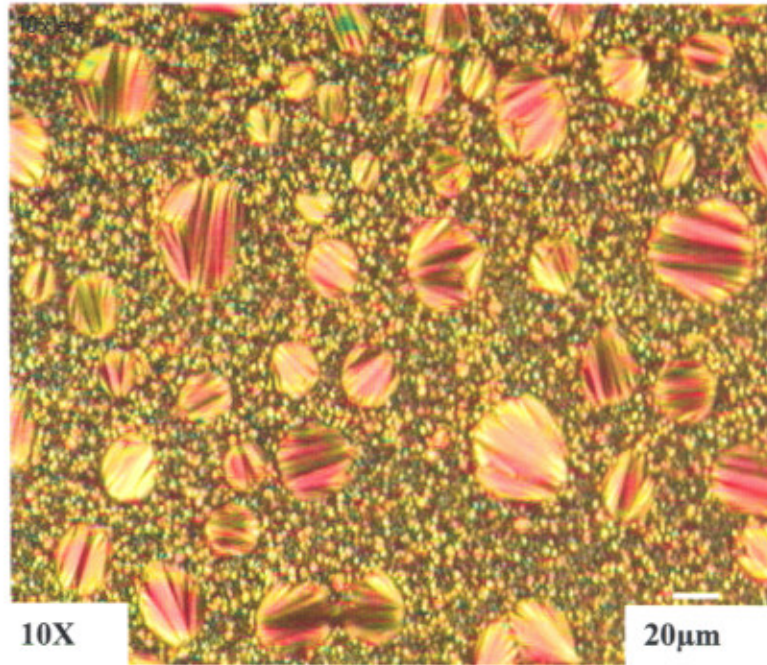
In the aligned PDFLC samples all the FLC materials align along the rubbing direction and adopt elongated droplets as shown in Fig. 2.10. We also see that in low viscosity polymer PDFLC sample, all the FLC droplets align easily in comparison to high viscosity polymer based PDFLC sample. We believe that in the high viscosity polymer, due to strong viscous force between the chains it is difficult to align the LC droplet than low viscosity PDFLC sample.



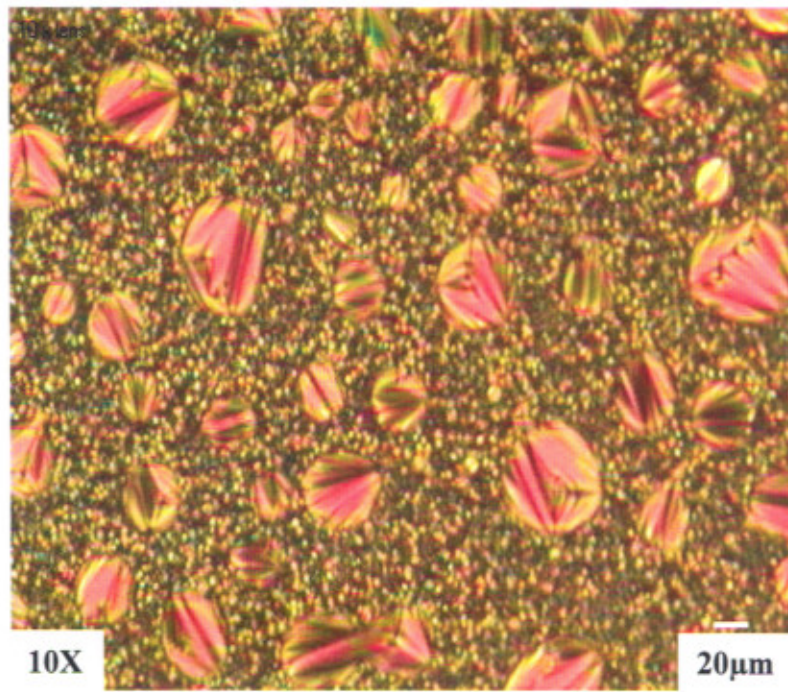
(a)



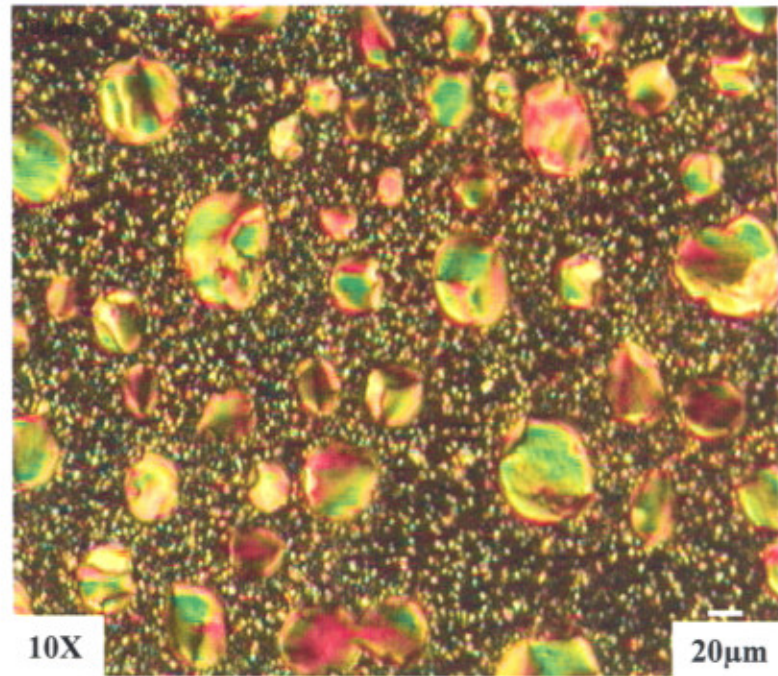
(b)



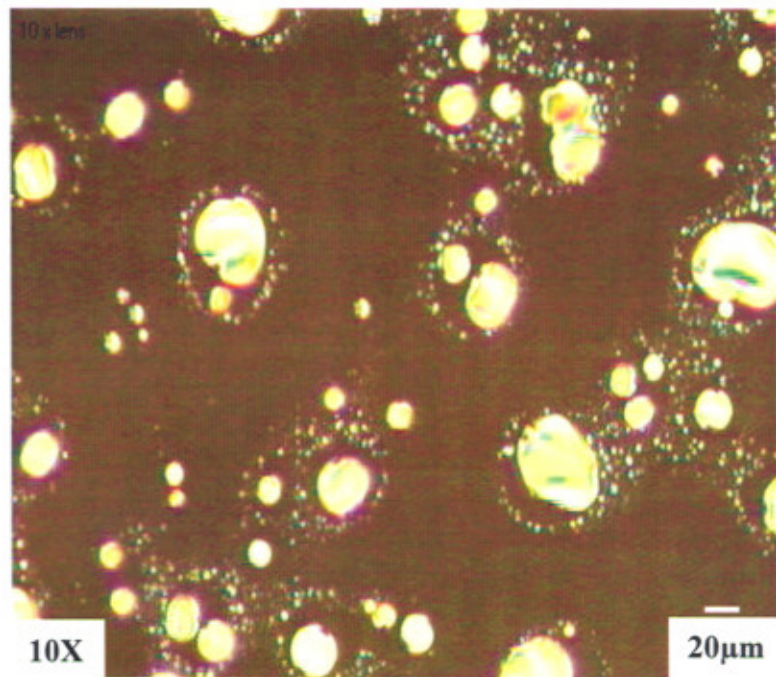
(c)



(d)

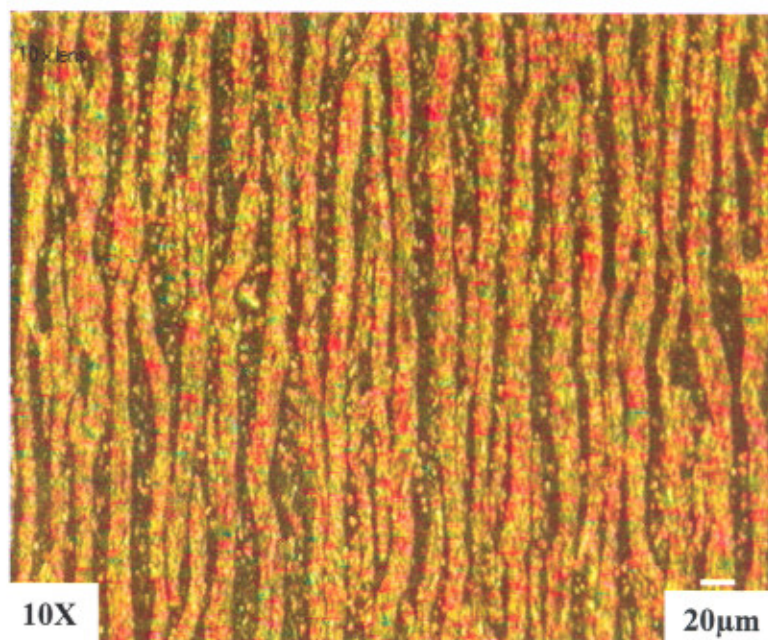


(e)

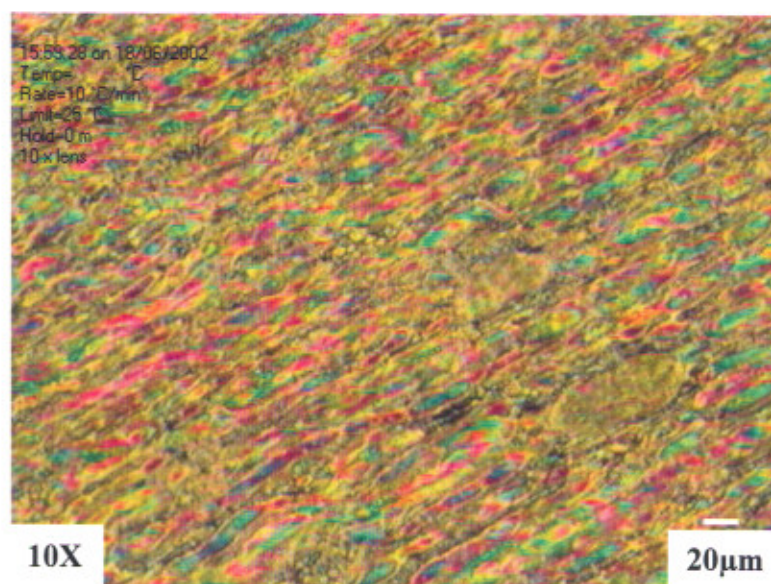


(f)

Fig. 2.9 Droplet morphology in unaligned PDFLC sample at temperatures ($^{\circ}\text{C}$) (a) 30 (b) 60 (c) 73 (d) 78 (e) 82 and (f) 91



(a)



(b)

Fig. 2.10 Alignment of FLC molecules dispersed in UV curable polymer viscosities (CPS) (a) 140 (b) 2500 at room temperature

REFERENCES

- [1] Data sheet, BDH, UK
- [2] Data sheet, Norland, NJ, USA
- [3] K. K. Raina, A. K. Gathania and B. Singh, *J. Phys. Condens. Matt.*, **11** (1999) 7061
- [4] P. S. Drazic, *Liquid Crystal Dispersion*, World Scientific, Singapore, (1995)
- [5] P. Malik, J. K. Ahuja and K. K. Raina, *Curr. Appl. Phys.*, **3** (2003) 325
- [6] G. Sumana and K. K. Raina, *Curr. Appl. Phys.*, **5** (2005) 277
- [7] P. J. Colling, *Liquid Crystal: Nature's Delicate Phase of Matter*, Princeton: University Press (1990)
- [8] P. J. Colling and Michael Hird, *Introduction to Liquid Crystal: Chemistry and Physics*, Taylor and Francis Ltd (1997)
- [9] S. Chandrasekhar, *Liquid Crystal 2nd Edn. Cambridge*: Cambridge University Press (1992)
- [10] P. G. De Gennes, *The Physics of Liquid Crystal*: Oxford University Press (1975)
- [11] I. C. Khoo, *Physics of Liquid Crystalline Materials* (Amsterdam: Golden and Breach) (1991)
- [12] S. S. Bawa A. M. Biradar and S. Chandra, *Jpn. J. Appl. Phys.*, **25** (1986) L 496
- [13] J. K. Ahuja and K. K. Raina, *Jpn. J. Appl. Phys.*, **39** (2000) 4076
- [14] G. H. Springer and D. A. Higgins, *J. Am. Chem. Soc.*, **122** (2000) 6801
- [15] D. A. Higgins, J. E. Hali and A. Xie, *Acc. Chem. Res.*, **38** (2005) 137

Chapter -3

Polymer Dispersed Nematic Liquid Crystal Systems

Overview

In this chapter phase separated polymer dispersed nematic liquid crystal and guest-host polymer dispersed nematic liquid crystal composite films were prepared by polymerization induced phase separation method. The detailed investigation of droplet morphology, droplet orientation and optical responses at different applied voltage and temperature are given. The effect of small amount of dichroic dye concentration on the droplet morphology and their electro- optic responses are also given.

The detailed preparation method of both the systems and their electro-optic and thermo-optic properties were investigated in detailed as a function of temperature, applied voltage and observed an unusual behaviour in PDNLC systems and explain the results on the basis of conductivity and dielectrics effects.

3.1 Review of Literature

Polymer dispersed liquid crystals (PDLCs) constitute a novel class of optical materials exhibiting interesting properties depending upon the preparation condition of PDLC samples, individual properties of the materials and various physical parameters. Various groups studied and explored the influence of polymer/LC composition, curing rate, curing temperature, preparation method on the electro-optic, thermo-optic properties and droplet morphology using nematic LC and different polymers. Review of literature by detailed electro-optic, thermo-optic and other droplet morphology related properties is being discussed as follows.

Fuh et al. [1] studied the effect of curing temperature, curing rate, density ratio of polymer on LC droplet size and electro-optical properties using nematic LC, E7 and EPON-305 polymer. It was concluded that the films cured at higher temperatures show a smaller and more uniform bipolar LC droplet size and better transmission properties.

Jain et al. [2] studied the electro-optic response in PDNLC sample as a function of frequency and applied voltage and size of LC droplet. They observed an optical memory effect in different LC droplet size and relate the memory effect with the relation of bipolar axes in different droplet size. The same group also investigated the switching response using a dual frequency addressable (DFA) liquid crystal mixture dispersing into a polymer by SIPS method. The decay and rise time of DFA-PDLC composite cell can be altered from a few thousand milliseconds to few hundred milliseconds at low and high frequency field. Kim et al. [3-4] studied the effect of polymer molecular weight on morphology and electro-optic properties of PDLC films. High molecular weight polymer gives high solution viscosity during the solvent evaporation process and makes the coalescence of LC domain difficult. Smaller LC domains contain more of tangentially oriented LC molecules on the wall, in bipolar configuration, to give higher values of V_{10} , V_{90} and τ_R . The Same group also reported a film prepared by 60/40 wt./wt. ratio of LC/polymer in PDLC film showed smaller threshold voltage, smaller rise time and higher transmittance.

Carter et al. [5] studied the morphology of PDLC as a function of polymer, LC composition, curing temperature and UV curing power. They observed no significant change in domain size with change in the curing temperature. They suggested that for

low switching voltage and high luminance, PDLC cells should be polymerised under conditions, which are below the coalescence temperature. Simoni et al. [6-8] studied the effect of UV curing intensity, exposure time, UV dose on phase separation process in UV cured PDLC and explored the idea of PDLC materials as optical switches.

Nastal et al. [9] also reported the influence of curing progress on electro-optical and switching properties of PDLC systems. Karapinar [10] reported the electro-optical response of PDLC films and found that higher LC concentration leads to the larger droplet size and hence low threshold voltage of the film.

The temperature dependence on electro-optical properties of PDLC films has been investigated rarely. Han [11] studied the effect of temperature and electro-optical characteristics of PDLC film formed by PIPS method using a nematic LC, TL213 and polymer PN313 and observed an unusual behaviour of temperature dependence on transmission properties at a fixed voltage and explained possible origin on the basis of conductivity effects. Amundson [12] gave the transmission properties at various temperatures for PDLC film based on E7/ NOA-65. Fuh et al. [13] investigated PDLC film based on E7/EPON 305 and found that a plot of transmission as a function of temperature should have broad peaks. Recently Sharma et al. [14] suggested the evidence for droplet orientation and interfacial charges in PDLC film. The additional charge build-up on the interface of the polymer and LC and its influence on the optical responses of PDLC cell were observed. Petti et al. [15-16] reported the fast switching time (rise time 190 μ sec and decay time 2msec) and higher contrast ratio 410 for PDNLC films.

Coloured PDLCs are formed by incorporating isotropic and dichroic dyes as a guest material in homogenous mixture of the PDLC. Dichroic dyes employed in PDLC films produce higher contrast than isotropic dyes. The electro-optic properties, droplet morphology of LC in a guest host polymer dispersed nematic liquid crystal (GHPDNLC) samples were studied at various preparation conditions (aligned and unaligned), surface treatment, different dye concentration and laser intensity etc.

Wu et al. [17] examined the electro-optical properties of aligned azo dye doped PDNLC films. They showed that the contrast ratio of aligned dye doped PDNLC film is higher than non-aligned PDNLC film. Lee et al. [18] have proposed a method for improving the contrast ratio of PDLC using azo dye with the photo-pumping technique and noticed that

aligned dye doped PDLC film shows much higher contrast than those with randomly oriented dye molecules in polymer matrix.

Zhou et al. [19] studied and compared the thermo-optical properties of NOA based PDLC and a new type of metallomesogen based PDLC (MOM-PDLC). They showed that thermo-optical behaviour of NOA-65 based PDLC is better than MOM based PDLC film.

Wu et al. [20] reported the effect of dichroic dye in UV cured PDLC film and optimize the dye concentration to minimize the transmission and higher contrast. Higgins et al. [21-22] studied the optical microscopy studies in PDLC and dye doped PDLC systems using Near-Field Scanning Optical Microscopy (NSOM).

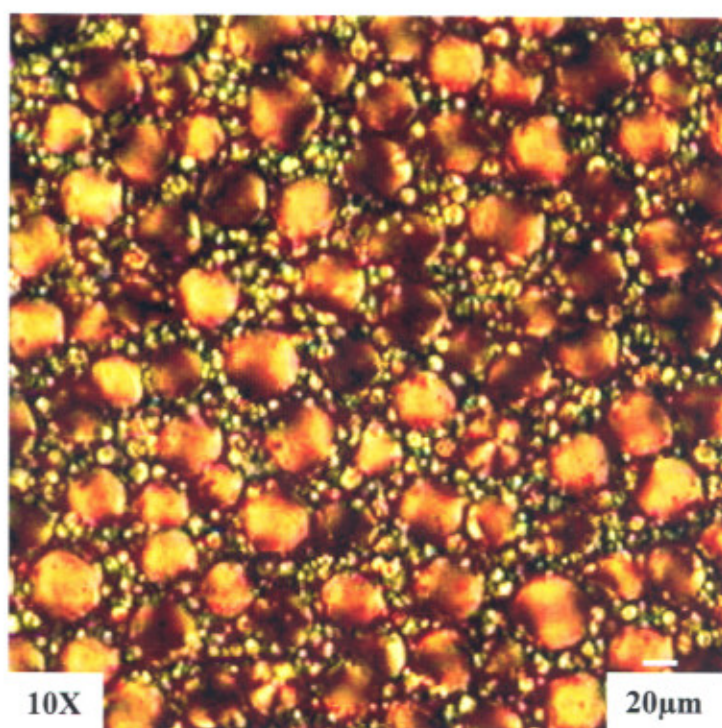
3.2 Results and discussion

3.2.1 Polymer dispersed nematic liquid crystal

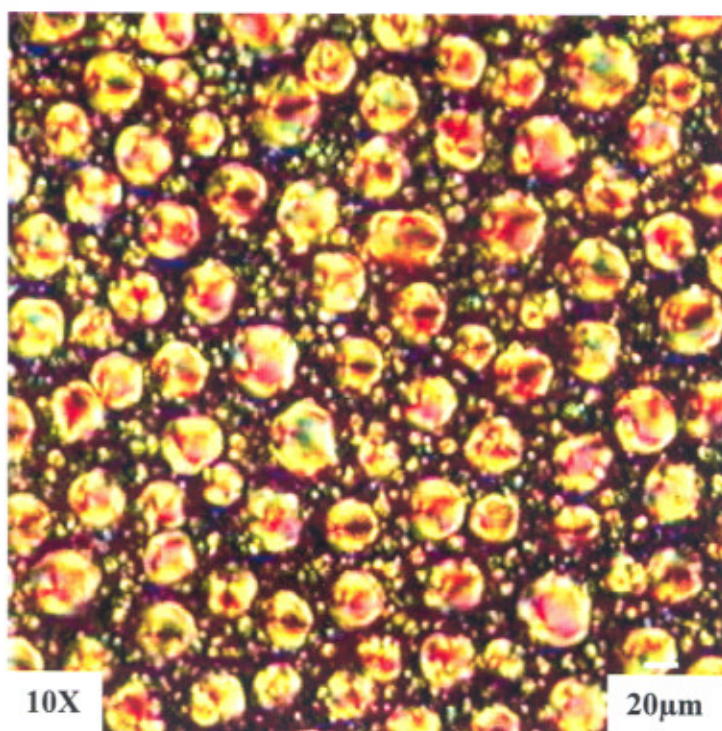
3.2.1.1 Droplet Morphology

Figure 3.1 shows the morphology of nematic LC droplets dispersed in polymer matrix under crossed polarizers at 55°C as a function of applied voltage (0, 5, 10 and 25V_{p-p}) at a frequency of 1 kHz respectively. In the absence of electric field [Fig. 3.1(a)], we notice that the LC droplets exhibits configurations like bipolar, radial, axial, and some other micro droplets between the void of two neighbouring droplets. The bipolar configuration is dominant in comparison to other configuration and their axes are randomly distributed in the polymer matrix.

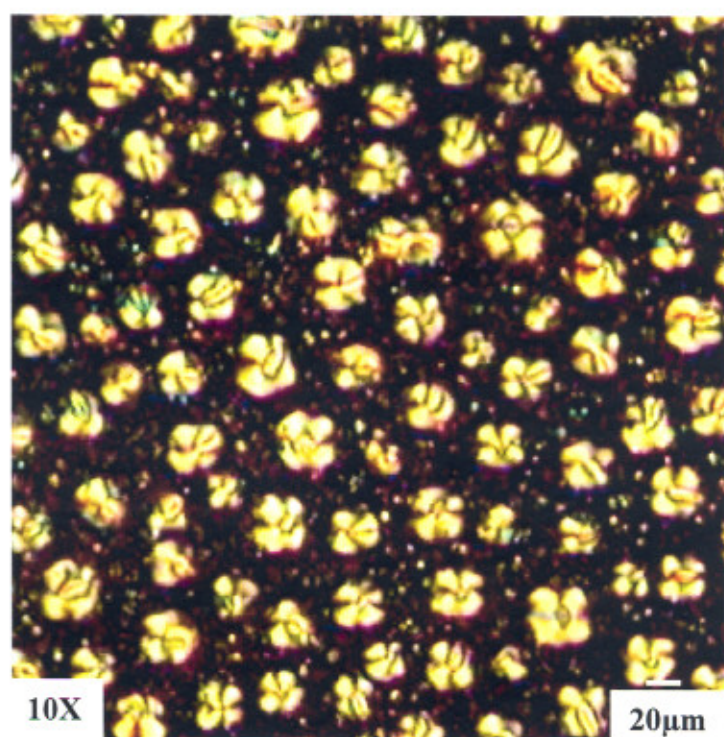
Interestingly at ~25V_{p-p} we observed, maltese type crosses [Fig. 3.1(d)] in which LC molecules and their corresponding bipolar axes are oriented along the direction of applied electric field. However in the intermediate voltage range (i.e.10-30V_{p-p}) droplet size and shape does not vary much but it showed an appreciable change in the droplet size below 10 volts. The average droplet size found in the range of 5-28 μm was almost independent of both applied voltage and temperature.



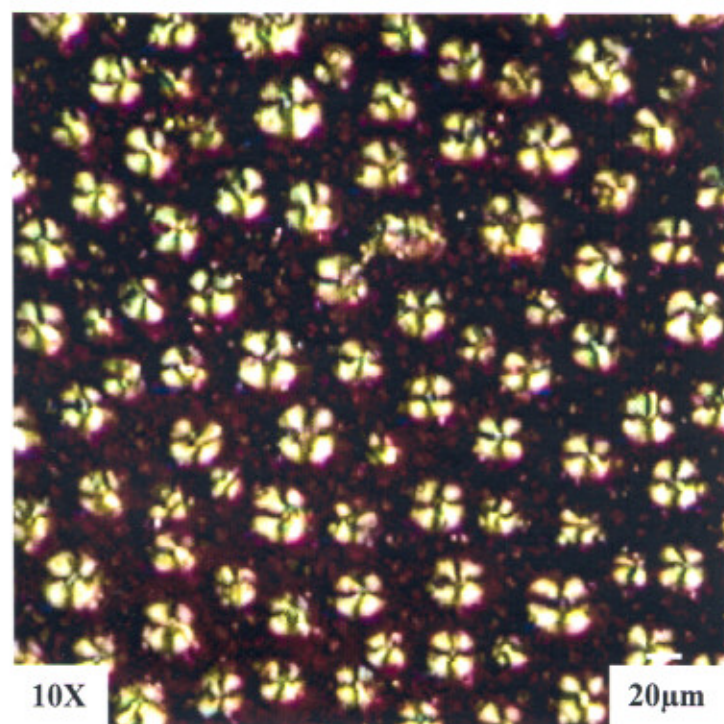
(a)



(b)



(c)



(d)

Fig. 3.1 Response of PDNLC sample to an applied voltages (V_{p-p}) (a) 0 (b) 5 (c) 10 and (d) 25 at 55°C

3.2.1.2 Electro-optic responses

The electric field inside the droplets of PDLC is not the same as the applied electric field, $E = V/d$, where V is the applied voltage and d the thickness of the PDLC film between the ITO electrodes. In fact the electric field can be different at different points inside the nematic droplets, but this variation was found to be small and therefore neglected.

Considering the isolated spherical nematic liquid crystal droplet in a polymeric material and assuming that the nematic LC behaves as an isotropic LC medium, the effective electric field E_{eff} across a nematic LC droplet can be computed by considering both conductivity and dielectric terms at different frequencies and can be written as [23, 24].

$$E_{eff} = E_a \frac{3\sigma_{pol}}{2\sigma_{pol} + \sigma_{LC}} \quad (\text{for conductive terms}) \quad (1a)$$

and

$$E_{eff} = E_a \frac{3\epsilon_{pol}}{2\epsilon_{pol} + \epsilon_{LC}} \quad (\text{for dielectric terms}) \quad (1b)$$

Where E_{eff} and E_a refer to the actual electric field across the droplets and the applied electric field, respectively. ϵ_{pol} and ϵ_{LC} are the dielectric constants and σ_{pol} and σ_{LC} are the conductivities of the polymer matrix and the LC respectively. Eq. 1(a) is valid at very low frequencies ($\omega \rightarrow 0$) where conductivity terms are dominant whereas Eq. 1(b) is significant at higher frequencies ($\omega \rightarrow \infty$). We feel that at high frequencies ($\omega \rightarrow \infty$), conductivity effect will become insignificant relative to dielectric effects, where ionic motion can be considered to be frozen out. Thus very few mobile ions generate a significant depolarization in the composite films. Comparatively, conductivity can dominate the dielectric terms at low frequencies ($\omega \rightarrow 0$).

The threshold field E'_{eff} for bipolar droplets broadened by their random orientation can be as given by the expression [25]

$$E'_{eff} = \frac{1}{R} \left[\frac{K(l^2 - 1)}{\epsilon_0 \Delta \epsilon} \right]^{\frac{1}{2}} \quad (2)$$

Where R denotes droplet radius and l its anisotropy (ratio of major to minor radius). K is effective elastic constant, d the film thickness and $\Delta\epsilon$ the dielectric anisotropy of the liquid crystal.

Applying Eq. (2) and Eq. 1(a, b) the threshold voltage V_{th} for a bipolar droplet was computed using the equation;

$$V_{th} = \frac{d}{R} \left[\frac{K(l^2 - 1)}{\epsilon_0 \Delta\epsilon} \right]^{1/2} \left[\frac{2\sigma_{Pol} + \sigma_{LC}}{3\sigma_{Pol}} \right]$$

or

$$V_{th} = \frac{d}{R} \left[\frac{K(l^2 - 1)}{\epsilon_0 \Delta\epsilon} \right]^{1/2} \frac{1}{3} \left[2 + \frac{\rho_{Pol}}{\rho_{LC}} \right]$$

or

$$V_{th} = \frac{d}{cR} \left[\frac{K(l^2 - 1)}{\epsilon_0 \Delta\epsilon} \right]^{1/2} \quad (3)$$

$1/c$ is related to the effectiveness of the field across the droplets due to a dielectric or conductivity mismatch between the LC droplets and surrounding polymer matrix [23].

The prefactor 'c' is given by $\frac{3\sigma_{Pol}}{(\sigma_{LC} + 2\sigma_{Pol})}$.

Separating out the temperature dependent terms, Eq. (3) can be written in the form [11, 26]

$$V_{th} \propto (K/\Delta\epsilon)^{1/2} \quad (4)$$

Both K and $\Delta\epsilon$ are the function of the liquid crystal order parameter and they decrease with increasing temperature and thus V_{th} also behaves in the same manner as predicted by the theory [27].

Wu et al. [23] and Kelly et al. [24] also considered this criteria for PDNLC films and correlated it to the V_{th} through the factor 'c' [Eq.3].

In this system, we observed an unusual behaviour of V_{th} as a function of temperature (i.e. V_{th} increases with increasing temperature). We have tried to explain this behaviour on the basis of average droplet size distribution in the matrix and reduction of effective voltage

across the nematic liquid crystal droplets in a dielectric film when subjected to an alternating electric field. The ionic conductivity may have also contributed to this effect (both the LC as well as the polymer are commercially available materials and may contain some ionic impurities). Figure 3.2(a-d) [extracted from the optical textures given in Fig. 3.1] represents a schematic illustration of how field-induced effect on the LC droplets embedded in the polymer matrix may reorient at various field intensities. We believe that the external field may not act directly on the LC droplet, thus giving rise to generation of extra- charges stored (space charges due to interfacial polarization) at the polymer liquid crystal interface and other disclination sites.

From Eq. 1(a, b) and Eq. 3 it can be seen that V_{th} is inversely proportional to effective field across the LC droplets. The role of conductivity in PDLC films is more complex than other systems due to the inhomogeneous nature of the cell. In PDLC films, the ionic movements can set up a depolarization field with the application of an applied electric field. Depolarization field opposes the applied field and reduces the effective field across the LC droplet. The competition between the depolarization field and the applied field at higher voltage may in turn reduce the total effective field across the LC droplet thus contributing to the higher V_{th} .

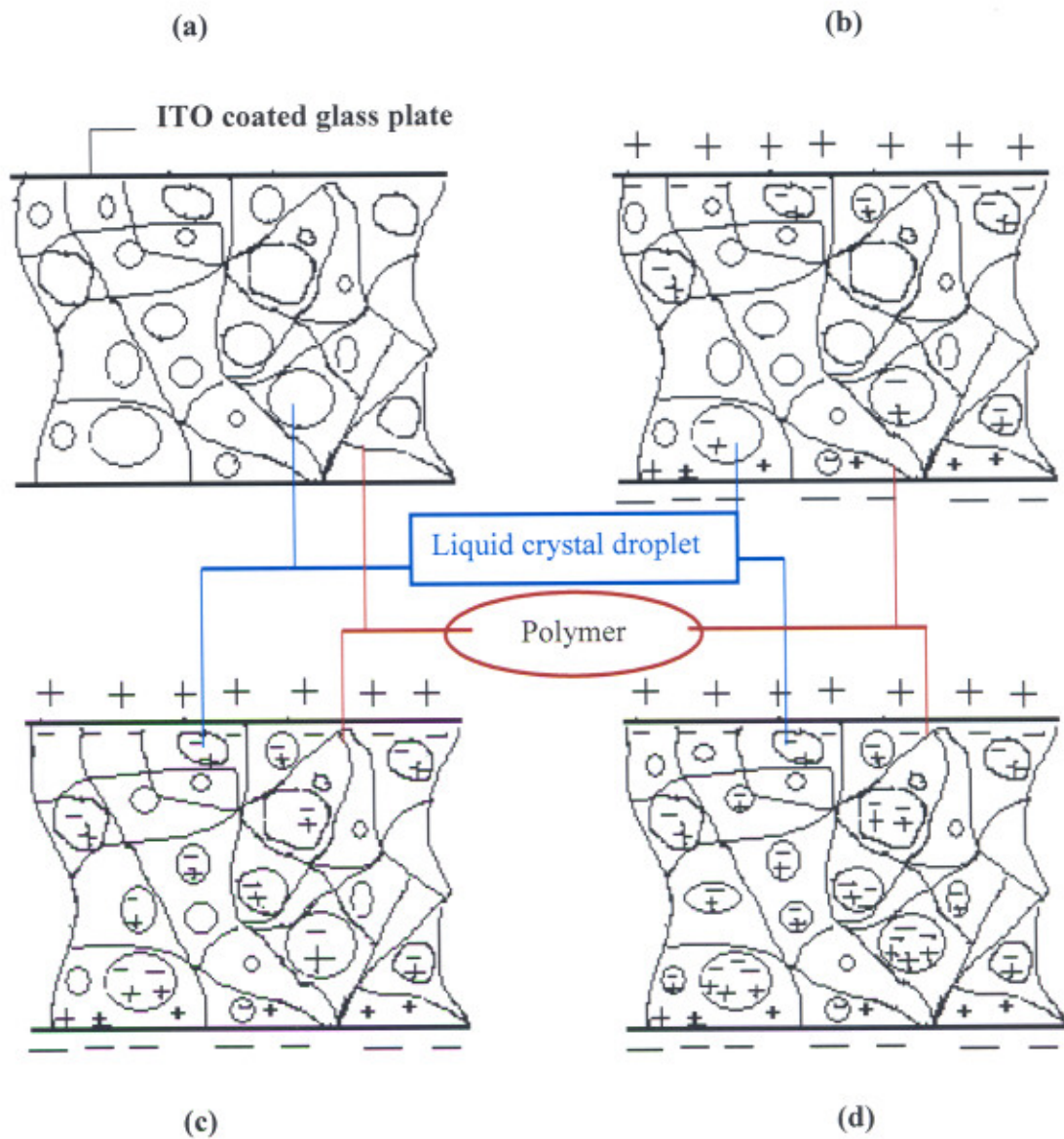


Fig. 3.2 Hypothetical illustration of field induced effect on LC droplets embedded in polymer matrix

3.2.1.3 Thermo-optic responses

The voltage dependence of the output transmission at different temperatures at a frequency of 50 Hz is shown in Fig. 3.3. It depicts that as temperature increases, the transmission curve shift to higher applied voltage and about 85% optical transmission was achieved at field strength of $2\text{V}/\mu\text{m}$. The transmission characteristics corresponding to V_{10} , V_{50} and V_{90} are shown in Fig. 3.3 [inset].

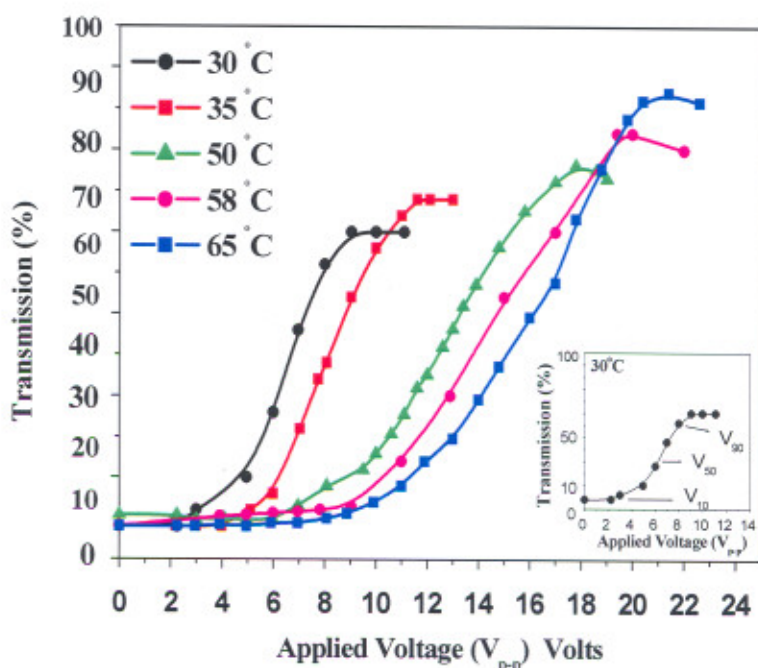


Fig. 3.3 Applied voltage dependence of the output transmission at different temperatures

V_{10} , V_{50} , and V_{90} refer to the applied voltage required to achieve 10%, 50% and 90% of the ultimate transmission at saturating voltages respectively. A closer explanation of the temperature dependence on the variation of applied voltage corresponding to different threshold voltages (V_{10} , V_{50} and V_{90}) is shown in Fig. 3.4. The threshold voltage across the LC droplets increases with the increase of temperature due to the increase of conductivity of composite films. It can be seen from Fig. 3.5(a, b) that LC droplet size is independent of applied voltage and temperature. Figure 3.5(a) shows that below $10V_{p-p}$, significant change in LC droplet size was observed. However above $10V_{p-p}$, droplet size was almost independent of temperature and applied voltage.

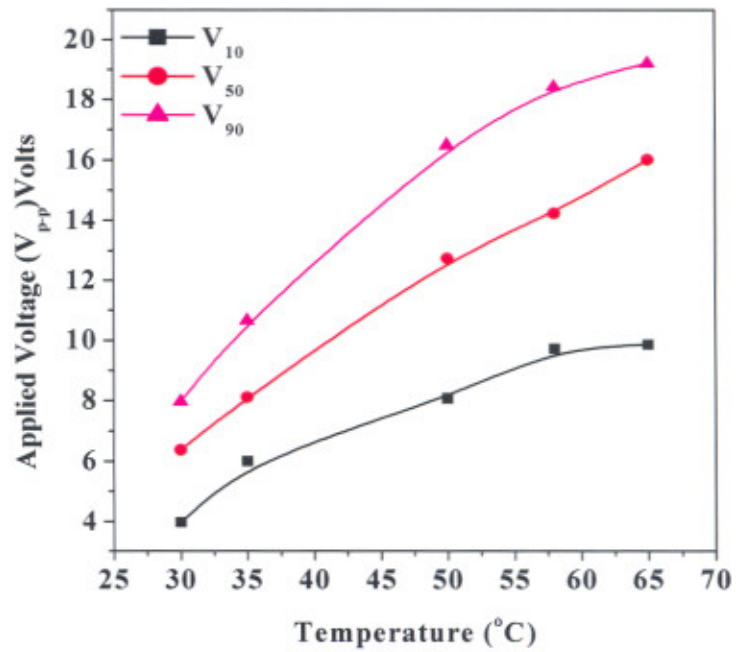
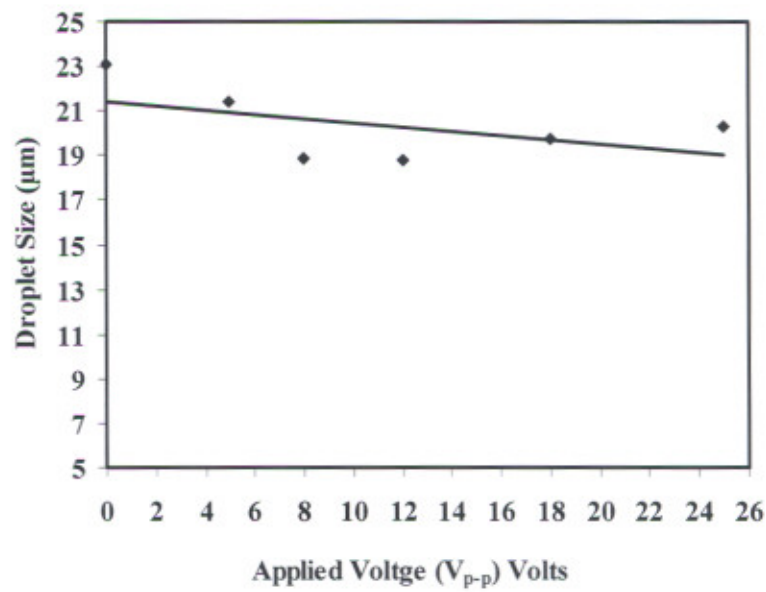


Fig. 3.4 Temperature dependence of the applied voltage corresponding to V_{10} , V_{50} and V_{90}



(a)

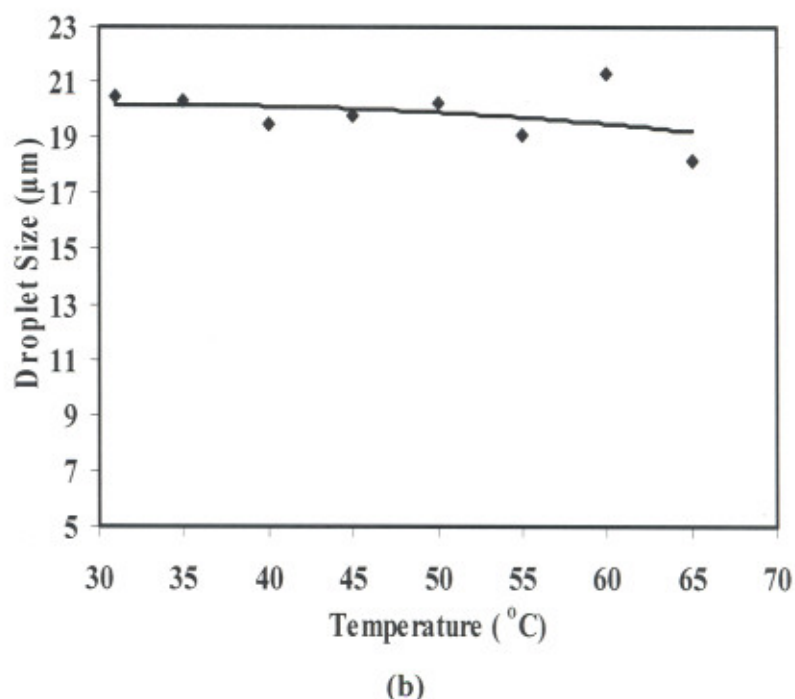


Fig. 3.5 Variation of liquid crystal droplet size as a function of (a) applied voltage at 55°C and (b) temperature at constant applied voltage (20V_{p-p}, $f = 1$ kHz)

3.2.2 Guest-host polymer dispersed nematic liquid crystals

3.2.2.1 Droplet Morphology

Figure 3.6 shows a typical illustration of the molecular arrangement of dye and LC in polymer matrix in the GHPDNLC sample without and with electric field. In the absence of electric field, the LC droplet and dye molecules were randomly distributed in polymer matrix. However few dye molecules get elongated towards LC molecules due to their inherent property (i.e. dye molecules align towards the LC molecule) and others aligned completely in the direction of applied electric field of sufficient strength. A blue color indicates the dichroic dye mixed in liquid crystal droplet as shown in Fig. 3.6.

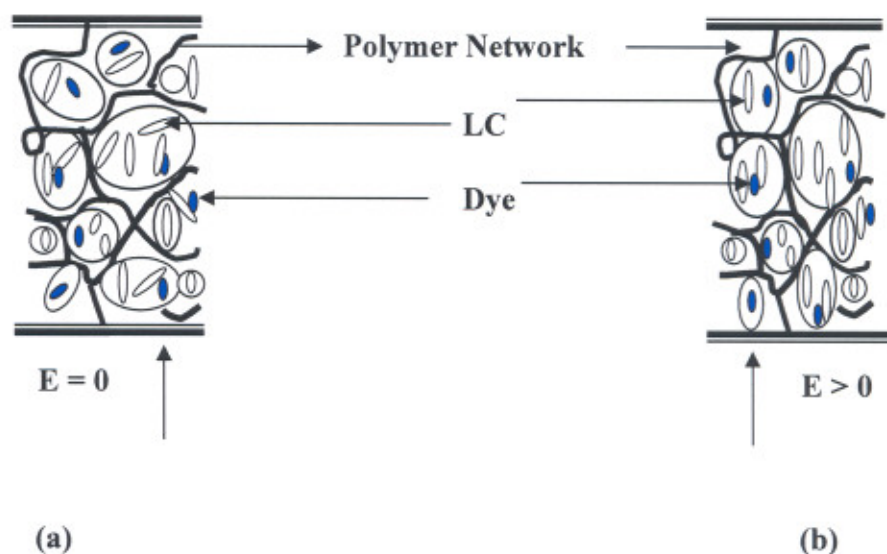
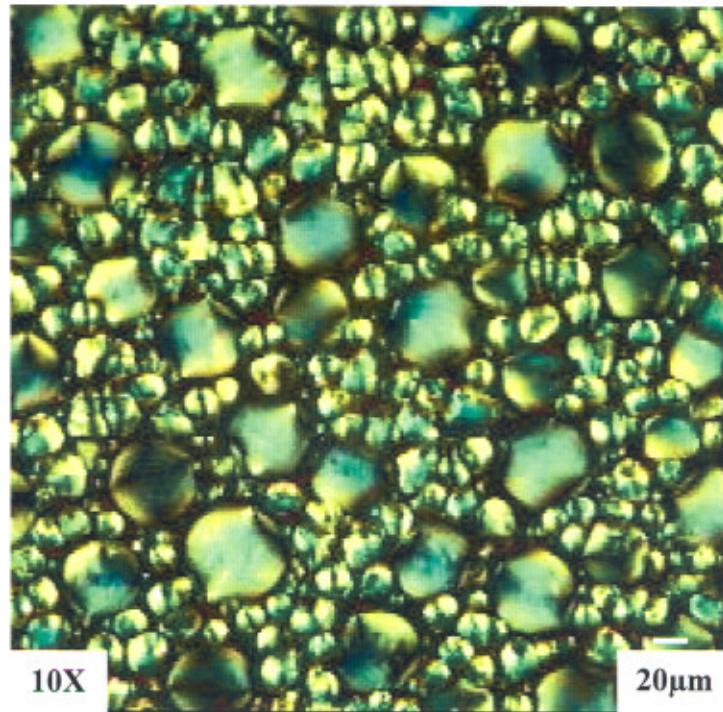
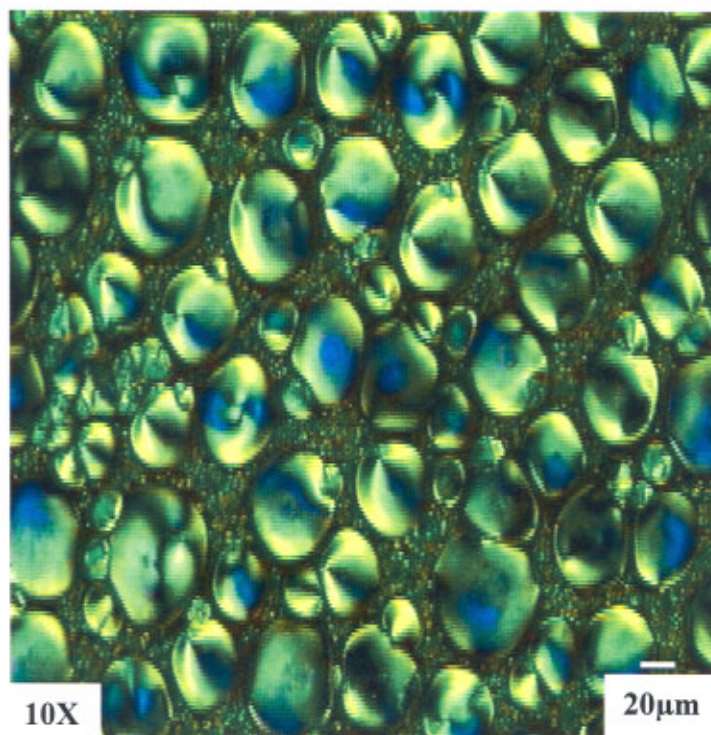


Fig. 3.6 Schematic representation of LC and dye molecular arrangements in GHPDNLC sample cell without and with electric field, (a) $E = 0$ and (b) $E > 0$

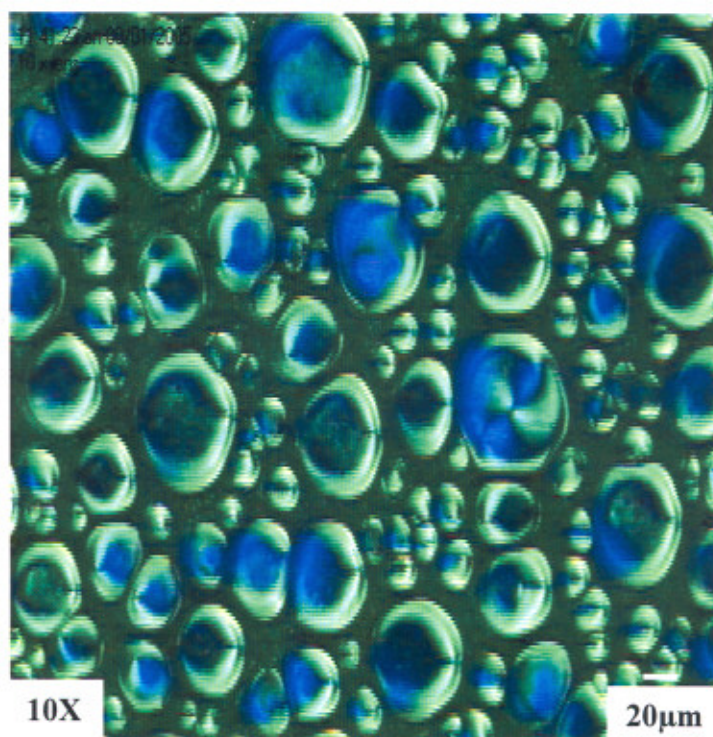
The effect of small amount of dichroic dye (1%, 2% and 4%) wt./wt. on LC droplet dispersed in polymer matrix in the absence of bias field is shown in Fig. 3.7. Here we noticed that with increase of dye concentration (from 1% to 4%), the absorbance in 4% GHPDNLC sample is higher than 2% and 1% samples respectively. Fig. 3.8 shows the UV-VIS spectra in the anthraquinone dye corresponding to 1% and 4% GHPDNLC samples. We believe that the higher absorption on 4% concentration leads to lower transmission of the guest host device. Thus 1% guest-host sample gives better transmission than higher dye concentration samples. The obtained micro-texture in Fig. 3.7 shows that bipolar configuration is dominant in comparison to others configurations (radial, axial). The size of LC droplets was noticed in the range of $\sim 10\text{-}40\ \mu\text{m}$ in all the systems and their sizes are independent of electric field and temperature.



(a)



(b)

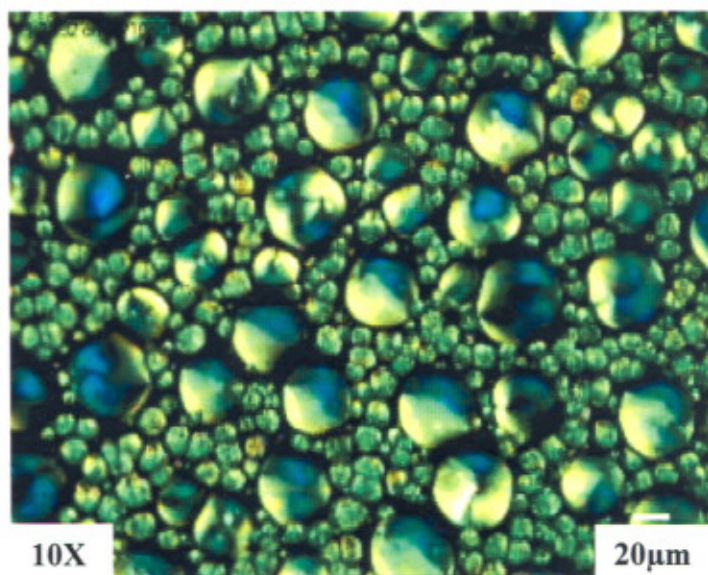


(c)

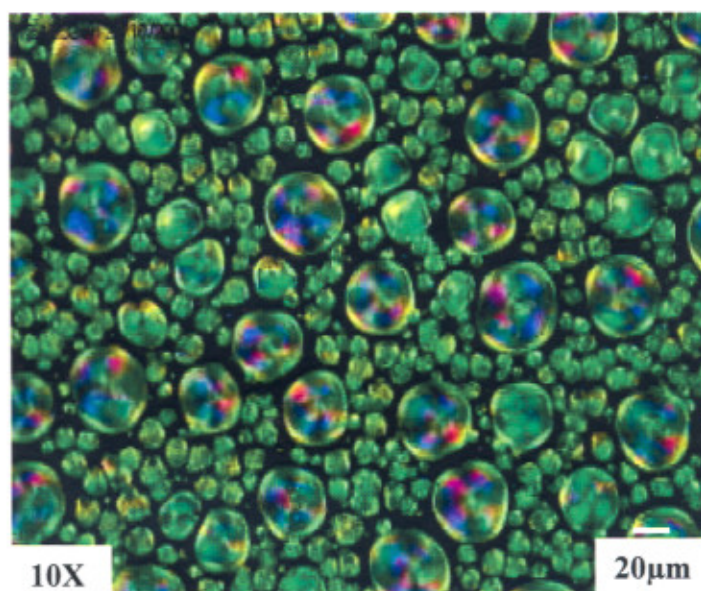
Fig. 3.7 Influence of dye concentration (a) 1% (b) 2% and (c) 4% on LC droplet morphology in polymer matrix

3.2.2.2 Electro-optic responses

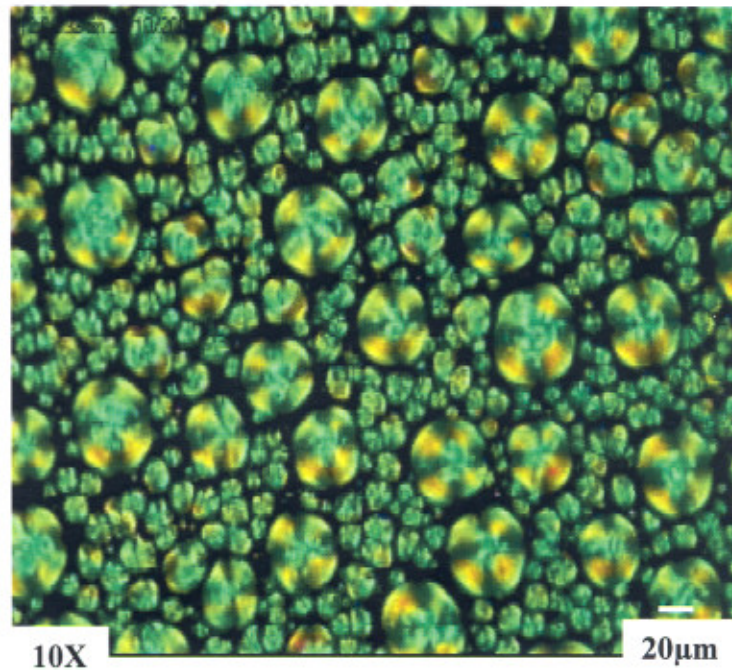
At relatively low voltage ($\sim 10V_{p-p}$) it was observed that the LC droplet orientation does not change vary much, however at higher voltage ($\sim 80V_{p-p}$) maltese type crosses [Fig. (3.8)] were appeared in the 1% dye concentration guest-host sample. Similar droplet behaviour was observed for 2% and 4% guest-host samples but relatively at higher voltage. The increase in applied voltage with increasing dye concentration may be due to the partial increase of viscosity of the GHPDNLC samples.



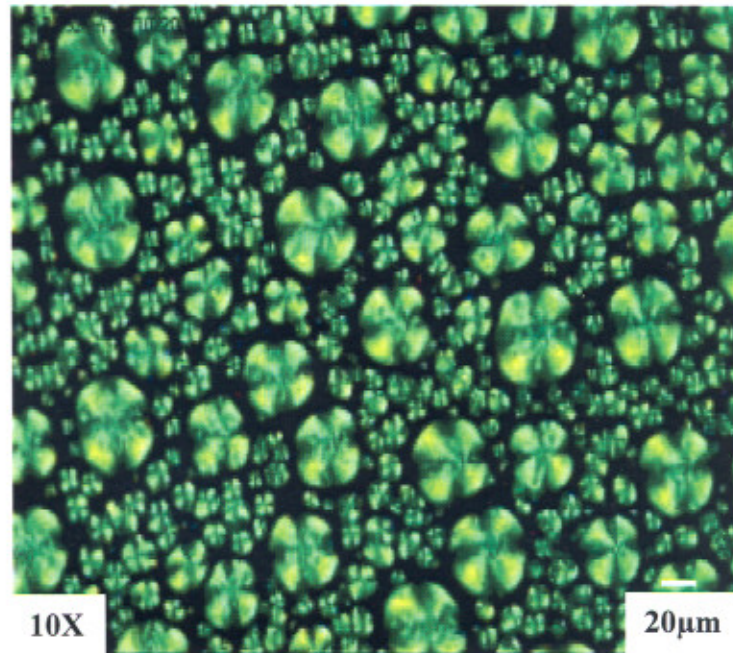
(a)



(b)



(c)



(d)

Fig. 3.8 Optical textures of GHPDNLC sample at various applied voltage ($f = 500\text{Hz}$) (a) $0V_{P-P}$ (b) $10V_{P-P}$ (c) $30V_{P-P}$ and (d) $100V_{P-P}$ at room temperature

The optical transmission as a function of applied voltage dependence at different dye concentration is given in Fig. 3.9. It shows that about 55% transmission can be achieved in ~1% GHPDNLC sample over 2% and 4% GHPDNLC samples. It can be concluded from Fig. 3.9 that ~ 1% dye shows higher transmission than 4% sample.

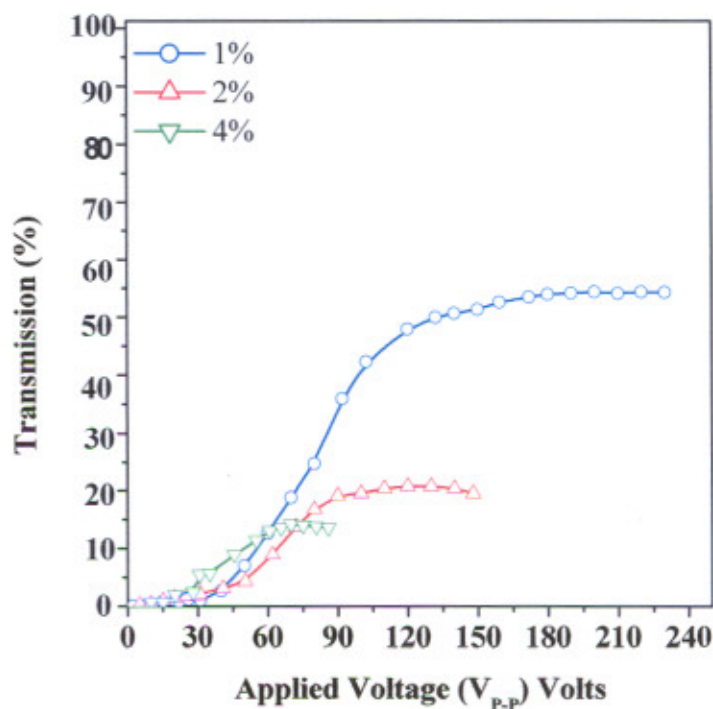


Fig. 3.9 Variation of optical transmission as a function of applied voltage ($f = 500\text{Hz}$) at different dye concentration

3.2.2.3 Thermo-optic responses

The voltage dependence of the output transmission at different temperatures for 1% GHPDNLC sample is shown in Fig. 3.10. It depicts that as temperature increases, the transmission increases primarily due to the decrease in order parameter. Similarly Fig. 3.11 shows temperature dependence on transmission characteristic. It is seen that the optical transmission increases non-linearly at lower voltage but at higher voltage there is a steep rise in transmission preferentially due to strong alignment of LC molecules with the external field.

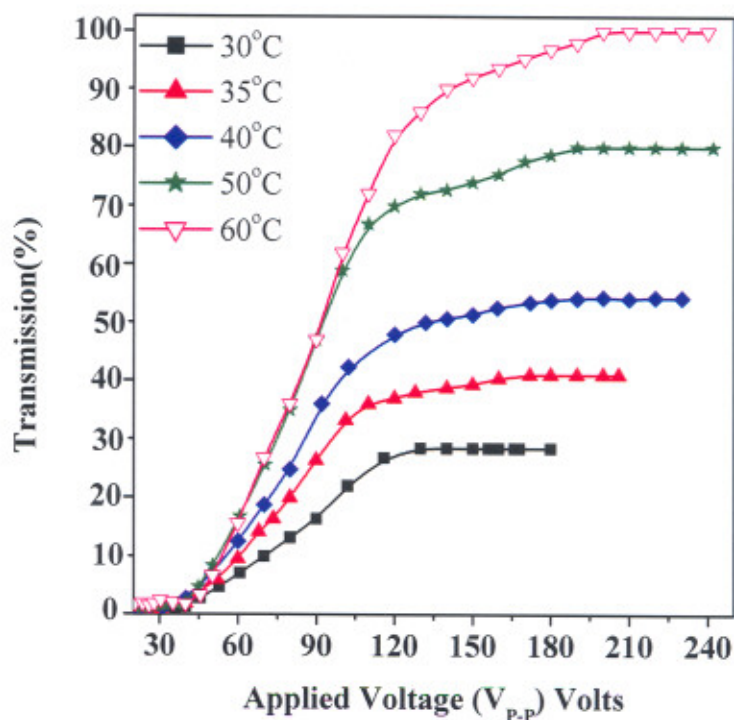


Fig. 3.10 Variation of optical transmission as a function of applied voltage ($f = 500$ Hz) at different temperatures for 1% dye concentration GHPDNLC sample

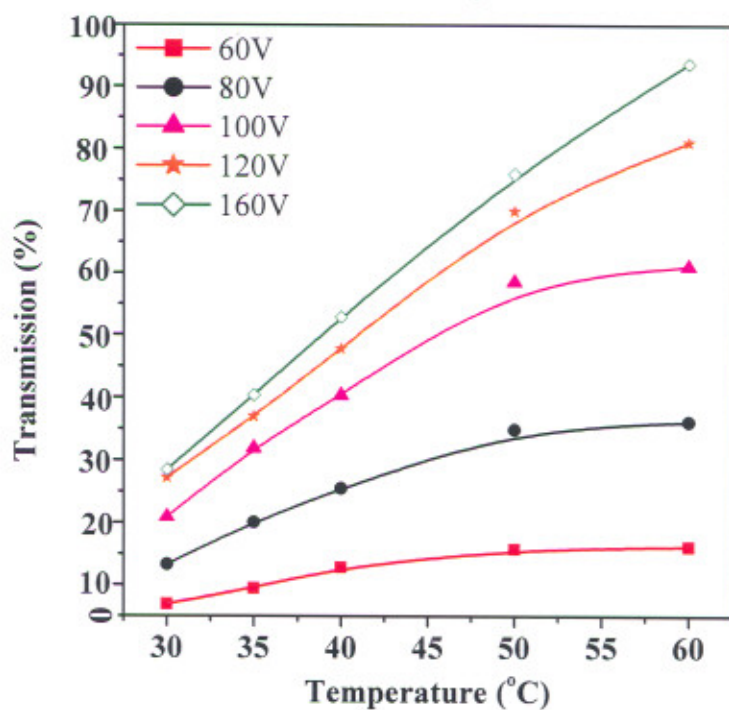


Fig. 3.11 Optical transmission as a function of temperature at different applied bias voltage

A closer explanation of the temperature dependence on the variation of applied voltage corresponding to different threshold voltages (V_{10} , V_{50} and V_{90}) is shown in Fig. 3.12. The slight increase in applied voltage with temperature may be due to the increase in conductivity of the composite films because of nature of multi-component systems [28].

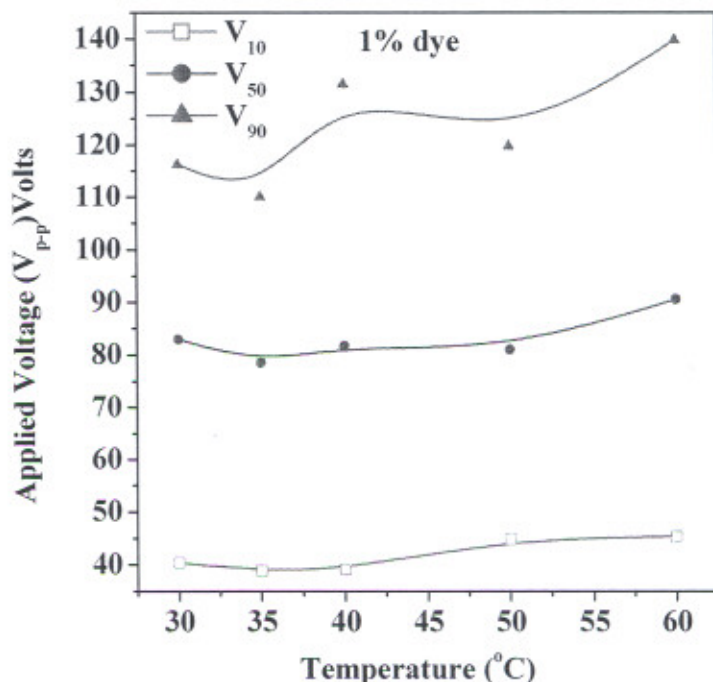


Fig. 3.12 Bias voltage as a function of temperature at V_{10} , V_{50} and V_{90}

3.2.2.4 Electro-optic responses

The optical response time such as rise time (τ_r) allows us to define not only the electro-optical properties of the condensed materials but allow their performance for practical applications. τ_r is defined as the time required for transmission change from 10 to 90% upon switching the film ON.

The response time is computed as [13].

$$\frac{1}{\tau_r} = \frac{1}{\gamma_1} \left[\Delta\epsilon E^2 + \frac{K(I^2 - 1)}{R^2} \right] \quad (5)$$

Where γ_1 is the rotational viscosity coefficient, E is the applied electric field, and other symbols bear the same meaning defined earlier. For larger voltages, τ_r is given by

$$\tau_r \cong \frac{\gamma_1}{\Delta\epsilon E^2} \quad (6)$$

$$\text{or } \tau_r \propto \frac{1}{E^2}$$

Fig. 3.13 shows the voltage dependence of the magnitude of response time at different dye concentration. It can be seen that τ_r decreases with increasing the applied voltage and follow the same behaviour as predicted by the theory (Eq.6). A fluctuating behaviour was noticed at 2% dye concentration GHPDNLC sample. It may be due to the some other different dynamic responses when the system passes from ON to OFF state. It was found that ~1% GHPDNLC sample shows faster response time than 4% GHPDNLC.

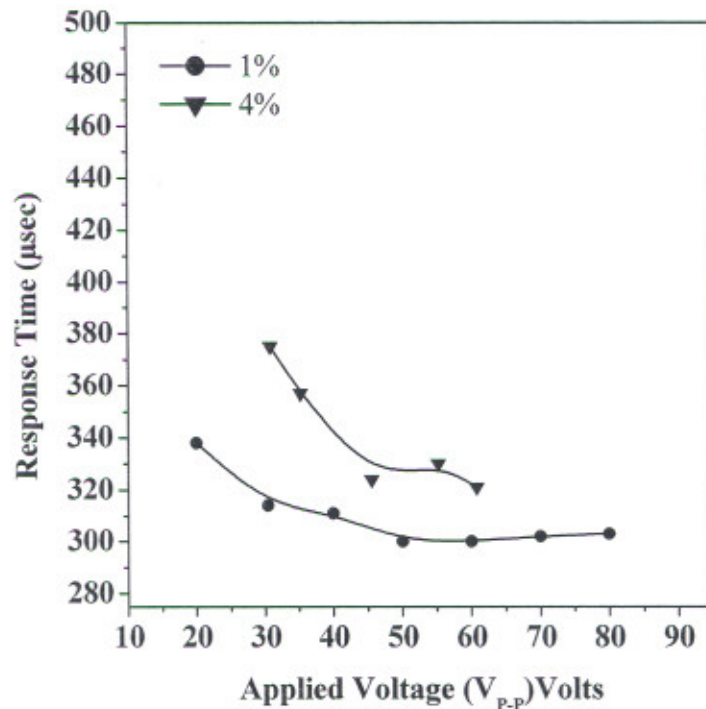


Fig. 3.13 Response time of a GHPDNLC samples as a function of bias voltage

REFERENCES

- [1] A. Y. G. Fuh, K. L. Hung, C. H. Lin, H. C. Lin and I. M. Jiang, *Chinese J. of Phys.*, **28** (1990) 551
- [2] S. C. Jain and R. S. Thakur, *Appl. Phys. Lett.*, **61** (1992) 1641
- [3] B. K. Kim, Y. S. OK and C. H. Choi, *J. Poly. Sci.: Part B: Poly. Phys.*, **33** (1995) 707
- [4] B. K. Kim and Y. S. OK, *J. Poly. Sci.: Part B: Poly. Phys.*, **32** (1994) 561
- [5] S. A. Carter, J. D. Legrange, W. White, J. Boo and P. Wiltzius, *J. Appl. Phys.*, **81** (1997) 5992
- [6] S. D. Bella, L. Lucchetti and F. Simoni, *Mol. Cryst. Liq. Cryst.*, **320** (1998) 139
- [7] F. Simoni and O. Francescangeli, *Intern. J. Polymeric Mater.*, **45** (2000) 381
- [8] L. Lucchetti and F. Simoni, *J. Appl. Phys.*, **88** (2000) 3934
- [9] E. Nastal, E. Zuranska and M. Mucha, *J. Appl. Poly. Sci.*, **71** (1999) 455
- [10] R. Karapinar, *Tr. J. of Phys.*, **22** (1998) 227
- [11] J. W. Han, *Liq. Cryst.*, **28** (2001) 1487
- [12] K. Amundson, *Phys. Rev. E.*, **53** (1996) 2412
- [13] A. Y. G. Fuh, T. C. Ko, Y. N. Chyr, C. Y. Hung, *Jpn. J. Appl. Phys.*, **32** (1993) 3526
- [14] S. C. Sharma, L. Zhang, A. J. Tapiwala, P. C. Jain, *Phys. Rev. Lett.*, **87** (2001) 105501
- [15] L. Petti, P. Mormile and W. J. Blau, *Opt. and Las. Engg.*, **39** (2003) 369
- [16] L. Petti, P. Mormile, Y. Ren, M. Abbate, P. Musto, G. Ragosta and W. J. Blau, *Liq. Cryst.*, **28** (2001) 1831
- [17] J. J. Wu, C. M. Wang, W. Y. Li and S. H. Chen, *Jpn. J. Appl. Phys.*, **37** (1998) 6434
- [18] S. H. Lee, T. K. Lim and K. S. Park, *J. Appl. Phys.*, **83** (2002) 208
- [19] J. Zhou, L. Petti, P. Mormile and A. Roviello, *Optics Communications*, **231** (2004) 263
- [20] J. J. Wu, C. M. Wang, and S. H. Chen, *Jpn. J. Appl. Phys.*, **35** (1996) 2681
- [21] G. H. Springer and D. A. Higgins, *J. Am. Chem. Soc.*, **122** (2000) 6801

- [22] D. A. Higgins, J. E. Hali and A. Xie, *Acc. Chem. Res.*, **38** (2005) 137
- [23] B. G. Wu, J. H. Erdmann and J. W. Doane, *Liq. Cryst.*, **5** (1989) 1453
- [24] J. Kelly and D. Seekola, *Proc. SPIE*, **1257** (1990) 17
- [25] J. Erdmann, J. W. Doane, S. Zumer and G. Chidichimo, *Proc. SPIE*, **1080** (1989) 32
- [26] J. W. Han, T. J. Kang and G. Park, *J. Kor. Phys. Soc.*, **36** (2000) 156
- [27] S. Chandrashekar, *Liq. Cryst.* 2nd Edn., Cambridge University Press (1992)
- [28] P. Malik and K. K. Raina, *Opt. Mat.*, **27** (2004) 613

Chapter -4

Polymer Dispersed Ferroelectric Liquid Crystal Systems

Overview

During the last three decades, FLC has gained incredible importance due to their novel electro-optic behaviour, fast switching speed and memory effects. Their dispersion in polymer matrix has further increased way for their use as fast switching flexible displays materials. An effort has gone in to investigate their FLC properties in UV curable adhesive with varying polymer viscosities and surface properties. A complete electro-optic characterization was made.

4.1 Review of Literature

Ferroelectric liquid crystal (FLC) are known for very fast switching electro-optic effects. Switching time of about few μsec or even less is not unusual in these materials. Thus efforts have been made to use these LC materials for PDLC devices.

The dispersion of ferroelectric smectic C liquid crystal in a polymer matrix gives rise to several interesting electro-optic effects. The switching field of polymer dispersed PDFLC sample depends on a variety of factors amongst which film morphology plays a crucial role [1-3]. This is determined by composition, cure rate, nature, kind of polymer and also the mutual solubility of ferroelectric liquid crystal and pre-polymer [4-6]. It is thus obvious that PDFLCs are very complex systems that require precise morphological and processing control. Several research groups [7-8] investigated the behavior of ferroelectric liquid crystal (FLC) in polymer matrix although little effort has gone into understanding their morphological behavior on the basis of polymer viscosity and different configurations.

In contrast to nematic and cholesteric, the value of response time (τ) was two order of magnitude higher than the switching times of the pure monomer, while the value of spontaneous polarization and phase transition temperature were slightly lower than expected.

In this chapter an attempt has been made to study the effect of polymer viscosity and surface treatment on the switching properties and droplet morphology and other physical parameters. Phase separated unaligned and aligned PDFLC samples were investigated. A brief literature review in this area by various researcher and technologists are given. Komitov et al. [9] obtained a pre-alignment of the liquid crystal by stretching the PDFLC film prepared by TIPS method and obtained a switching time of 128 μsec at 60V_{p-p}. Karapinar et al. [10] reported the electro-optic properties of FLC material dispersed in polymer matrix and aligned the FLC by shearing during the phase separation process. Shearing was done by gently shearing a slide during the exposure of the sample to UV light. Zyryanov et al. [11] have created a scattering PDLC display using a FLC material DOBAMBC.

Lee et al. [8] studied very large elliptical droplets, which are attached to the surfaces of an aligning substrate and investigated that rubbing process in PDFLC significantly

improves the electro-optic switching times. This group suggested that the phase sequence and pitch ($<4 \mu\text{m}$) of FLC material also influence the size and shape of LC droplets. Molsen et al. [12] predicted that a bistable switching effect occurs in PDFLC films when the droplet size is sufficiently small. Patel et al. [13] have observed bistable switching in PDFLC samples using the ferroelectric mixture ZLI-3654.

Heppke et al. [14] reported the electro-clinic effect in chiral smectic A material dispersed in UV polymer and noticed switching time 100 μsec to 170 μsec . Pozhidaev et al. [15] studied PDFLC samples and compared the electro-optic properties with pure FLC (FLC 3309C) material. The spontaneous polarization (P_s) value decreases one order of magnitude in comparison to pure FLC material. He suggested that a decrease in P_s may be due to the non-switching region existed near the polymer boundaries and strong anchoring of LC droplet with the polymer wall. An increase in SmC*/SmA* transition in PDFLC sample by about 4.1K higher than FLC was noticed. This unexpected shift may be due to strong interaction with the surrounding polymer.

Kundu et al. [16] reported the influence of UV polymer on electro-optic properties of FLC in PDFLC samples and observed a decrease in P_s and increase in switching time.

Uniformly aligned droplets of small size can also be used to achieve multi-stable switching by means of anti-ferroelectric liquid crystal. The possibility of aligning FLC in PDFLC film by shearing or stretching provides the application of linear, bistable and multi-stable effects with switching times down to 20 μsec .

A summary of the earlier investigation reveals that in PDFLCs (a) thicker cells gaps can be employed, which simplifies manufacturing (b) the polymer induces added stability to protect against mechanical shock failure (c) the feasibility of PDFLC in fast switching application is expected to lead to many exciting basic studies in the future.

4.2 Experimental

4.2.1 Polarization switching effects

It is one of the most precise methods for the measurement of electro-optic parameters in FLC and PDFLC materials [17]. The experimental setup used for the measurements of electro-optic parameters is shown in the Fig 4.1. Here the triangular voltage (V_{IN}) is applied across the PDFLC sample and the output (V_o) is taken across a standard resistor R. The electric field was applied to the PDFLC sample through an electrode connected to conducting ITO substrates by a function generator and output is obtained on a four channels digital storage oscilloscope (Tektronix TDS 2024 having 2.0 GS/s sample rate and 200 MHz bandwidth) interfaced with computer for further data acquisition. The current and voltage pulses were detected on a digital storage oscilloscope across a resistor.

In order to study the molecular re-orientation processes associated with the helix dynamics, the symmetric triangular wave pulses were applied to the samples. It reorients the dipoles between two stable polarization states (Up and Down). As the field is switched on, molecular alignment in the form of voltage drop is detected on the storage oscilloscope.

We believe that in the PDFLC sample within the ferroelectric phase range, for a certain applied voltage V_{IN} , the current I response consists

- (a) capacitive term I_C (a differentiating component which shows an abrupt jump when the slope of applied voltage changes abruptly)
- (b) ionic conduction term I_R
- (c) the third term is polarization current I_P , due to the charge induced by the dipole realignment in the form of polarization hump.

The schematic representation of these responses is shown in Fig. 4.2.

The Instantaneous value of the output current over resistor R can be presented as

$$I = I_R + I_C + I_P = \frac{V_{IN}}{R} + C \frac{dV_{IN}}{dt} + \frac{dP}{dt} \quad (4.1)$$

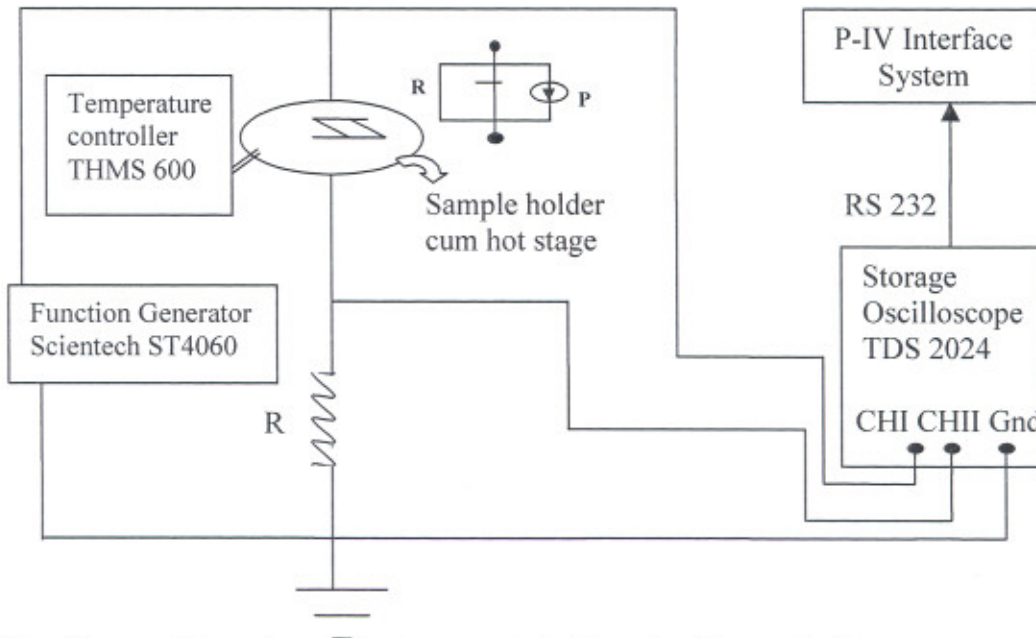


Fig. 4.1 Experimental set up to study the polarizing switching response using reversal field technique

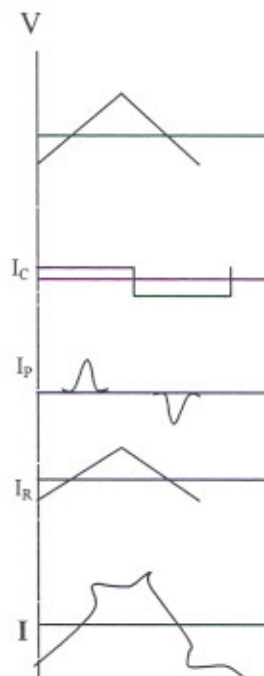


Fig. 4.2 Waveform of the output waveform by the resistor method

4.2.2 Measurement of spontaneous polarization (P_s)

The spontaneous polarization is the macroscopic polarization, which the sample attains due to the coupling of molecular polarization P with the electric field E within the smectic layer. The sample gets poled and attains a macroscopic polarization. At this stage the helix of the FLC in PDFLC mixture confined in the cell of a particular thickness unwinds, the macroscopic polarization becomes non-zero and the sample gets spontaneously polarized. This polarization was determined by applying the symmetric triangular wave (100Hz frequency and sufficient voltage) and separating the resistive and capacitive term from the polarization term by drawing a base line.

The hump of the polarization is directly associated with dipole reorientation, corresponding to the switching between uniform stable states. Every reorienting dipole imparts a charge impulse and contributes to the polarizing reversal peak. Thus the peak incorporates total contribution of reorientation dipoles while switching between uniform states.

The area under the hump is a measure of the spontaneous polarization, which is given by

$$P_s = \frac{A(i \times t)}{R(\text{Area of Sample})} \quad (4.2)$$

Where $A(i \times t)$ is the area under the curve measured by integrating the polarization hump in terms of voltage and time [17,18]. Thus by calculating the area of the curve by knowing current and time representing along the Y-axis and X-axis, respectively the P_s can be determined.

The magnitude of P_s in the ferroelectric phase of PDFLC films decrease with the rise of temperature and finally becomes zero at T_c^*A , it obey the power law and given by the equation

$$P_s = P_o(T_c - T)^\beta \quad (4.3)$$

The critical exponent β should be 0.5 predicted by the mean field theory.

4.3 Results and discussion

4.3.1 Droplet morphology

4.3.1 (a) Unaligned polymer dispersed ferroelectric liquid crystal films

Figure 4.3(a-d) shows the micro-textures of unaligned PDFLC films in order of increasing viscosity at a magnification of 10X. It can be seen from the Fig. 4.3 that LC droplets are randomly distributed in larger and micro LC droplet size in the polymer matrix. It is seen that with increase of polymer viscosity, the droplet size of ferroelectric liquid crystal also increases. The observed droplets are not completely circular thus precise measurements size were measured by taking the mean of major to minor axis droplet diameter of around 25-30 random droplets. The measured LC droplet size was found to be in the range of 5-55 μm . The measured droplet sizes as a function of polymer viscosity are given in Fig. 4.4

According to the Stoke's equation, the terminal velocity V_t of a dispersed droplet driven by the sedimentation force is given as [17,19-20].

$$V_t = \frac{2g(\rho_p - \rho_{LC}) \cdot R^2}{9\mu} \quad (4.4)$$

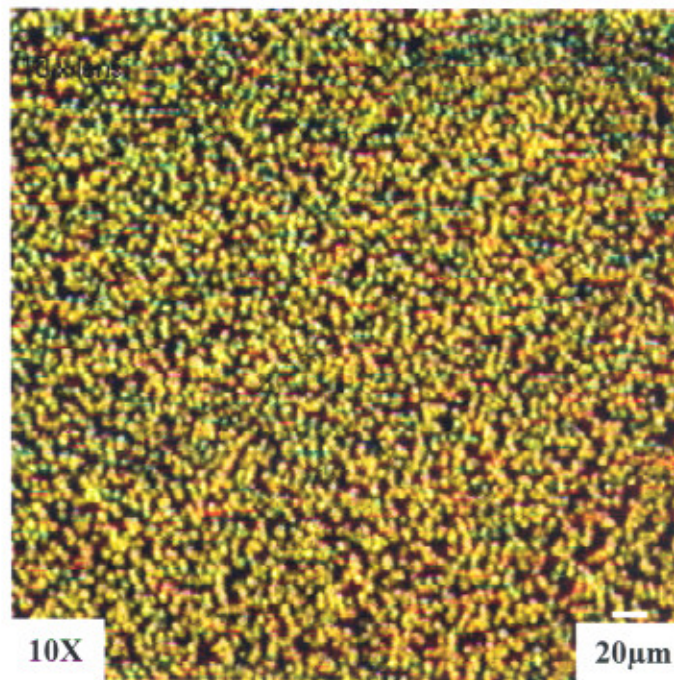
Where

V_t = Terminal velocity of dispersed liquid crystal droplet driven by sedimentation force

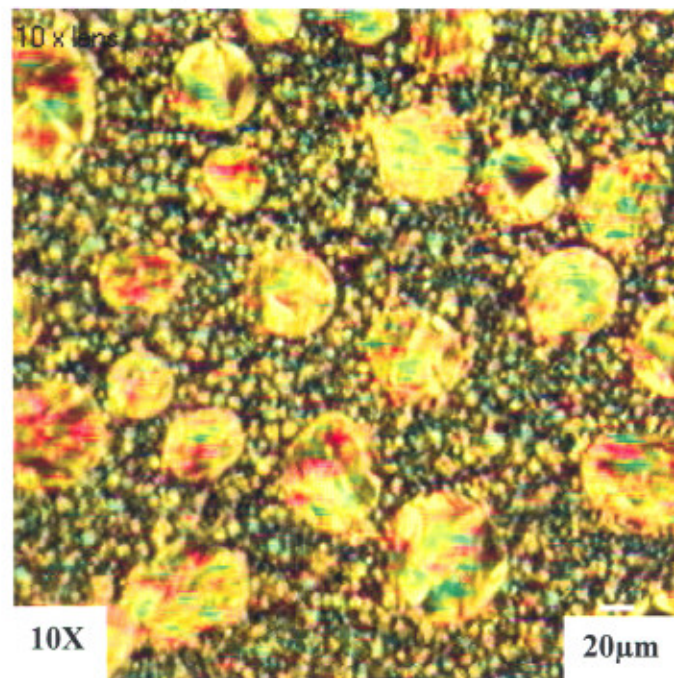
g = Gravitational acceleration

ρ_p, ρ_{LC} = Density of polymer and liquid crystal respectively

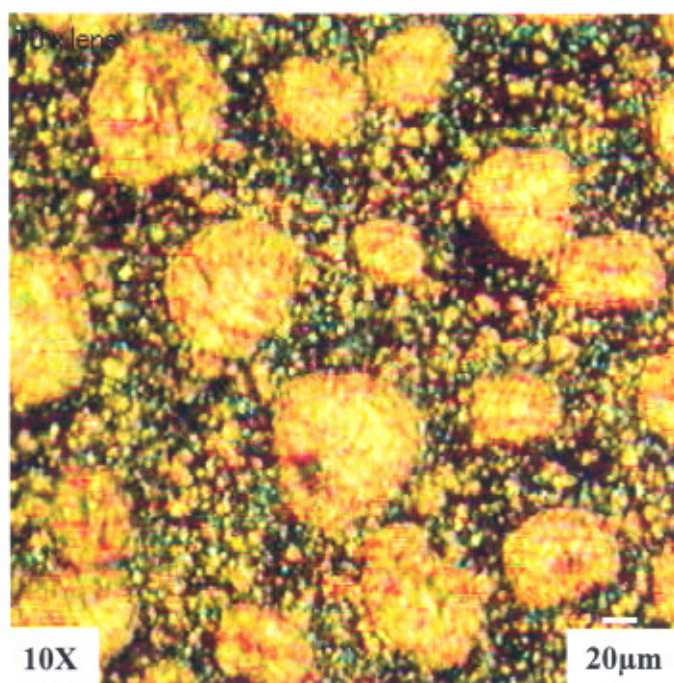
R is the radius of the liquid crystal droplet in PDLC system and μ represent the polymer viscosity. The sedimentation-induced motion can lead to collision between the droplets. As a result the size uniformity of the droplets is expected to be more uniform as ρ_{LC}/ρ_p approaches unity. From the equation (4.4), it is clear that the liquid crystal droplet size and its uniformity are dependent on the sedimentation force as well as the polymer viscosity. As the polymer viscosity increases, the liquid crystal droplet size also increases. The agreement between the theory and our experiments has been found to be good.



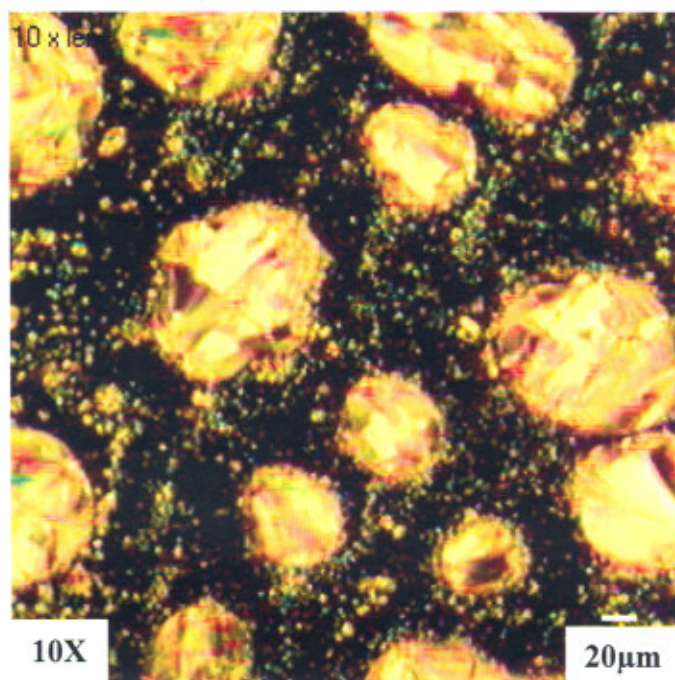
(a)



(b)



(c)



(d)

Fig. 4.3 Liquid crystal droplet morphology of unaligned PDFLC sample at polymer viscosities (CPS) (a) 140 (b) 1000 (c) 2500 and (d) 5000

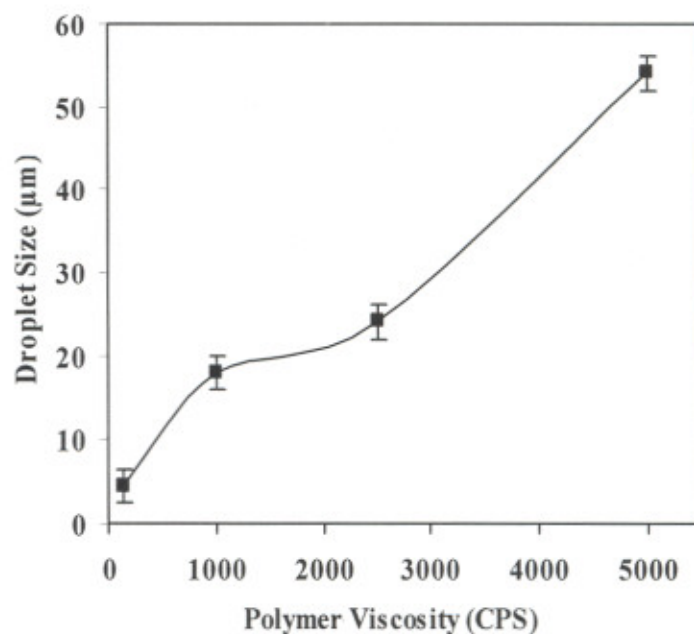
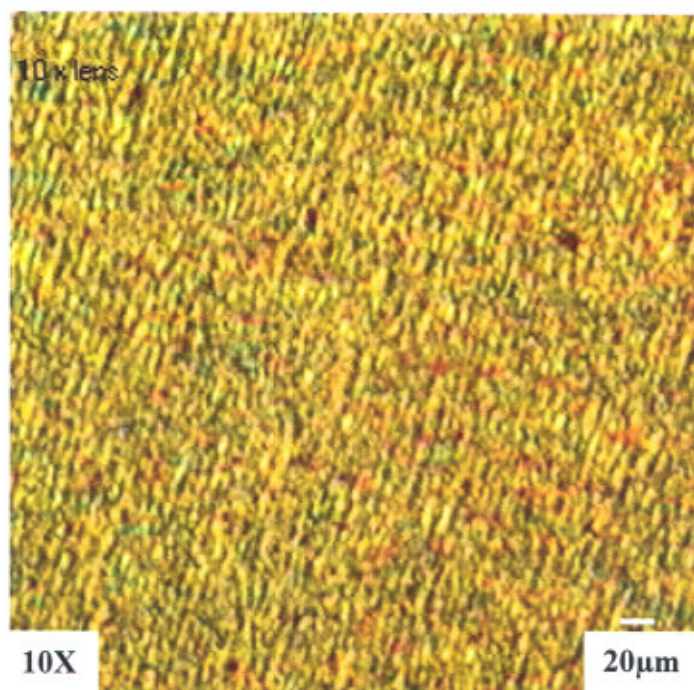


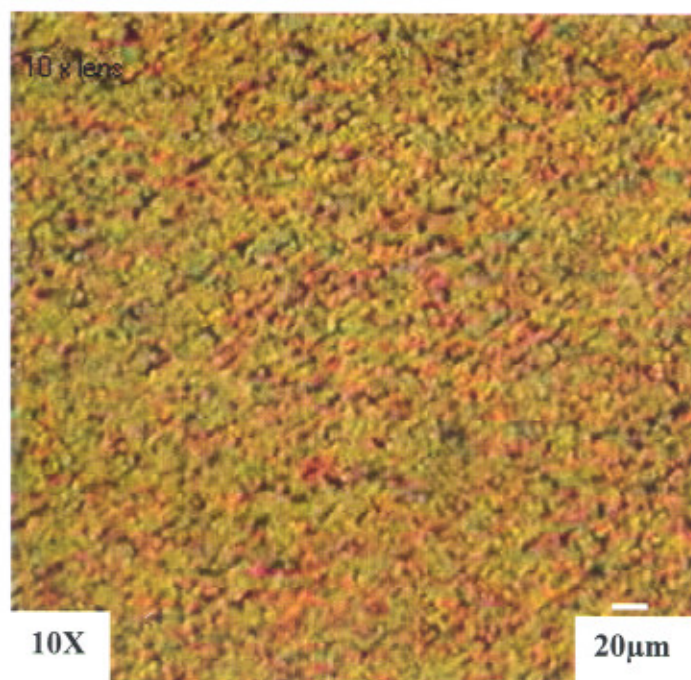
Fig. 4.4 Variation of liquid crystal droplet size as a function of polymer viscosity in unaligned PDFLC at 30°C

4.3.1 (b) Aligned polymer dispersed ferroelectric liquid crystal films

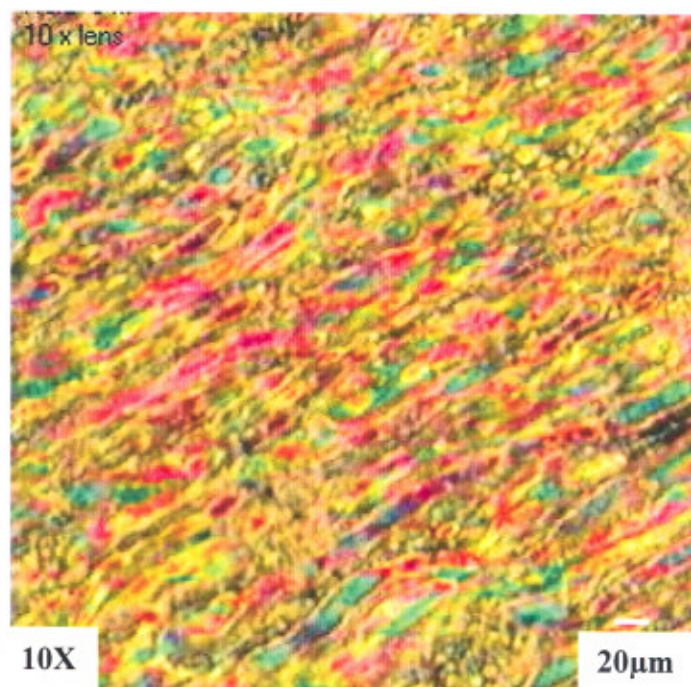
The micro-texture of aligned PDFLCs are shown in Fig. 4.5(a-d) respectively. It is seen that all the liquid crystal droplets are elongated along the rubbing direction but the alignment of liquid crystal droplets decreases with increase of polymer viscosity. Figure 4.5(a) represents that at lower viscosity, all the liquid crystal droplets are well aligned, and that may make it useful for fast switching and flexible displays. In Fig. 4.5(d), it is seen that at higher polymer viscosity liquid crystal droplets are not well aligned as compared to low polymer viscosity PDFLC film. This may be due to the difficulty in droplet formation in high viscous polymer matrix because of the high surface force exerted by polymer on liquid crystal droplets.



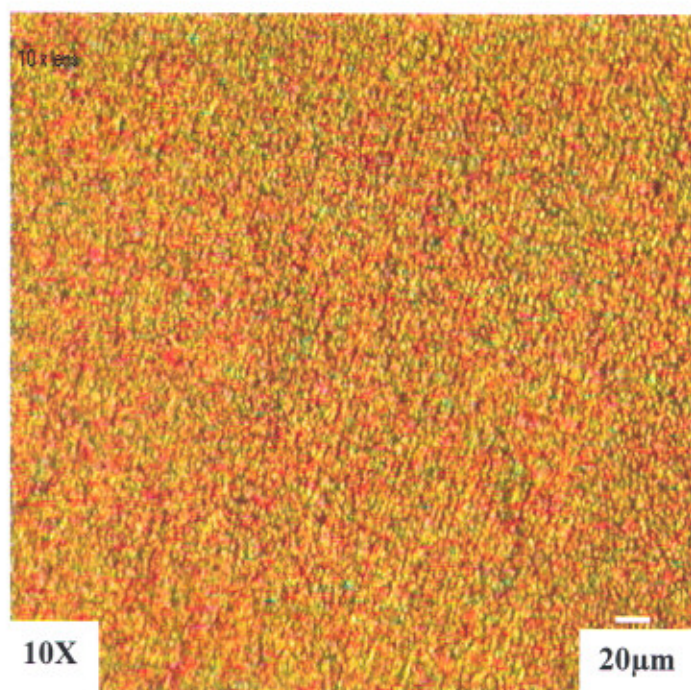
(a)



(b)



(c)



(d)

Fig. 4.5 Polymer viscosity dependence on the alignment of liquid crystal droplets in aligned PDFLC samples at polymer viscosities (CPS) 140 (b) 1000 (c) 2500 and (d) 5000

4.3.2 Electro-optic and thermo-optic studies in PDFLC films

4.3.2(a) Temperature dependence on spontaneous polarization

The spontaneous polarization gives information about the internal structure of the mesophase and also about the quality of the phase separation since it is directly correlated to the fraction of switching molecules.

A symmetric triangular wave applied to PDFLC film reorients the dipoles between two stable polarization states (i.e., UP and DOWN). As the field was switched on, the molecular realignment in the form of voltage drop was detected on the storage oscilloscope across a standard resistance R ($\sim 100 \text{ k}\Omega$).

The spontaneous polarization as a function of temperature for UV cured aligned PDFLC composite films at room temperature 30°C in presence of an applied voltage ($100 \text{ V}_{\text{p-p}}$, 100 Hz) is shown in Fig. 4.6.

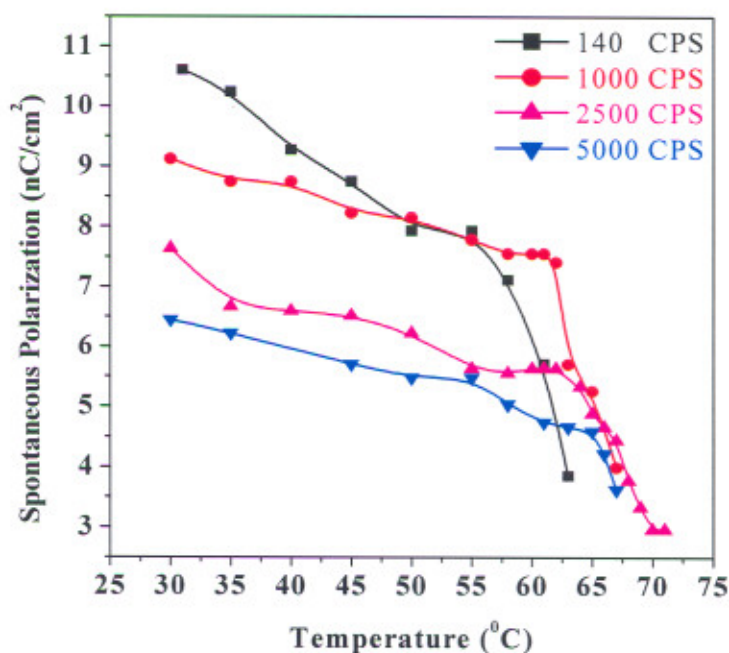


Fig. 4. 6 Temperature dependence on spontaneous polarization in aligned PDFLC sample

The oscilloscope trace for low viscosity (NOA-73) aligned PDFLC systems at different temperature at a fixed applied voltage ($100V_{p-p}$, Freq 100 Hz) are shown in Fig. 4.7.

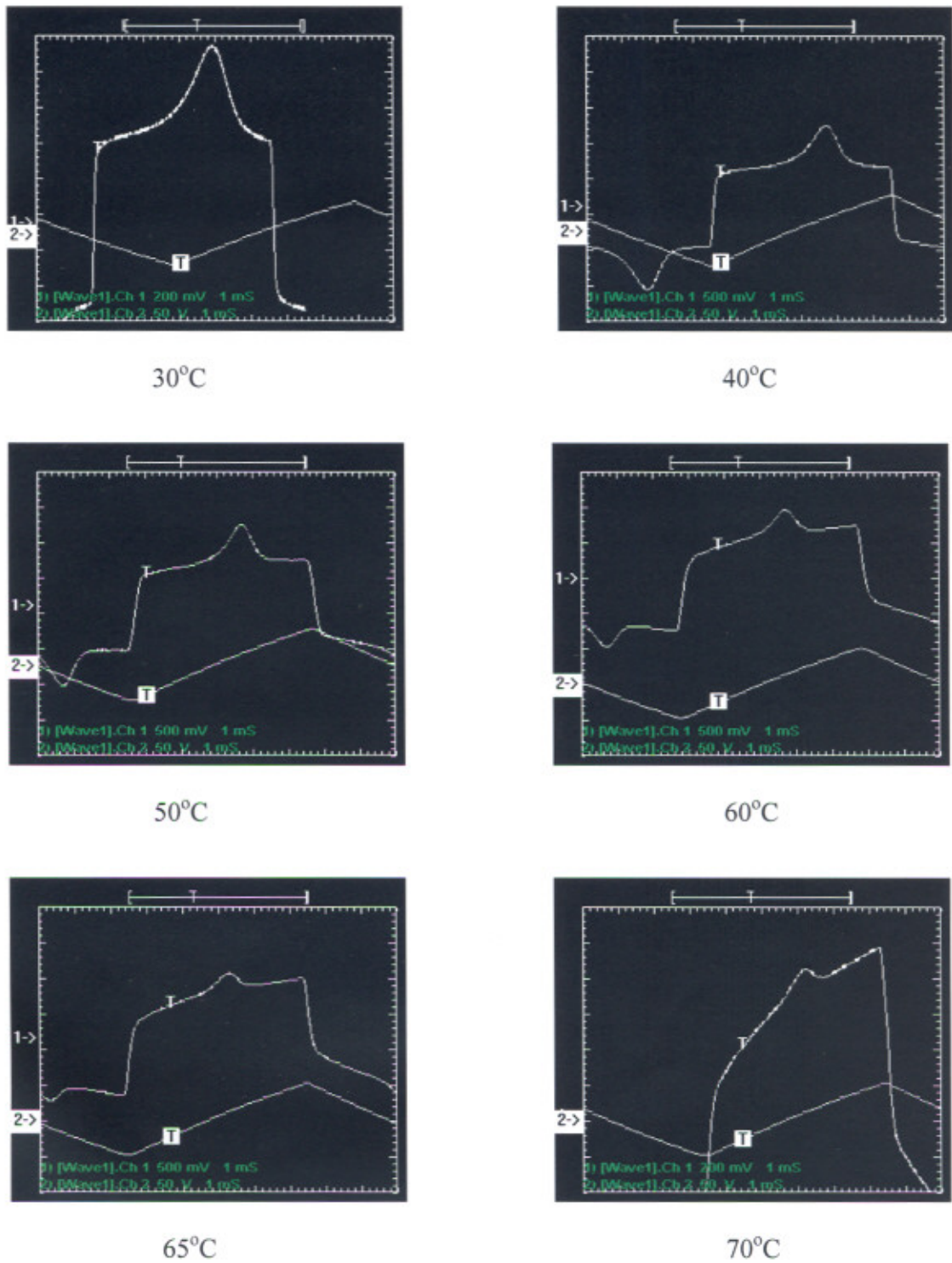


Fig. 4.7 Waveform of polarization hump at different temperatures ($^{\circ}C$)
 (a) 30 (b) 40 (c) 50 (d) 60 (e) 65 and (f) 70

It was observed that the peak area of the output wave form decreases with increasing the temperature and minimum at higher temperature.

It is observed that with increase of temperature, spontaneous polarization decreases. At SmC^* - SmA transition temperature (T_c^*A), P_s suddenly drops to a very small value. Our results indicate that the aligned PDFLC sample of lower polymer viscosity (NOA-73) shows higher P_s ($\sim 10.60 \text{ nC/cm}^2$) than the sample with higher polymer viscosity (NOA-68) [$P_s \sim 6.45 \text{ nC/cm}^2$] whereas the pure ferroelectric liquid crystal mixture (ZLI-3654) has a P_s ($\sim 23 \text{ nC/cm}^2$) at 30°C . A similar temperature dependence behavior on P_s at different polymer viscosity for unaligned PDFLC samples is also shown in Fig. 4.8.

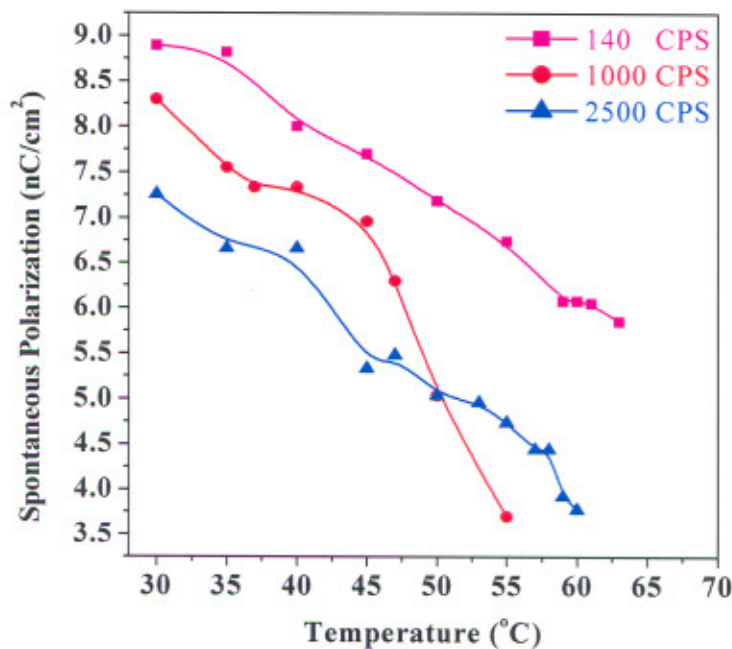


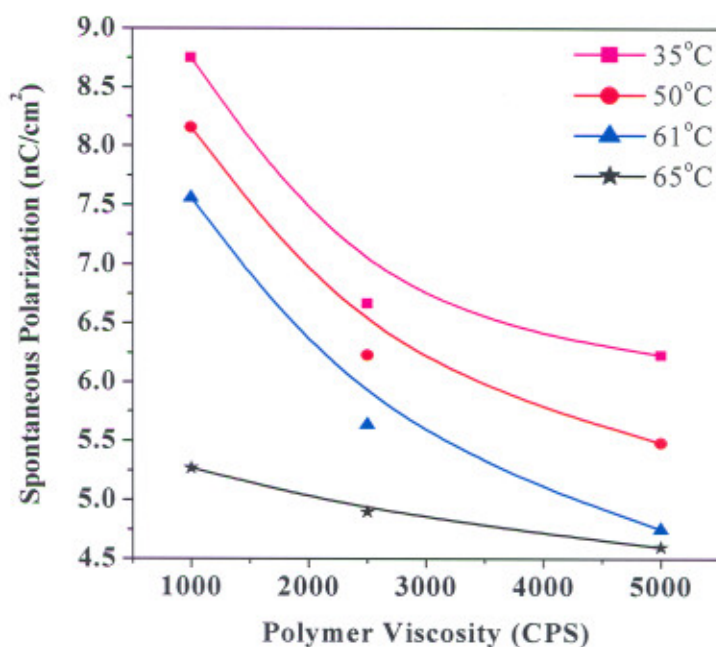
Fig. 4.8 Temperature dependence on spontaneous polarization in unaligned PDFLC sample

It was also observed that aligned PDFLC films show relatively higher value of P_s than unaligned PDFLC samples. It may be due to fact that in aligned samples FLC molecules easily orient from one state to another states due to week anchoring than unaligned LC droplets dispersed into the polymer matrix. Fig. 4.6 and Fig. 4.8 indicate that lower viscosity (NOA-73) unaligned PDFLC sample show lower value of P_s ($\sim 8.89 \text{ nC/cm}^2$)

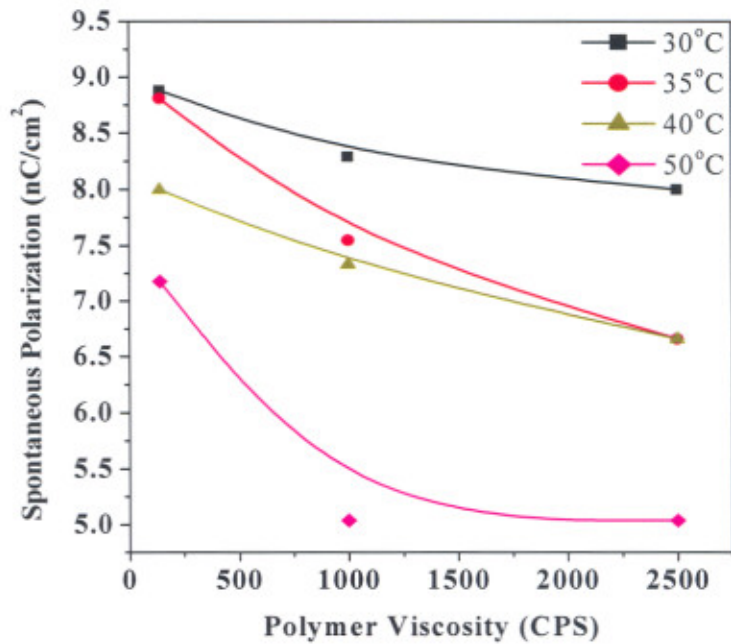
than the aligned PDFLC sample ($P_s \sim 10.60 \text{ nC/cm}^2$) at 30°C whereas the pure ferroelectric liquid crystal mixture (ZLI-3654) has a $P_s (\sim 23 \text{ nC/cm}^2)$ at 30°C . Thus the polymer viscosity affects P_s and lowers it by about 50% in low viscosity polymer matrix and about 30% in high viscosity polymer matrix for aligned PDFLC samples. Approximately 40% in low viscosity polymer matrix and about 30% in high viscosity polymer matrix were also observed in unaligned PDFLC samples. This variation is small when we approach to the T_{C^*A} . Over the whole temperature range studied, we found that polarization decreases but at the same time flexibility in the composite films has enhanced. Our result indicates that aligned PDFLC systems shows fast switching at lower viscosity.

4.3.2 (b) Effect of polymer viscosity on spontaneous polarization

A typical P_s dependence of PDFLC films as a function of polymer viscosity at different temperatures is shown in Fig. 4.9. It is observed that P_s decreases with the increasing polymer viscosity. Our results indicate that both the systems follow the Arrhenius behaviour over the entire viscosity range. Further studies are in progress to characterize these materials for electro-optic device applications.



(a)



(b)

Fig. 4.9 Effect of polymer viscosity on spontaneous polarization at different temperatures in (a) aligned PDFLC sample (b) unaligned PDFLC sample

4.3.2 (c) Bias voltage dependence on optical responses

Fig. 4.10 shows the effect of applied voltage on optical transmission at different polymer viscosities in unaligned PDFLC films at room temperature (30°C).

Better optical response was observed in sample having higher polymer viscosity (e.g. 2500 CPS) than at 140 CPS and 1000 CPS although there is a similar trend. It is due to the formation of larger LC droplet in higher viscosity polymer and enhancement in the optical transmission. The transmission increases linearly with voltage but saturates at higher voltages giving about 80% transmission.

Fig. 4.11 shows the applied voltage dependence on rise time for unaligned PDFLC sample at room temperature. It was observed that in all the samples rise time decreases exponentially with increasing applied voltage and minimum in lower viscosity (140 CPS) system. It can be concluded that low polymer viscosity sample shows faster switching time than high viscosity (2500 CPS) PDFLC samples. Further experiments are in progress to ascertain correlation between these parameters.

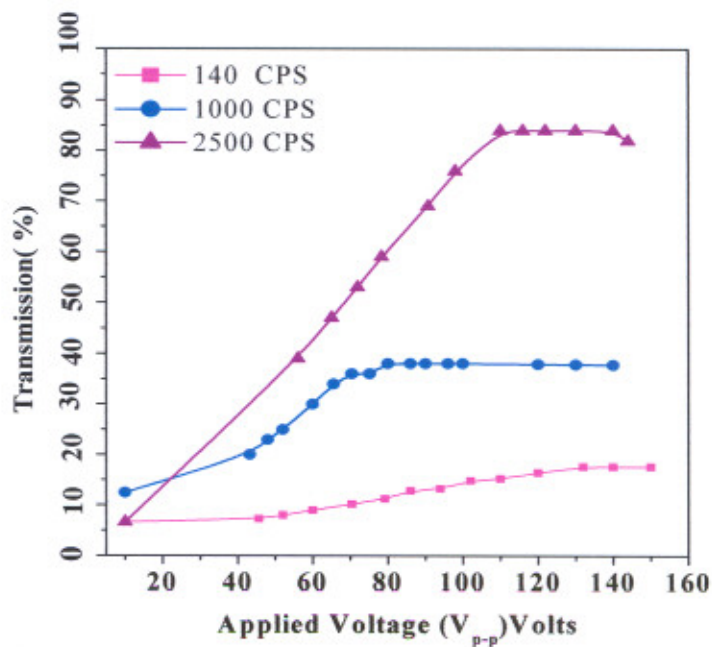


Fig. 4.10 Optical transmission as a function of applied voltage in polymers of different viscosities

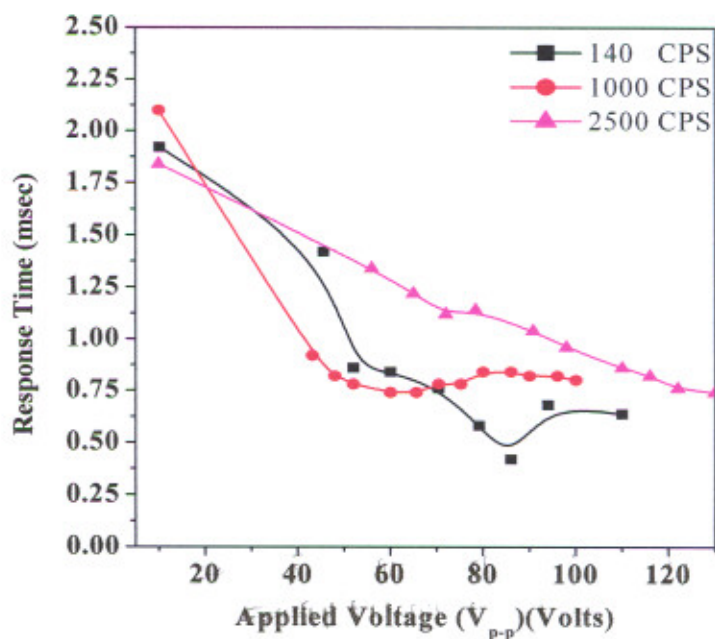


Fig. 4.11 Response time as a function of applied voltage in different polymer viscosities for unaligned PDFLC samples at room temperature

REFERENCES

- [1] J. L. Fergason, *SID Digest*, **68** (1985)
- [2] H. G. Craighead, J. Cheng and S. Hackwood, *Appl. Phys. Lett.*, **40** (1982) 22
- [3] H. Liu, H. Duig and J. R. Kelly, *Mol. Cryst. Liq. Cryst.*, **26** (1995) 99
- [4] J. W. Han, T. J. Kaxg and G. Park, *J. Kor. Phys. Soc.*, **36** (2000) 156
- [5] P. P. Kandu, G. Verma and K. K. Raina, *J. Appl. Poly. Sci.*, **87** (2003) 284
- [6] G. Sumana and K. K. Raina, *J. Appl. Poly. Sci.*, **87** (2003) 1209
- [7] H. S. Kitzerow, H. Molsen and G. Heppke, *Appl. Phys. Lett.*, **60** (1992) 25
- [8] K. P. Lee, S.W. Suh and S. D. Lee, *Appl. Phys. Lett.*, **64** (1994) 718
- [9] L. Komitov, S. T. Lagerwall, B. Stebler, R. Aloe, G. Chidichimo, N. A. Clark and D. Walba, *14 Inter. Liq. Cryst. Conf.*, Pisa (Italy), (1992)
- [10] R. Karapinar, M. O. Neill, *J. Phys. D; Appl. Phys.*, **31** (1998) 900
- [11] V. Y. Zyryanov, S. L. Smorgon and V. F. Shabanov, *SID Digest* (1992) 776
- [12] H. Molsen and H. S. Kitzerow, *J. Appl. Phys.*, **75** (1994) 710
- [13] P. Patel, D. Chu, J. L. West and S. Kumar, *Soc. Inf. Disp. Dig. XXV*, (1994) 845
- [14] G. Heppke, H. S. Kitzerow and H. Molsen, *Mol. Cryst. Liq. Cryst.*, **237** (1993) 471
- [15] E. P. Pozhidaev, D. Ganzke, V.Ya. Zyryanov, S. L. Smorgon, and W. Haase, *Liq. Cryst.*, **29** (2002) 1305
- [16] S. Kundu, T. Ray, S. K. Roy, W. Haase and R. Dabrowski, *Ferrotelectrics*, **282** (2003) 239
- [17] P. Malik, J. K. Ahuja and K. K. Raina, *Curr. Appl. Phys.*, **3** (2003) 325
- [18] J. K. Ahuja and K. K. Raina, *Jpn. J. Appl. Phys.*, **39** (2000) 4076
- [19] A. Fuh and O. Caporaletti, *J. Appl. Phys.*, **66** (1989) 5278
- [20] G. Sumana and K. K. Raina, *Curr. Appl. Phys.*, **5** (2005) 277

Chapter -5

Conclusions

Conclusions

- ❖ The present research work was an attempt to understand the process of liquid crystal dispersion in polymer matrix, process of phase separation, their interaction with polymer and affects of various parameters like electric field, surface alignment, role of polymer viscosity, temperature and droplet size and its distribution etc. on the electro-optic, thermo-optic, droplet and their orientational behaviour. The effect of small amount of dichroic dye on the droplet morphology, optical responses and electro-optic properties has been given.
- ❖ The droplet morphology of PDNLC systems indicates the random distribution of bipolar droplets typically of size 5-28 μm at low voltage. These droplets turned to maltese types crosses at a relatively higher voltage ($\sim 25V_{p-p}$). Our results show that their size was almost independent of applied voltage as well as temperature.
- ❖ The threshold voltage (V_{th}) in PDNLC films increases with temperature. This behaviour has been explained on the basis of average droplet size distribution in the polymer matrix and reduction in effective voltage across the NLC droplets. We believe that the increase of V_{th} as a function of temperature may be due to conductivity variations because of presence of multi-component mixtures. An optical transmission of about $\sim 85\%$ at field strength of $\sim 2V/\mu\text{m}$ was noticed.
- ❖ In the case of GHPDNLC materials, similar types of droplets (bipolar) as in PDNLC were also observed and these droplet turns to maltese types crosses at much higher field ($\sim 80V_{p-p}$) than required PDNLC sample. $\sim 1\%$ dye doped GHPDNLC system shows better optical transmission ($\sim 55\%$ at $20V/\mu\text{m}$) over 4% dye doped GHPDNLC. It may be due to the higher absorbance in 2% and 4% GHPDNLC samples.
- ❖ Better optical and electro-optic responses were noticed in aligned PDFLC system. The increasing polymer viscosity also affects the switching properties and our results indicate that the measured value of P_s was 10.6 nC/cm^2 , and 8.8 nC/cm^2 for aligned and unaligned PDFLC samples respectively. P_s decreases in both the systems with increasing the temperature and low viscosity sample shows better

optical responses due to larger droplet size formed in low viscosity PDFLC samples.

Thapar Institute of Engg: & Technol
PATIALA-147001
CENTRAL LIBRARY

92220

25 DEC 2005